2017

Influence of topography and moisture and nutrient availability on green alder function on the low arctic tundra, NT

Katherine Louise Black Ms.
Wilfrid Laurier University, blac8490@mylaurier.ca

Jennifer Lynn Baltzer Dr.
Wilfrid Laurier University, jbaltzer@wlu.ca

INFLUENCE OF TOPOGRAPHY AND MOISTURE AND NUTRIENT AVAILABILITY ON GREEN ALDER FUNCTION ON THE LOW ARCTIC TUNDRA, NT

by

Katherine Louise Black

(B.Sc. Wildlife Biology and Conservation, University of Guelph, 2015)

THESIS

Submitted to the Department of Biology

Faculty of Science

in partial fulfillment of the requirements for the

Master of Science in Integrative Biology

Wilfrid Laurier University

2017

Abstract

The Arctic has warmed by at least 3°C over the past 50 years and this rapid warming is expected to continue. Climate warming is driving the proliferation of shrubs across the tundra biome with implications for energy balance, climate, hydrology, nutrient cycling, and biodiversity. Changes in tundra plant water use attributable to shrub expansion are predicted to increase evapotranspirative water loss which may amplify local warming and reduce run-off. However, little is known about the extent to which shrubs will enhance evapotranspirative water loss in these systems. Direct measures of shrub water use are needed to accurately predict evapotranspiration rates and the associated hydrological and energetic impacts.

In addition, it is crucial that we understand the abiotic factors that drive shrub distribution and physiological function to forecast further changes in tundra ecosystem function. Shrubs are expanding in areas that have a higher potential of accumulating moisture, such as drainage channels and hill slopes. Shrub expansion may be limited by variation in water and nutrient availability across topographic gradients. Nevertheless, the associations between shrub function and abiotic limitations remain understudied.

To address these knowledge gaps, we measured sap flow, stem water potential, and a range of functional traits of green alder (*Alnus viridis*) shrubs and quantified water and nutrient availability in shrub patches on the low arctic tundra of the Northwest Territories. Frost table depth was a significant negative driver of sap flow and underlies decreased surface water availability with thaw. This was further supported through significantly lower stem water potential values as the growing season progressed. Shrubs in upslope locations had significantly lower water potentials relative to shrubs in

downslope locations, demonstrating topographic variation in shrub water status. Shrubs in channels and at the tops of patch slopes significantly differed in leaf functional traits representing leaf investment, productivity, and water use efficiency. Channel shrubs reflected traits associated with higher resource availability and productivity whereas shrubs at the tops of patches reflected the opposite. This work provides insight into the abiotic drivers of tall shrub water use and productivity, both of which will be essential for predicting ecosystem function.

Acknowledgements

Very special thanks to my supervisor, Dr. Jennifer Baltzer. You provided excellent guidance and helpful suggestions throughout my M.Sc. and trusted me with a lot of responsibility. Thanks to you, I have learned more than I ever imagined I could during my grad studies. I believe my experience working with you will allow me to excel in my future career. I would also like to thank the rest of my committee members, Dr. Philip Marsh and Dr. Kevin Stevens, for their helpful suggestions and comments regarding project conception, fieldwork, and writing. Thank you to Dr. Tristan Long for being a very thorough external examiner.

To the 'Baltzer Army' – Dr. Nicola Day, Geneviève Degré-Timmons, Allison McManus, Jason Paul, Jenna Rabley, Kirsten Reid, Ana Sniderhan, Katherine Standen, Cory Wallace, Meagan Warkentin, and Alison White – I am so grateful for our science and pep talks, your never-ending help and support, and most of all, our friendship. Thank you for always cheering me on; my experience would not have been the same without all of you.

I would like to thank the Trail Valley Creek research team members for all of their help in and out of the field. Warm thanks to Tom Giguere, Jenna Rabley, Cory Wallace, and Emily Way-Nee for their assistance with field data collection. Thank you to Newton Tran for his fabulous technical assistance with post-field data processing. Thank you to Dr. Aaron Berg, Dr. Tracy Rowlandson, Will Woodley, and Beth Wrona for their advice on soil moisture measurements, and thanks to Beth for providing the soil moisture calibrations. Thanks to Phil Mann for his help with meteorological data processing. To

the Group of Seven (you know who you are) – thanks for the great fun in the field through full embracement of tundra madness.

Thank you to all of my friends and family members for their endless encouragement. To my Mom and Dad, thanks for always being my number one fans. Your consistent praise has helped maintain my morale and motivation throughout my academic career. To my brother, Mike, thank you for your constant support and interest in my work. Amanda Knoepfli and Dave Pimiskern, thank you for being the best friends I could ever ask for – your continuous words of wisdom and comic relief were greatly appreciated. Lastly, thank you to my partner, Brent Harbers, and his amazing family for their unconditional love and support. Brent, I am greatly appreciative of your patience and the reassurance you provided me throughout my university experience.

Table of Contents

List of tables

Table 2.5: Compilation of a series of studies investigating evapotranspiration (ET) rates ($mm \cdot day^{-1}$) of different tundra vegetation assemblages on the arctic tundra to facilitate qualitative comparison of our estimates of mean green alder patch transpiration to tundra ET values in the literature. The 'Mean ET' column shows the average ET value for the growing season investigated in the compared studies. We calculated green alder patch water flux for early in the growing season (E), during peak water use (P), and late in the growing season (L).

Table S1: 2015 and 2016 sample sizes for the number of green alder patches investigated, the number of topographic positions per patch (consistent across all patches), the number of green alders per topographic position (top, middle, bottom, channel; see Fig. 2.1 for depiction of these positions) and the total number of green alders studied. These sample sizes correspond with all measurements excluding stem water potential (see Table S2).

Table S2: 2015 and 2016 sample sizes for the number of green alder patches investigated, the number of topographic positions per patch (consistent across all patches), the number of green alders per topographic position (top, middle, bottom, channel; see Fig. 2.1 for depiction of these positions), and the total number of green alders measured for stem water potential. All stem water potential measurements were performed at the patch closest to the Trail Valley Creek research station for logistical ease.

Table S3: List of candidate linear mixed effects models used to assess the relative importance of water availability, nutrient availability, and topography on green alder water use (mean daily sap flow during abiotic measurements) during the 2015 growing season. The random effect term was 'individual' nested within 'patch' to account for our spatially-nested sampling design ('patch') and repeated measures ('individual').

Table S4: List of candidate linear mixed effects models used to assess the relative importance of water availability, nutrient availability, and topography on green alder water use (mean daily sap flow during abiotic measurements) during the 2016 growing season. The random effect term was 'individual' nested within 'patch' to account for our spatially-nested sampling design ('patch') and repeated measures ('individual').

Table S5: Pearson's correlation matrix to test for collinearity between continuous predictors for the 2015 growing season. Leaf N represents percent nitrogen in green alder leaves. We excluded collinear variables from models using a cut-off correlation coefficient of $r = 0.3$.

Table S6: Pearson's correlation matrix to test for collinearity between continuous predictors for the 2016 growing season. Leaf N represents percent nitrogen in green alder leaves. NH_4^+ (ammonium), NO_3^- (nitrate), P (dihydrogen phosphate and hydrogen phosphate), and K^+ (potassium) represent ion supply rate in the soil beneath green alders during the growing season. We excluded collinear variables from models using a cut-off correlation coefficient of $r = 0.3$ (variables with $r > 0.3$ are bolded). Based on this correlation matrix, soil moisture (5 cm) and K^+ were excluded from models.

Table S7: Random effects output for a linear mixed effects model used to test for differences in mean stem water potential (Ψ_{stem}) of green alders among topographic positions and measurement periods (early, mid-, and late season) as well as among topographic positions (top, middle, bottom, channel; see Fig. 2.1 for depiction of these positions) during different measurement periods (interactive effect). 'Individual' was used as a random effect to account for repeated measures.

Table S8: AIC_c-based rankings from best to worst for nine candidate linear mixed effects models predicting green alder sap flow (SF_{daily}) during the 2015 growing season. Model rankings were based on AIC_c (corrected Akaike's information criterion) values and the associated statistics (Burnham and Anderson, 1998). The associated statistics shown are the difference between each model and the minimum AIC_c model (Δi), the number of parameters per model (K), the log-likelihood values (LogLik), the Akaike weights (w_i), the amount of variation in SF_{daily} that the fixed effects of each model accounted for (pseudo marginal R^2; R^2_m), and the total amount of variation in SF_{daily} that each model accounted for (pseudo conditional R^2; R^2_c; fixed effects and random effects combined). The random effect term was 'individual' nested within 'patch' to account for our spatially-nested sampling design ('patch') and repeated measures ('individual').

Table S9: AIC_c-based rankings from best to worst for 10 candidate linear mixed effects models predicting green alder sap flow (SF_{daily}) during the 2016 growing season. Model rankings were based on AIC_c (corrected Akaike's information criterion) values and the associated statistics (Burnham and Anderson, 1998). The associated statistics shown are the difference between each model and the minimum AIC_c model (Δi), the number of parameters per model (K), the log-likelihood values (LogLik), the Akaike weights (w_i), the amount of variation in SF_{daily} that the fixed effects of each model accounted for (pseudo marginal R^2; R^2_m), and the total amount of variation in SF_{daily} that each model accounted for (pseudo conditional R^2; R^2_c; fixed effects and random effects combined). For all models, the random effect term was 'individual' nested within 'patch' to account for our spatially-nested sampling design ('patch') and repeated measures ('individual').

Table S10: Random effects output for the AICc-selected linear mixed effects model predicting green alder sap flow during the 2015 growing season. The random effect term was 'individual' nested within 'patch' to account for our spatially-nested sampling design ('patch') and repeated measures ('individual').

Table S11: Random effects output for the AICc-selected linear mixed effects model predicting green alder sap flow during the 2016 growing season. The random effect term was 'individual' nested within 'patch' to account for our spatially-nested sampling design ('patch') and repeated measures ('individual').

Table S12: Loadings of a principal components analysis used to reduce functional traits of green alders into gradients that explain variation in resource use strategies in multivariate trait space. Principal components 1-3 cumulatively explained 82.8% of the variation in the functional trait dataset. The magnitude and directionality of the loadings of our three retained principal components indicate that principal components 1 and 2 can be thought of as separate functional trait spectra. The first principal component explained a gradient in leaf investment and productivity: increasing leaf N (leaf nitrogen concentration) and decreasing C:N (leaf carbon to nitrogen ratio) and LMA (leaf mass per area). The second principal component explained a gradient in water use efficiency: increasing LA:SA (leaf area to sapwood area ratio) and decreasing leaf $\delta^{13}C$ (integrated water use efficiency). The third principal component was mainly explained by mean daily cumulative sap volume during peak physiological activity (SF_{peak}).

List of figures

Fig. 2.3: (a) Scatterplot showing mean stem water potential (Ψ_{stem}) of green alders (± standard error) measured early in the growing season (June 18), mid-season (July 26), and late in the growing season (August 21) of 2015. Mean Ψ_{stem} significantly differed across a topographic gradient such that downslope locations generally had higher Ψ_{stem} values than upslope locations. Mean Ψ_{stem} also significantly differed across a seasonal gradient such that green alders had higher Ψ_{stem} values earlier in the season relative to mid-season and lower Ψ_{stem} values at the end of the season relative to mid-season. There was no significant interactive effect between topographic position and study year (Table 2.1). (b) Scatterplot showing mean late season Ψ_{stem} of green alders during the 2015 (August 21) and 2016 (August 9) study years. Mean late season Ψ_{stem} significantly differed between study years. Green alders located on the top of the patch slope had significantly lower late season Ψ_{stem} values than downslope locations in 2015 but not in 2016 (Table 2.2).

Fig. 2.4: Scatterplots of the relationship between frost table depth and green alder sap flow (mean daily cumulative sap volume during abiotic measurements; SF_{daily}) during the 2015 (a) and 2016 (b) growing seasons. The two abiotic measurement periods during the 2015 growing season were: June 30-July 3 (early season) and August 19-22 (late season). The three abiotic measurement periods during the 2016 growing season were: June 28-29 (early season), July 13-19 (mid-season), and August 6 (late season). The dashed lines represent the overall regression between frost table depth and SF_{daily} (across early, mid-, and late season measurements). Based on the outputs of the AICc-selected linear mixed effect models used to assess the relative importance of water availability, nutrient availability, and topography on green alder sap flow during the 2015 and 2016 growing seasons (Tables 2.3 and 2.4, respectively), the main abiotic driver of green alder SF_{daily} for both years was frost table depth (2015: $p = 0.004$; 2016: $p= 0.005$).

Fig. 2.5: Bi-plot of principal component 1 against principal component 2 from a principal components analysis (PCA) used to reduce functional traits of green alders into gradients that explain variation in resource use strategies in multivariate trait space. Principal component 1 was driven by topography (ANOVA; *a priori* contrast: top vs. channel; $F_{3,19} = 8.058$, $p = 0.009$), with channel shrubs clearly separating out from those at the tops of patches. Green alders in channels were characteristic of higher leaf N (leaf nitrogen concentration) and lower C:N (leaf carbon to nitrogen ratio), LMA (leaf mass per area), and leaf $\delta^{13}C$ (integrated water use efficiency). Shrubs at the top of the patches were characterized by the opposite suite of traits. Mean daily cumulative sap volume during peak physiological activity (SF_{peak}) was unimportant in this bi-plot as indicated by its small arrow. LA:SA (leaf area to sapwood area ratio) represents whole-plant water use efficiency. The amount of variation explained by each principal component is indicated on each axis. Colour version available online.

Fig. S1: Map of the lower portion of the Trail Valley Creek research basin indicating the locations of sap flow meter-instrumented shrubs for the 2015 (orange circles) and 2016 (blue triangles) growing seasons. The yellow star indicates the location of the Trail Valley Creek research station base camp. Colour version available online.

Fig. S2: Linear regression between stem diameter and sapwood thickness for the green alder stem cross-sections collected during the 2016 growing season. The equation of the fitted line and stem diameter information measured during the 2015 growing season were used to estimate sapwood thickness for the stem cross-sections collected during the 2015 growing season.

Fig. S3: Linear regression between dry leaf area and fresh leaf area per scanned batch of green alder leaves (n = 25 batches of leaves; 20 leaves per batch; 400 leaves total) for the 2016 growing season. Following removal of sap flow meters, all leaves were removed from instrumented stems to measure total stem leaf area. Due to the large number of leaves, fresh leaf scans for all instrumented stems was not feasible. To address this, we developed a relationship between fresh leaf area and dry leaf area using a subsample of fresh leaves which were scanned in batches and their batch areas measured. These leaves were then oven dried for 48 hours at 70°C and re-scanned to determine dry leaf area and the subsequent fresh to dry leaf area relationship. All remaining leaves were oven-dried, scanned in batches, and the fresh to dry leaf area relationship was used to correct for leaf shrinkage in the large batches. The fresh area of each batch was summed for each instrumented stem to obtain total stem leaf area. All leaf area measurements were performed using WinFOLIA (v. 2004a, Regent Instruments Inc., Ville de Québec, QC, CA).

Fig. S4: Continuous tracing of daily cumulative stem sap flow for four shrubs (one per topographic position: top, middle, bottom, and channel) during the 2015 growing season (approximately early June to late August). Despite technical issues that prevented us from calculating the total (cumulative) volume of sap used by green alder stems during the 2015 and 2016 growing seasons, the four shrubs used in this figure had full datasets that are representative of the general seasonal variation in sap flow experienced by our study shrubs in both 2015 and 2016. Colour version available online.

Fig. S5: (a) Bi-plot of principal component 1 against principal component 2 from a principal components analysis used to reduce functional traits of green alders into gradients that explain variation in resource use strategies in multivariate trait space. (b) Bi-plot of principal component 1 against principal component 3. (c) Bi-plot of principal component 2 against principal component 3. The amount of variation explained by each principal component is indicated on each axis. Principal component 1 explained a gradient in productivity, leaf investment, and leaf water use efficiency: decreasing leaf N (leaf nitrogen concentration) and increasing leaf C:N (carbon to nitrogen ratio), LMA (leaf mass per area) and leaf $\delta^{13}C$ (integrated water use efficiency). Principal component 2 explained a gradient in leaf and whole plant water use efficiency: decreasing leaf $\delta^{13}C$ and increasing LA:SA (leaf area to sapwood area ratio). Principal component 3 represented mean daily cumulative sap volume during peak physiological activity (SF_{peak}).

Fig. 3.1: (a) Boxplot displaying soil moisture (%) measured at a 5 cm depth at eight locations along 10 green alder patch transects and 10 paired open tundra transects from June 30th-July 2nd, 2015 in the Trail Valley Creek research basin on the low arctic tundra of the Northwest Territories (the eight locations along each transect were pooled for analysis). Each box encompasses the middle 50% of the distributions. The horizontal line within each box denotes the median. The whiskers represent the minimum and maximum values. Outliers (represented by open circles) are values that are 1.5 times greater than the interquartile range. Soil moisture was significantly higher in open tundra sites than in green alder patches (linear mixed effects model; $p = 3.70 \times 10^{-3}$). (b) Scatterplot showing the relationship between green alder density and soil moisture measured at a 5 cm depth (soil moisture measured in patches as explained above). Soil moisture data were pooled such that an average soil moisture per patch could be calculated (each point represents shrub density in a patch). Soil moisture significantly decreased with shrub density (simple linear regression; $p = 0.013$, $R^2 = 0.56$). Data in (a) and (b) were collected and analyzed by C. Wallace.

Fig. 3.2: Scatterplots of average nodule biomass per shrub vs. ordinated green alder functional traits representing leaf investment, productivity, and water use for 16 green alders in the Trail Valley Creek research basin. Ordinated functional traits are represented by the scores of three principal component axes. Estimates of average nodule biomass per shrub were obtained from Rabley (2017). Average nodule biomass was not a significant predictor of principal component 1 (a), 2 (b), or 3 (b) (Table 3.1).

Fig. 3.3: Scatterplots of square root-transformed total nodule biomass per shrub vs. ordinated green alder functional traits representing leaf investment, productivity, and water use for 16 green alders in the Trail Valley Creek research basin. Ordinated functional traits are represented by the scores of three principal component axes. Estimates of total nodule biomass per shrub were obtained from Rabley (2017). Square root (total nodule biomass) was not a significant predictor of principal component 1 (a), 2 (b), or 3 (b) (Table 3.1).

Fig. 3.2: Scatterplots of square root-transformed nodule count per shrub vs. ordinated green alder functional traits representing leaf investment, productivity, and water use for 16 green alders in the Trail Valley Creek research basin. Ordinated functional traits are represented by the scores of three principal component axes. Estimates of nodule count per shrub were obtained from Rabley (2017). Square root (nodule count per shrub) was not a significant predictor of principal component 1 (a), 2 (b), or 3 (b) (Table 3.1).

Chapter 1: General introduction and literature review

1.1 Arctic amplification

It is widely accepted that increased concentrations of greenhouse gases in the atmosphere have contributed to global warming (e.g., IPCC, 2013). In recent decades, the Arctic has experienced increases in surface temperatures at more than twice the global rate (Serreze *et al.*, 2009; Screen & Simmonds, 2010). Specifically, over the past 50 years, the Arctic has warmed by ~3°C while global temperatures have only increased by ~0.6°C (ACIA, 2004). It is predicted that arctic warming will continue to increase at an accelerating rate, a phenomenon known as 'arctic amplification' (Serreze *et al.*, 2000; Hinzman *et al.*, 2005; Francis & Vavrus, 2012).

The Arctic warms faster than other regions of the planet largely because reductions in snow and ice cover result in decreased reflectivity and thus increased absorption of incoming radiation, which in turn heats the surrounding ground and ocean (Comiso, 2006; Screen & Simmonds, 2010). This relationship leads to a positive feedback in which loss of snow and ice creates more warming regionally, further accelerating loss of snow and ice (Kaplan & New, 2006). Arctic amplification has had a wide range of consequences for high latitude ecosystems, such as increased rates of permafrost thaw and slumping (Lantz & Kokelj, 2008), increased frequency and severity of tundra fires and the subsequent release of carbon to the atmosphere (Mack *et al.*, 2011), and major changes in tundra vegetation composition, distribution, and density (Walker & Wahren, 2006).

1.2 Climate-warming induced tundra shrub expansion

A significant increase in shrub cover is occurring across the tundra biome due to rapid climate warming (Sturm *et al.*, 2001a; Hinzman *et al.*, 2005; Tape *et al.*, 2006; Forbes *et al.*, 2010; Loranty & Goetz, 2012; Fraser *et al.*, 2014). Low-growing shrubs are increasing in size, tall shrubs are becoming more prevalent, and shrubs are colonizing areas that were previously shrub-free (Sturm *et al.*, 2001a; Elmendorf *et al.*, 2012). The short growing season and low temperatures in the Arctic would typically limit the growth of shrubs due to the low energy input to support productivity, but climate warming has stimulated shrub growth and reproduction (Hobbie & Chapin, 1998; Lantz *et al.*, 2010).

Remote sensing techniques and fine-scale mapping provide strong visual evidence of the expansion of shrubs in tundra landscapes during recent decades (Tape *et al.*, 2006; Lantz *et al.*, 2013). Using high resolution satellite imagery and repeat aerial photographs, Fraser *et al.* (2014) found that 85% of the surface of ~15,000 km^2 of the western Canadian Arctic had a positive trend in normalized difference vegetation index (NDVI; a measure of vegetation productivity based on spectral characteristics of the land surface) or 'greening' from 1985 to 2011. Based on their comparisons of aerial photograph pairs from 1980 and 2013, Fraser *et al.* (2014) attributed this greening of their study area to increased canopy cover of erect dwarf and tall shrubs. Lantz *et al.* (2013) used soft copy stereo visualization of aerial photographs to map fine-scale changes in shrub tundra of ~3,000 km^2 of the western Canadian Arctic. They found that mean tall shrub cover of the Mackenzie Delta Uplands increased by 15.8% (± 3.6%) from 1972 to 2004. These studies as well as others document the rapid greening of tundra environments coincident with recent climate warming.

Ground studies further support an increase in shrub abundance in the Arctic congruent with warming. Both naturally and experimentally warmed tundra plots have demonstrated increases in shrub growth (Chapin *et al.*, 1995; Wahren *et al.*, 2005; Walker & Wahren, 2006; Elmendorf *et al.*, 2012). Dendrochronological analyses performed by Hallinger *et al.* (2010) in northern Sweden showed that average radial and vertical growth of dwarf juniper shrubs (*Juniperus nana*) significantly increased in recent decades, and this growth was positively correlated with warmer summer temperatures. Dwarf juniper shrubs at higher elevations above the treeline of Mount Slåttatjocka in northern Sweden were also younger and had greater increases in growth in recent decades than shrubs at lower elevations (Hallinger *et al.*, 2010), indicating that dwarf juniper shrubs have recently colonized higher elevations and are growing at a rapid rate. Annual radial growth rates in *Salix pulchra* and *Betula nana* shrubs from 1948 to 2006 also increased with warmer summer temperatures in northeastern Siberia (Blok *et al.*, 2011). Consequently, both plot-level studies and growth ring analyses corroborate visual observations of increased productivity and extent of tundra shrubs.

1.3 Feedbacks and implications of tundra shrub expansion

Shrub expansion across the Arctic is projected to continue at an accelerating rate. As climate warming continues, it is predicted that approximately half of the vegetation across the Arctic will transition to taller physiognomic states by 2050, with woody cover increasing by as much as 52% (Pearson *et al.*, 2013). This continued shrub expansion is predicted to have profound implications for tundra ecosystems mainly due to changes in albedo and evapotranspiration, which will likely result in an overall positive feedback to regional warming and shrub productivity (Bonfils *et al.*, 2012)

Shrub canopies act as dark surfaces that decrease albedo (reflectivity) and increase net surface long-wave radiation, leading to local atmospheric warming throughout the year and a potentially larger-scale positive feedback to climate warming (Chapin *et al.*, 2005). Lantz *et al.* (2013) found that tall shrub sites in the western Canadian Arctic had, on average, decreased albedo and elevated near-surface ground temperatures from the onset of snowmelt and throughout the growing season compared to dwarf shrub sites. Tall shrub canopies can protrude above winter snow cover, and this has been shown to result in winter albedo values being 30% lower than at sites where dwarf shrubs were buried by snow, which can cause earlier snow melt under tall shrubs (Sturm *et al.*, 2005a). Sturm *et al.* (2005a) estimated that the predicted transition from open tundra to shrub tundra in the Arctic could produce a 69-75% increase in absorbed solar radiation by shrubs during the winter due to the increased area of dark and tall shrub canopies protruding above the snow. These large increases in long-wave radiation due to reductions in albedo are expected to result in a positive feedback to atmospheric heating with the potential to further promote shrub growth under climate warming (Chapin *et al.*, 2005; Pearson *et al.*, 2013).

Tall, dense shrub canopies capture more snow than sites without shrubs, and thicker snow packs insulate soils beneath shrubs (Sturm *et al.*, 2005b; Myers-Smith & Hik, 2013). Sturm *et al.* (2001b) found that snow cover below shrubs in arctic Alaska was on average ~40% deeper than snow cover on tussock tundra, leading to snow-ground interface temperatures in April to be approximately 3°C warmer beneath shrubs than in open tundra areas. Sturm *et al.* (2001b) hypothesized that warmer winter soils associated with snow capture may promote greater winter microbial activity which may lead to

enhanced nitrogen mineralization. If this hypothesis is true, then snow insulation could lead to a positive feedback to shrub growth by enhancing nitrogen availability in the spring. In addition, increased snow capture by shrubs results in an uneven distribution of snow across different tundra landscape types (e.g., shrub patches, open tundra, drifts) which can dramatically alter spring run-off processes through accelerated snowmelt in shrub patches (Marsh & Pomeroy, 1996; Essery *et al.*, 1999; Endrizzi & Marsh, 2010; Marsh *et al.*, 2010).

An increase in tundra shrub cover is anticipated to result in increased summer evapotranspiration, and thus increased atmospheric water vapour concentrations (Swann *et al.*, 2010; Lawrence & Swenson, 2011). Increases in atmospheric moisture due to potentially enhanced evapotranspiration are projected to increase long-wave radiation as a result of the radiative forcing of water vapour (Swann *et al.*, 2010). Based on climate scenarios that incorporate unrestricted dispersal and colonization of arctic vegetation, evapotranspiration is expected to increase by up to 13% across the entire Arctic by 2050 (Pearson *et al.*, 2013), most of which will likely be attributable to erect shrubs. The predicted increase in radiative forcing accompanying increased evapotranspiration is modelled to be 1.5 times larger than the predicted forcing associated with decreases in albedo (Swann *et al.*, 2010). The combined effect of decreased albedo and increased evapotranspiration from a 20% increase in shrub cover north of 60°N is expected to increase annual arctic tundra temperatures by 0.66°C-1.84°C (Bonfils *et al.*, 2012).

Increased evapotranspiration by shrubs has consequences for tundra surface hydrology and permafrost dynamics (Fig. 1.1). Large-scale increases in evapotranspiration could reduce tundra basin discharge simply because more and larger

shrubs would be effectively depleting the available water supply in soils and releasing it into the atmosphere. Drier soils below shrubs would likely reduce run-off because increased empty pore space in dry soils results in an increased water requirement to fill pores before run-off occurs (Tape *et al.*, 2011). Lower soil moisture below shrubs from increased evapotranspiration may result in reduced seasonal thaw (thinner active layer) due to reduced thermal conductivity of the soil (Hinkel *et al.*, 2001). A thinner active layer may increase run-off (in opposition to above) and restrict shrub rooting depth and growth as plant roots cannot penetrate permafrost (Benninghoff, 1952). However, regional warming from increased evapotranspiration is overall estimated to contribute to permafrost thaw and degradation (Lawrence & Swenson, 2011; Bonfils *et al.*, 2012) which may increase seasonal thaw and summer soil temperatures. Warmer soil temperatures during the growing season could enhance root function, soil microbial activity, nutrient supply, and overall shrub physiological function and productivity (Chapin, 1983; Rustad *et al.*, 2001; Keuper *et al.*, 2012a).

Although shrub expansion is predicted to accelerate regional warming (Swann *et al.*, 2010; Bonfils *et al.*, 2012; Pearson *et al.*, 2013), there are also some important processes that may offset the positive shrub expansion-climate feedbacks. Shrub expansion increases shading of the ground surface (Chapin *et al.*, 1995) which can cool soils during the growing season. Myers-Smith and Hik (2013) found that soil temperatures in Yukon Territory in July were on average ~2°C cooler under *B. glandulosa* and *Salix* spp. canopies compared to open tundra. Cooler soil temperatures beneath shrub canopies in the summer can reduce seasonal thaw. Indeed, Blok *et al.* (2010) found that the presence of *B. nana* canopies in northeastern Siberia resulted in a

~9% shallower frost table due to a lower ground heat flux compared to plots where *B. nana* was removed. Shading by shrubs has been shown to reduce the amount of short-wave radiation incident on snow cover (Marsh *et al.*, 2010), which can cause longer snow cover after the initial melt period (Sturm *et al.*, 2001b). Accordingly, the cooling effects of canopy shading on active layer thickening may offset the warming effects associated with decreased albedo and increased evapotranspiration during the growing season.

1.4 Issues with predicting the impacts of increased evapotranspiration by shrubs

The current models developed to predict the magnitude and impacts of increased evapotranspiration of woody plants in the Arctic (Swann *et al.*, 2010; Bonfils *et al.*, 2012; Pearson *et al.*, 2013) have several flaws due to the difficulty of incorporating the complexity of interactions between climate, plant distribution and productivity, and abiotic and biotic factors. Swann *et al*.'s (2010) estimates of changes in evapotranspiration were modelled from a simple vegetation transition from bare ground to deciduous forest north of 60°N rather than the shift from current arctic vegetation to increased shrub cover. The transition of tundra to forest on the arctic tundra is not probable within this century mainly due to time lags between change in climate and migration of trees, whereas shrub expansion is occurring much more rapidly (Rupp *et al.*, 2001; Epstein *et al.*, 2004; Chapin *et al.*, 2005). Thus, Swann *et al.* (2010) may have overestimated the magnitude of increase of evapotranspiration in tundra systems. Pearson *et al*.'s (2013) ecological niche models relied on statistical associations rather than biological mechanisms of range shifts of several arctic vegetation classes without explicit mention of the specific impact of shrubs on evapotranspiration. The authors also acknowledge that they did not account for the important feedbacks associated with shrub

expansion, such as increased subnivean temperatures and the associated potential increase in nutrient availability (Sturm *et al.*, 2001b, 2005b), and thus their models may have underestimated evapotranspiration. Bonfils *et al.* (2012) provide the most comprehensive model yet to test the impact of tundra shrub expansion on regional climate by accounting for variation in shrub height, winter albedo feedbacks, and permafrost-shrub relationships. But, as most climate models cannot account for all of the intricacies of shrub expansion, Bonfils *et al.* (2012) did not account for several mechanisms relating to vegetation structure, phenology, or snow accumulation in shrub patches. None of the aforementioned models account for the fact that the rate of vegetation expansion in the Arctic differs across both spatial and temporal scales (Epstein *et al.*, 2013). Although these models provide informative estimates of broad scale trends, little is known about the water use of tundra shrubs or variation in shrub function across landscape positions. Accurate estimates of model parameters (i.e., direct measures of shrub water use) are necessary for accurately predicting future evapotranspiration rates and the associated hydrological and energetic impacts in tundra ecosystems.

1.5 The influence of topographic gradients, moisture availability, and nutrient availability on tundra shrub expansion

In addition to needing direct measures of shrub water use to accurately predict the consequences of evapotranspirative water loss, it is crucial that we understand the abiotic factors that drive shrub distribution and physiological function to forecast changes in tundra vegetation. Since multiple factors interact to influence the expansion of shrubs in tundra ecosystems, it is difficult to determine which specific factors will control the growth and recruitment of a shrub species at a given location. We can use observations of

landscape patterns of shrub expansion to make predictions about why shrubs are expanding in certain locations. Shrubs are mainly expanding in wetter tundra sites, such as floodplains, drainage channels, and the slopes and toes of hills (Epstein *et al.*, 2004; Tape *et al.*, 2006, 2012; Fig. 1.2). The topography of a landscape has a large impact on vegetation distribution because it controls the spatial variability in hydrologic conditions (Sørensen *et al.*, 2006). The distribution of snow and the flow of surface water are largely influenced by the slope and aspect of landforms (Swanson *et al.*, 1988). Naito and Cairns (2011) reported a significant relationship between shrub development and topographically-derived characteristics of the northern Brooks Range and North Slope uplands of Alaska. Using a time series of aerial photographs of the region, they found that the average total area of shrub cover from the 1970s to the 2000s increased by ~24%, and within that area and time frame, average total area of shrub cover in floodplains increased by ~40%. Chapin *et al.* (1988) found that average shoot mass of *B. nana* shrubs located in water tracks in arctic Alaska was ~18 mg·shoot^{-1} more compared to *B. nana* shrubs located on adjacent non-water tracks. Cameron and Lantz (2016) concluded that rapid green alder (*Alnus viridis* ssp. *fruticosa*) expansion at disturbed roadsides in the Northwest Territories was promoted by increases in soil moisture. These studies imply that the availability of moisture and other topographically-derived characteristics are important drivers of shrub expansion.

Other studies suggest that shrub growth in tundra ecosystems is limited primarily by nutrient rather than moisture availability. A study performed by Keuper *et al.* (2012) at Siberian and Swedish tundra sites found that three years of experimentally increased (approximately doubled) summer precipitation had no effect on total annual aboveground

biomass production of *B. nana*-dominated tundra, suggesting that shrub productivity is not water limited. Chapin *et al.* (1995) tested the effects of nutrient addition on tundra plant communities in arctic Alaska by providing experimental plots with supplemental nitrogen and phosphorous. From 1983 to 1989, average total peak-season aboveground biomass of *B. nana* shrubs in control plots without nutrient additions increased by ~108 $g \cdot m^{-2}$ whereas nutrient addition plots increased by ~444 $g \cdot m^{-2}$. Additionally, Shaver and Chapin (1980) found that primary productivity of shrubs in arctic Alaska was limited by nitrogen availability. These results therefore suggest that nutrient limitations may have a larger impact on shrub expansion than water limitations, as it is widely known that the tundra is a nitrogen-limited biome (Haag, 1974; Shaver & Chapin, 1980, 1986; Bowman & Conant, 1994; Theodose & Bowman, 1997). However, nutrient cycling rates and plant productivity are often greater in wetter tundra sites (Chapin *et al.*, 1988; Matthes-Sears *et al.*, 1988; Hastings *et al.*, 1989) so it is likely that the combined effects of topography, water, and nutrients are important for predicting the distribution and productivity of shrubs.

1.6 Green alder

The main deciduous shrubs that are experiencing pan-Arctic expansion are green alder (*A. viridis*; Fig. 1.3), willow (*Salix* spp.), and birch (*Betula* spp.; Tape *et al.*, 2006; Lantz *et al.*, 2013). These shrubs increase in cover by expanding the boundaries of existing shrub patches, infilling existing shrub patches, and/or increasing individual shrub size (Sturm *et al.*, 2001a; Tape *et al.*, 2006). Most tundra shrub expansion studies focus on the climatic drivers and subsequent impacts of willow and birch expansion, whereas

far fewer studies have investigated the abiotic constraints on green alder physiological function.

Green alder is expanding rapidly across the low Arctic. In the previously mentioned study in which Lantz *et al.* (2013) reported an average absolute increase of 15.8% in total shrub cover over the western Canadian Arctic from 1972 to 2004, a mean relative increase of 68.1% in green alder stem density was observed. Repeat photography also demonstrates an increase in green alder cover in arctic Alaska over the last 50 years (Tape *et al.*, 2006). Although green alder productivity is increasing in the Arctic, little is known about this species in the context of tundra shrub expansion. However, green alder is well studied in other ecosystems, and information from these studies can provide insight into how green alder may function in tundra ecosystems.

Green alder has several subspecies that are found across the northern hemisphere, with centres in Alaska, northwestern Canada, northern Europe, the European Alps, and Siberia (Bühlmann *et al.*, 2016). Green alder is known as a pioneer or early successional species (Wiedmer & Senn-Irlet, 2006) as it tends to colonize and invade disturbed sites with recently exposed mineral soils, high light availability, and high soil moisture (Mitchell & Ruess, 2009), such as avalanche slides (Wiedmer & Senn-Irlet, 2006), abandoned pastures (Bühlmann *et al.*, 2016), burned tundra sites (Lantz *et al.*, 2010), roadsides (Cameron & Lantz, 2016), old seismic lines (Kemper & Macdonald, 2009), abandoned drilling mud sumps (Johnstone & Kokelj, 2008), and permafrost thaw slumps (Lantz *et al.*, 2009). Green alder is a successful colonizer mainly due to its climatic hardiness and partnership with two root symbionts: ectomycorrhizas that are important for water and nutrient uptake (mainly phosphorous) and the formation of root nodules by

Frankia bacteria that fix atmospheric nitrogen (N; Mejstrik & Benecke, 1969; Benecke, 1970; Bissonnette *et al.*, 2014; Fig. 1.4). Some *Alnus* spp. have been shown to rely on *Frankia* to meet 70-100% of their N needs (Hurd *et al.*, 2001; Myrold & Huss-Danell, 2003) and no non-nodulated alder has ever been observed under natural conditions (Chaia *et al.*, 2010). In addition to its N-fixing abilities, green alder is able to grow rapidly after seed establishment due to its clonal growth form which leads to the formation of dense patches of shrubs 1-4 m in height, making it virtually impossible to differentiate individuals through simple visual observation (Wiedmer & Senn-Irlet, 2006). These traits have allowed green alder to recently expand not only across tundra ecosystems, but also across montane systems, such as subalpine regions in the western Alps and the Balkan and Carpathian Mountains (Anthelme *et al.*, 2007; Boscutti *et al.*, 2014; Bühlmann *et al.*, 2016).

The expansion of green alder in montane systems has had major implications for ecosystem functioning. Bühlmann *et al.* (2016) found that green alder expansion in a former grassland in the Swiss Alps rapidly converted an N-poor grassland into a highly productive shrubland that resulted in N saturation and increased turnover of N and C. The persistence of green alder in montane systems through clonal reproduction is predicted to inhibit the succession of late successional forest species and thus may reduce the C storage potential of the landscape (Anthelme *et al.*, 2002; Hiltbrunner *et al.*, 2014). In addition to altering the N and C cycles of montane ecosystems and inducing N losses through leaching and gaseous emissions, the expansion of N-fixing green alder can reduce plant diversity through competitive exclusion (i.e., shading, homogenizing soil; Anthelme *et al.*, 2007; Hiltbrunner *et al.*, 2014). These reductions in plant diversity can

alter trophic composition and structure; Anthelme *et al.* (2001) found that dense alder stands in the French Alps caused significant reductions in soil arthropod biomass, which may in turn reduce the diversity of insectivores. Similar shrub-induced impacts on biodiversity have been observed in tundra systems. For example, large-scale increases in shrub cover have caused substantial reductions in lichen cover due to increased shading and litter accumulation by tall shrubs like green alder (Fraser *et al.*, 2014). Lichen is a significant forage for caribou, consequently green alder expansion may negatively influence caribou populations and traditional hunting and herding practices (Myers-Smith *et al.*, 2011).

Since montane systems are also strongly nutrient-limited (Bassin *et al.*, 2013), green alder expansion has the potential to transform tundra ecosystems by introducing large amounts of N, altering soil microclimate, and increasing rates of soil organic matter accumulation (Rhoades *et al.*, 2001; Hiltbrunner *et al.*, 2014). Since soil N infertility enhances N-fixation rates by *Frankia* in green alder (Benecke, 1970), N-fixation should be crucial in the establishment and growth of green alder on the tundra. Although green alder N input rates are not known for the low Arctic, Mitchell and Ruess (2009) estimated that green alders along a secondary successional chronosequence in interior Alaska contribute 2.5-6.6 kg $N \cdot ha^{-1} \cdot year^{-1}$. This provides insight into what N input rates of green alder may be like on the tundra, where nitrogenase activity may be more limited due to colder and shorter growing seasons (Winship & Tjepkema, 1985). Although green alder is well-known for its role in altering ecosystem nutrient cycling, virtually nothing is known about the impacts of *Alnus* spp. on ecosystem water fluxes despite their clear importance in ecosystem function and structure.

1.7 Rationale behind this research

The associations between shrub expansion and abiotic limitations remain understudied, and only limited field measures have been undertaken to further understand the moisture and nutrient constraints on shrub expansion as the climate warms. The abiotic constraints on green alder physiological function are of particular interest because this species has the potential to substantially change tundra ecosystems by the mechanisms described above. Green alder's N-fixing abilities, its persistence via clonal growth, and its relatively large size also give this shrub a strong competitive advantage over other tundra vegetation. Investigating green alder function and the associated abiotic constraints will provide insight into the factors that control shrub distribution and productivity. Refining and characterizing the factors that influence green alder expansion in the context of climate change is essential for predicting the future state of the Arctic.

We also highlight the need for field measures of tundra shrub water use so that predictive models can be used to predict broad-scale evapotranspiration rates. As the largest tundra shrub undergoing expansion, green alder likely has higher evapotranspirative potential than the lower-growing shrubs that are expanding, and thus characterizing green alder water use is critical in understanding and forecasting the impacts of tall shrub expansion on surface hydrology and energy regimes.

1.8 Study aim

The aim of this study was to improve the current understanding of tundra shrub function by answering the following questions: 1) How much water do green alders use?; 2) How do topography and associated gradients in water and nutrients influence green alder physiological function (water use)?; and 3) How variable are functional traits

among green alder individuals and is this variability attributable to shrub distribution along topographic and resource gradients?

Green alder water use was quantified through measurements of stem water potential and sap flow. Stem water potential provides a measurement of water stress experienced by an individual (McCutchan & Shackel, 1992) and thus allowed us to determine seasonal and topographic variation in water limitations experienced by green alders during the growing season. Sap flow is defined as the movement of water and minerals through the conducting tissue of a plant (Kramer & Boyer, 1995) and is an indication of transpiration (Swanson, 1994), thereby providing insight into shrub water use and physiological function. We scaled estimates of stem sap flow per shrub to green alder patch water fluxes so that estimates of shrub patch transpiration can be incorporated into hydrological models predicting the impacts of tundra shrubbing. Metrics of water availability (surface soil moisture and frost table depth) and nutrient availability (soil inorganic nutrients, leaf nitrogen concentration, and frost table depth) and topographic position were used to predict sap flow to determine which abiotic factors drive green alder water use and physiological function. Functional traits allow us to understand trade-offs that determine ecological strategies as well as identify attributes of plants that are responsible for those trade-offs, thus providing information about the causal mechanisms of plant distribution and function (Reich, 2014). We used functional traits associated with water and nutrient use to determine whether green alders in downslope locations of shrub patches utilize resource strategies associated with higher resource environments and productivity relative to upslope locations.

We expect there to be a gradient in water and nutrient availability that corresponds with the topography of green alder patches. Downslope locations should have higher resource availability than upslope locations due to the downslope movement of water and nutrients along water tracks and greater capture of snow in channels and on hill slopes (with aspects and slopes that lead to deposition) due to the distribution of snow by prevailing winds. Green alders in downslope locations should therefore have functional traits that are associated with higher resource availability and productivity compared to upslope locations. We hypothesize that water availability will be the main driver of green alder physiological function (sap flow) since alders should have a direct nutrient source from their N-fixing symbiont. This study was performed during the summers of 2015 and 2016 at Trail Valley Creek (TVC) in the Northwest Territories (68º44'N, 133º30'W).

1.9 Thesis overview

The first chapter of this thesis is a general introduction to climate warming in the Arctic, climate warming-induced tundra shrub expansion, and the implications of shrub expansion. This information provides the broader subject matter and background necessary to understand the more succinct introduction in the manuscript of Chapter 2. This chapter also includes a detailed section on what is currently known about green alder, which is the study species used for the manuscript in Chapter 2. I then provide the study aim and hypotheses but further support and reasoning for these can be found in the introduction in the manuscript of Chapter 2.

The second chapter has been formatted in preparation for submission as a manuscript to *Global Change Biology*. This manuscript is co-authored by my M.Sc.

supervisor, Dr. Jennifer Baltzer. My role in the manuscript involved co-development of the study design, all data collection, data analyses, and development and revision of the manuscript. This manuscript answers the research questions outlined in section 1.8.

The third and final chapter acts as a general discussion, which includes a summary of the main research findings, collaboration involved in this work (in the context of integrative biology), and future research regarding this work.

1.10 References

ACIA (2004) *Impacts of a Warming Arctic: Arctic Climate Impact Assessment*. Cambridge University Press, Cambridge, UK.

Anthelme F, Grossi JL, Brun J, Didier L (2001) Consequences of green alder expansion on vegetation changes and arthropod communities removal in the northern French Alps. *Forest Ecology and Management*, **145**, 57–65.

Anthelme F, Cornillon L, Brun J (2002) Seconday succession of *Alnus viridis* (Chaix) DC. in Vanoise National Park, France: Coexistence of sexual and vegetative strategies. *Annals of Forest Science*, **59**, 419–428.

Anthelme F, Villaret J, Brun J (2007) Shrub encroachment in the Alps gives rise to the convergence of sub-alpine communities on a regional scale. *Journal of Vegetation Science*, **18**, 355–362.

Bassin S, Volk M, Fuhrer J (2013) Species composition of subalpine grassland is sensitive to nitrogen deposition, but not to ozone, after seven years of treatment. *Ecosystems*, **16**, 1105–1117.

Benecke U (1970) Nitrogen fixation by *Alnus viridis*. *Plant and Soil*, **33**, 30–48.

Benninghoff WS (1952) Interaction of vegetation and soil frost phenomena. *Arctic*, **5**, 34–44.

Bissonnette C, Fahlman B, Peru KM, Khasa DP, Greer CW, Headley JV, Roy S (2014) Symbiosis with *Frankia* sp. benefits the establishment of *Alnus viridis* ssp. *crispa* and *Alnus incana* ssp. *rugosa* in tailings sand from the Canadian oil sands industry. *Ecological Engineering*, **68**, 167–175.

Blok D, Heijmans MMPD, Schaepman-Strub G, Kononov AV, Maximov TC, Berendse F (2010) Shrub expansion may reduce summer permafrost thaw in Siberian tundra. *Global Change Biology*, **16**, 1296–1305.

Blok D, Sass-Klaassen U, Schaepman-Strub G, Heijmans MMPD, Sauren P, Berendse F (2011) What are the main climate drivers for shrub growth in northeastern Siberian tundra? *Biogeosciences*, **8**, 1169–1179.

Bonfils CJW, Phillips TJ, Lawrence DM, Cameron-Smith P, Riley WJ, Subin ZM (2012) On the influence of shrub height and expansion on northern high latitude climate. *Environmental Research Letters*, **7**, 1-9. DOI: 10.1088/1748-9326/7/1/015503.

Boscutti F, Poldini L, Buccheri M (2014) Green alder communities in the Alps: Phytosociological variability and ecological features. *Plant Biosystems*, **148**, 917–934.

Bowman WD, Conant RT (1994) Shoot growth dynamics and photosynthetic response to increased nitrogen availability in the alpine willow *Salix glauca*. *Oecologia*, **97**, 93–99.

Bühlmann T, Körner C, Hiltbrunner E (2016) Shrub expansion of *Alnus viridis* drives former montane grassland into nitrogen saturation. *Ecosystems*, **19**, 968–985.

Cameron EA, Lantz TC (2016) Drivers of tall shrub proliferation adjacent to the Dempster Highway, Northwest Territories, Canada. *Environmental Research Letters*, **11**, 1-11. DOI: 10.1088/1748-9326/11/4/045006.

Chaia EE, Wall LG, Huss-Danell K (2010) Life in soil by the actinorhizal root nodule endophyte *Frankia*: A review. *Symbiosis*, **51**, 201–226.

Chapin FS (1983) Direct and indirect effects of temperature on arctic plants. *Polar Biology*, **2**, 47–52.

Chapin FS, Fetcher N, Kielland K, Everett KR, Linkins AE (1988) Productivity and nutrient cycling of Alaskan tundra: Enhancement by flowing soil water. *Ecology*, **69**, 693–702.

Chapin FS, Shaver GR, Giblin A, Nadelhoffer K, Laundre J (1995) Responses of arctic tundra to experimental and observed changes in climate. *Ecology*, **76**, 694–711.

Chapin FS, Sturm M, Serreze MC et al. (2005) Role of land-surface changes in arctic summer warming. *Science*, **310**, 657–660.

Comiso JC (2006) Arctic warming signals from satellite observations. *Weather*, **61**, 70–76.

Elmendorf SC, Henry GHR, Hollister RD et al. (2012) Plot-scale evidence of tundra vegetation change and links to recent summer warming. *Nature Climate Change*, **2**, 453–457.

Endrizzi S, Marsh P (2010) Observations and modeling of turbulent fluxes during melt at the shrub-tundra transition zone 1: Point scale variations. *Hydrology Research*, **41**, 471–491.

Epstein HE, Beringer J, Gould WA et al. (2004) The nature of spatial transitions in the Arctic. *Journal of Biogeography*, **31**, 1917–1933.

Epstein HE, Myers-Smith IH, Walker DA (2013) Recent dynamics of arctic and sub-arctic vegetation. *Environmental Research Letters*, **8**, 1-6. DOI: 10.1088/1748-9326/8/1/015040.

Essery R, Li L, Pomeroy J (1999) A distributed model of blowing snow over complex terrain. *Hydrological Processes*, **13**, 2423–2438.

Forbes BC, Fauria MM, Zetterberg P (2010) Russian Arctic warming and "greening" are closely tracked by tundra shrub willows. *Global Change Biology*, **16**, 1542–1554.

Francis JA, Vavrus SJ (2012) Evidence linking arctic amplification to extreme weather in mid-latitudes. *Geophysical Research Letters*, **39**, 1–6.

Fraser RH, Lantz TC, Olthof I, Kokelj SV, Sims RA (2014) Warming-induced shrub expansion and lichen decline in the western Canadian Arctic. *Ecosystems*, **17**, 1151–1168.

Haag RW (1974) Nutrient limitations to plant production in two tundra communities. *Canadian Journal of Botany*, **52**, 103–116.

Hallinger M, Manthey M, Wilmking M (2010) Establishing a missing link: Warm summers and winter snow cover promote shrub expansion into alpine tundra in Scandinavia. *New Phytologist*, **186**, 890–899.

Hastings SJ, Luchessa SA, Oechel WC, Tenhunen JD (1989) Standing biomass and production in water drainages of the foothills of the Philip Smith Mountains, Alaska. *Holarctic Ecology*, **12**, 304–311.

Hiltbrunner E, Aerts R, Bühlmann T et al. (2014) Ecological consequences of the expansion of N_2-fixing plants in cold biomes. *Oecologia*, **176**, 11–24.

Hinkel KM, Paetzold F, Nelson FE, Bockheim JG (2001) Patterns of soil temperature and moisture in the active layer and upper permafrost at Barrow, Alaska: 1993–1999. *Global and Planetary Change*, **29**, 293–309.

Hinzman LD, Bettez ND, Bolton WR et al. (2005) Evidence and implications of recent climate change in northern Alaska and other arctic regions. *Climatic Change*, **72**, 251–298.

Hobbie SE, Chapin FS (1998) An experimental test of limits to tree establishment in arctic tundra. *Journal of Ecology*, **86**, 449–461.

Hurd T, Raynal D, Schwintzer C (2001) Symbiotic N_2 fixation of *Alnus incana* ssp. *rugosa* in shrub wetlands of the Adirondack Mountains, New York, USA. *Oecologia*, **126**, 94–103.

IPCC (2013) *Climate Change 2013: The Physical Science Basis*. Cambridge University Press, Cambridge.

Johnstone JF, Kokelj SV (2008) Environmental conditions and vegetation recovery at abandoned drilling mud sumps in the Mackenzie Delta region, Northwest Territories, Canada. *Arctic*, **61**, 199–211.

Kaplan JO, New M (2006) Arctic climate change with a 2˚C global warming: Timing, climate patterns and vegetation change. *Climatic Change*, **79**, 213–241.

Kemper JT, Macdonald SE (2009) Directional change in upland tundra plant communities 20-30 years after seismic exploration in the Canadian low-Arctic. *Journal of Vegetation Science*, **20**, 557–567.

Keuper F, van Bodegom PM, Dorrepaal E, Weedon JT, van Hal J, van Logtestijn RSP, Aerts R (2012a) A frozen feast: Thawing permafrost increases plant-available nitrogen in subarctic peatlands. *Global Change Biology*, **18**, 1998–2007.

Keuper F, Parmentier FJW, Blok D et al. (2012b) Tundra in the rain: Differential vegetation responses to three years of experimentally doubled summer precipitation in Siberian shrub and Swedish bog tundra. *Ambio*, **41**, 269–280.

Lantz TC, Kokelj SV (2008) Increasing rates of retrogressive thaw slump activity in the

Mackenzie Delta region, N.W.T., Canada. *Geophysical Research Letters*, **35**, 1–5.

Lantz TC, Kokelj SV, Gergel SE, Henry GHR (2009) Relative impacts of disturbance and temperature: Persistent changes in microenvironment and vegetation in retrogressive thaw slumps. *Global Change Biology*, **15**, 1664–1675.

Lantz TC, Gergel SE, Henry GHR (2010) Response of green alder (*Alnus viridis* subsp. *fruticosa*) patch dynamics and plant community composition to fire and regional temperature in north-western Canada. *Journal of Biogeography*, **37**, 1597–1610.

Lantz TC, Marsh P, Kokelj SV (2013) Recent shrub proliferation in the Mackenzie Delta Uplands and microclimatic implications. *Ecosystems*, **16**, 47–59.

Lawrence DM, Swenson SC (2011) Permafrost response to increasing arctic shrub abundance depends on the relative influence of shrubs on local soil cooling versus large-scale climate warming. *Environmental Research Letters*, **6**, 1-8. DOI: 10.1088/1748-9326/6/4/045504.

Loranty MM, Goetz SJ (2012) Shrub expansion and climate feedbacks in arctic tundra. *Environmental Research Letters*, **7**, 1-3. DOI: 10.1088/1748-9326/7/1/011005.

Mack MC, Bret-Harte MS, Hollingsworth TN, Jandt RR, Schuur EAG, Shaver GR, Verbyla DL (2011) Carbon loss from an unprecedented arctic tundra wildfire. *Nature*, **475**, 489–92.

Marsh P, Pomeroy J (1996) Meltwater fluxes at an arctic forest-tundra site. *Hydrological Processes*, **10**, 1383–1400.

Marsh P, Pomeroy J, Pohl S (2008) Snowmelt processes and runoff at the arctic treeline: Ten years of MAGS research. In Cold Regions Atmospheric and Hydrologic Studies (Woo M). pp. 97-123. Berlin, Heidelberg: Springer.

Marsh P, Bartlett P, MacKay M, Pohl S, Lantz TC (2010) Snowmelt energetics at a shrub tundra site in the western Canadian Arctic. *Hydrological Processes*, **24**, 3603–3620.

Matthes-Sears U, Matthes-Sears WC, Hastings SJ, Oechel WC (1988) The effects of topography and nutrient status on the biomass, vegetative characteristics, and gas exchange of two deciduous shrubs on an arctic tundra slope. *Arctic and Alpine Research*, **20**, 342–351.

McCutchan H, Shackel K (1992) Stem-water potential as a sensitive indicator of water stress in prune trees (*Prunus domestica* L. cv. French). *Journal of the American Society for Horticultural Science*, **117**, 607–611.

Mejstrik V, Benecke U (1969) The ectotrophic mycorrhizas of *Alnus viridis* (Chaix) DC and their significance in respect to phosphorus uptake. *New Phytologist*, **68**, 141–149.

Mitchell JS, Ruess RW (2009) N_2 fixing alder (*Alnus viridis* spp. *fruticosa*) effects on soil properties across a secondary successional chronosequence in interior Alaska. *Biogeochemistry*, **95**, 215–229.

Myers-Smith IH, Hik DS (2013) Shrub canopies influence soil temperatures but not nutrient dynamics: An experimental test of tundra snow-shrub interactions. *Ecology and Evolution*, **3**, 3683–3700.

Myers-Smith IH, Forbes BC, Wilmking M et al. (2011) Shrub expansion in tundra ecosystems: Dynamics, impacts and research priorities. *Environmental Research Letters*, **6**, 1–15.

Myrold DD, Huss-Danell K (2003) Alder and lupine enhance nitrogen cycling in a degraded forest soil in northern Sweden. *Plant and Soil*, **254**, 47–56.

Naito AT, Cairns DM (2011) Relationships between arctic shrub dynamics and topographically derived hydrologic characteristics. *Environmental Research Letters*, **6**, 1-8. DOI:10.1088/1748-9326/6/4/045506.

Patankar R, Quinton WL, Hayashi M, Baltzer JL (2015) Sap flow responses to seasonal thaw and permafrost degradation in a subarctic boreal peatland. *Trees*, **29**, 129–142.

Pearson RG, Phillips SJ, Loranty MM, Beck PSA, Damoulas T, Knight SJ, Goetz SJ (2013) Shifts in arctic vegetation and associated feedbacks under climate change. *Nature Climate Change*, **3**, 673–677.

Reich PB (2014) The world-wide "fast-slow" plant economics spectrum: A traits manifesto. *Journal of Ecology*, **102**, 275–301.

Rhoades C, Oskarsson H, Binkley D, Stottlemyer B (2001) Alder (*Alnus crispa*) effects on soils in ecosystems of the Agashashok River valley, northwest Alaska. *Ecoscience*, **8**, 89–95.

Rupp TS, Chapin FS, Starfield AM (2001) Modeling the influence of topographic barriers on treeline advance at the forest-tundra ecotone in northwest Alaska. *Climatic Change*, **48**, 399–416.

Rustad LE, Campbell JL, Marion GM et al. (2001) A meta-analysis of the response of soil respiration, net nitrogen mineralization, and aboveground plant growth to experimental ecosystem warming. *Oecologia*, **126**, 543–562.

Screen JA, Simmonds I (2010) The central role of diminishing sea ice in recent arctic temperature amplification. *Nature*, **464**, 1334–1337.

Serreze MC, Walsh JE, Chapin FS et al. (2000) Observational evidence of recent change in the northern high-latitude environment. *Climatic Change*, **46**, 159–207.

Serreze MC, Barrett AP, Stroeve JC, Kindig DN, Holland MM (2009) The emergence of surface-based arctic amplification. *The Cryosphere*, **2**, 601–622.

Shaver GR, Chapin FS (1980) Response to fertilization by various plant growth forms in an Alaskan tundra: Nutrient accumulation and growth. *Ecology*, **61**, 662–675.

Shaver GR, Chapin FS (1986) Effect of fertilizer on production and biomass of tussock tundra, Alaska, U.S.A. *Arctic and Alpine Research*, **18**, 261–268.

Sørensen R, Zinko U, Seibert J (2006) On the calculation of the topographic wetness

index: Evaluation of different methods based on field observations. *Hydrological Earth Systems Sciences*, **10**, 101–112.

Sturm M, Racine C, Tape KD (2001a) Increasing shrub abundance in the Arctic. *Nature*, **411**, 546–547.

Sturm M, McFadden JP, Liston GE, Chapin FS, Racine CH, Holmgren J (2001b) Snow–shrub interactions in arctic tundra: A hypothesis with climatic implications. *Journal of Climate*, **14**, 336–344.

Sturm M, Douglas T, Racine C, Listen GE (2005a) Changing snow and shrub conditions affect albedo with global implications. *Journal of Geophysical Research*, **110**, 1–13.

Sturm M, Schimel J, Michaelson G et al. (2005b) Winter biological processes could help convert arctic tundra to shrubland. *BioScience*, **55**, 17.

Swann AL, Fung IY, Levis S, Bonan GB, Doney SC (2010) Changes in arctic vegetation amplify high-latitude warming through the greenhouse effect. *Proceedings of the National Academy of Sciences*, **107**, 1295–1300.

Swanson RH (1994) Significant historical developments in thermal methods for measuring sap flow in trees. *Agricultural and Forest Meteorology*, **72**, 113–132.

Swanson FJ, Kratz TK, Caine N, Woodmansee RG (1988) Landform effects on ecosystem patterns and processes. *BioScience*, **38**, 92–98.

Tape KD, Sturm M, Racine C (2006) The evidence for shrub expansion in northern Alaska and the pan-Arctic. *Global Change Biology*, **12**, 686–702.

Tape KD, Verbyla D, Welker JM (2011) Twentieth century erosion in arctic Alaska foothills: The influence of shrubs, runoff, and permafrost. *Journal of Geophysical Research: Biogeosciences*, **116**, 1–11.

Tape KD, Hallinger M, Welker JM, Ruess RW (2012) Landscape heterogeneity of shrub expansion in arctic Alaska. *Ecosystems*, **15**, 711–724.

Theodose TA, Bowman WD (1997) Nutrient availability, plant abundance, and species diversity in two alpine tundra communities. *Ecology*, **78**, 1861–1872.

Wahren CHA, Walker MD, Bret-Harte MS (2005) Vegetation responses in Alaskan arctic tundra after 8 years of a summer warming and winter snow manipulation experiment. *Global Change Biology*, **11**, 537–552.

Walker MD, Wahren CHA (2006) Plant community responses to experimental warming across the tundra biome. *Proceedings of the National Academy of Sciences*, **103**, 1342–1346.

Wiedmer E, Senn-Irlet B (2006) Biomass and primary productivity of an *Alnus viridis* stand - A case study from the Schächental valley, Switzerland. *Botanica Helvetica*, **116**, 55–64.

Winship L, Tjepkema J (1985) Nitrogen fixation and respiration by root nodules of *Alnus rubra* Bong.: Effects of temperature and oxygen concentration. *Plant and Soil*, **87**, 91–107.

1.11 Figures

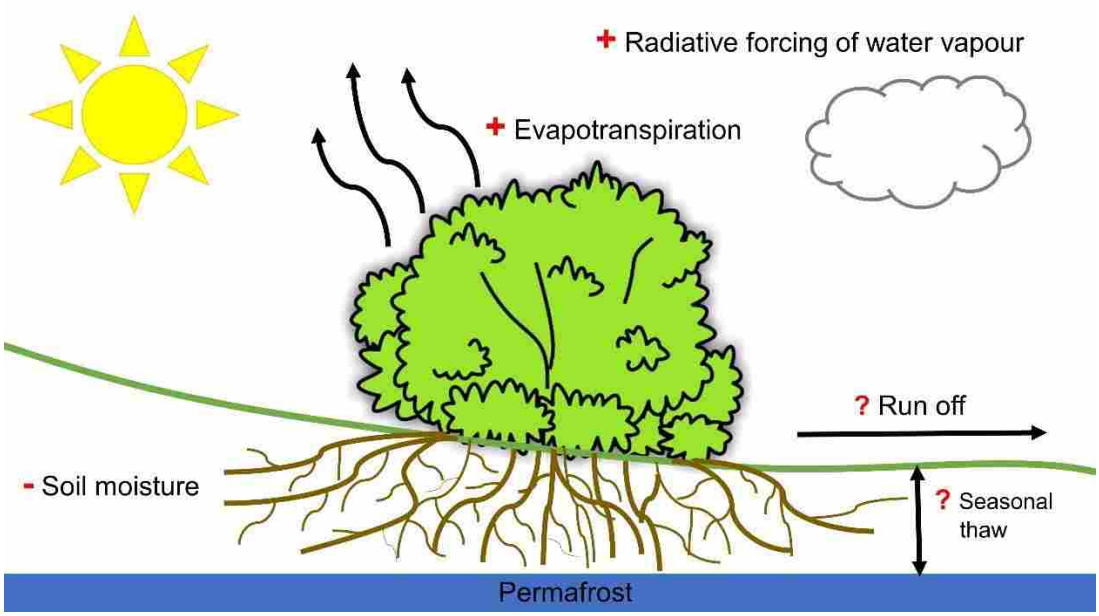

Fig. 3.1: Schematic diagram representing the potential implications of increased shrub evapotranspiration on tundra surface hydrology and permafrost dynamics during the growing season. Plus signs (+) represent an increase, minus signs (-) represent a decrease, and question marks (?) represent unknown directionality.

Fig. 1.2: Photographs showing tundra shrubs growing along water tracks on hill slopes. Photos were taken within the Trail Valley Creek research basin on the low arctic tundra of the Northwest Territories. Dark shrub canopies in water tracks at this site are mainly composed of green alder, willow, and dwarf birch. The top photo is courtesy of W. Woodley and the bottom photo is courtesy of J. Rabley.

Fig. 1.3: Photographs of green alder in the Trail Valley Creek research basin on the low arctic tundra of the Northwest Territories.

Fig. 1.4: Photograph of nitrogen-fixing *Frankia* nodules on green alder roots collected within the Trail Valley Creek research basin on the low arctic tundra of the Northwest Territories. Photo courtesy of J. Rabley.

Chapter 2: Topography determines green alder functional traits and water potential but not sap flow on the low arctic tundra, NT

In preparation for *Global Change Biology*

Title: Topography determines green alder functional traits and water potential but not sap flow on the low arctic tundra, NT

Running head: Topography drives alder functional traits

List of authors: Katherine L. Black and Jennifer L. Baltzer

Institute of origin: Department of Biology, Wilfrid Laurier University, Waterloo, Ontario, Canada, N2L 3C5

Corresponding author:
Jennifer Baltzer
Department of Biology
Waterloo, ON
N2L 3C5
Email: jbaltzer@wlu.ca
Telephone: (519) 884-0710 ext. 4188

Keywords: tundra shrub expansion, *Alnus viridis*, transpiration, abiotic limitations, functional traits, resource availability, frost table depth, climate warming

Type of paper: Primary research article

2.1 Abstract

Climate warming is driving the expansion of shrubs across the tundra biome with implications for further regional warming and increased shrub productivity. To make predictions about the consequences of shrub expansion, it is necessary to understand the abiotic factors that constrain shrub physiological function and distribution. Shrubs are preferentially expanding in areas that have a higher potential of accumulating moisture, such as hill slopes and drainage channels. We hypothesize that shrub function and distribution are limited by the availability of water and nutrients across topographic gradients. Nevertheless, the associations between shrub function, distribution, and abiotic limitations remain understudied. We measured sap flow, stem water potential, and a range of functional traits of green alder (*Alnus viridis*) shrubs and quantified water and nutrient availability in shrub patches on the low arctic tundra of the Northwest Territories. Thaw depth was a significant negative driver of sap flow and is linked with water limitations. Topographic position was not strongly associated with sap flow but it did determine stem water potential and leaf functional traits. Shrubs in downslope locations had significantly higher water potentials than upslope locations suggesting greater water limitation in upslope positions. Channel shrubs reflected traits associated with higher resource environments and greater productivity and growth relative to the slower-return strategy of shrubs at the tops of patch slopes. We offer estimates of seasonal variation in green alder sap flow and green alder patch transpiration supporting incorporation of shrub water use estimates into models predicting the magnitude and impacts of tundra shrubbing on evapotranspiration. Green alder is expanding rapidly across the low arctic tundra of the Northwest Territories and understanding the drivers of its expansion is essential for predicting future tundra conditions.

2.2 Introduction

A significant increase in shrub cover is occurring across the tundra biome due to rapid climate warming (e.g., Sturm *et al.*, 2001a; Forbes *et al.*, 2010). Evidence of shrub expansion has been documented through remote sensing techniques (Fraser *et al.*, 2014), fine-scale mapping (Lantz *et al.*, 2013), ground studies involving naturally- and experimentally-warmed plots (Chapin *et al.*, 1995; Elmendorf *et al.*, 2012), and dendrochronological assessments (Myers-Smith *et al.*, 2015). Tundra shrub expansion is projected to continue at an accelerating rate and is expected to have profound implications for tundra ecosystems mainly due to changes in albedo and evapotranspiration, which will likely result in an overall positive feedback to regional warming and shrub productivity (Bonfils *et al.*, 2012).

To accurately predict the consequences of shrub expansion it is necessary to understand the abiotic factors that constrain shrub distribution and physiological function on a landscape scale. Shrub expansion has occurred primarily in areas that have a higher potential of accumulating and draining moisture, such as drainage channels and the slopes and toes of hills (Naito & Cairns, 2011; Tape *et al.*, 2006, 2012). This spatial heterogeneity in shrub distribution suggests that water availability, and other features associated with the movement of water downslope and within basins, is a primary factor limiting shrub expansion. However, other studies suggest that shrub productivity in tundra ecosystems is limited primarily by nutrient rather than moisture availability (e.g., Chapin *et al.*, 1995; Keuper *et al.*, 2012a).

It is possible that topographic features, water availability, and nutrient availability interact to influence tundra shrub function. High soil water content in catchments is often

associated with nutrient availability due to the lateral transport of nutrients to plant roots in water and the increased solubility of nutrients for uptake by plants (Chapin *et al.*, 1988; Matthes-Sears *et al.*, 1988). Water flow downslope and within drainage basins not only transports nutrients but also increases active layer thickness, potentially providing shrub roots a larger volume of soil for nutrient and water acquisition (Hastings *et al.*, 1989; Ostendorf & Reynolds, 1993). The high thermal conductivity of water may cause an increase in soil heat flux in moist tundra sites which could promote root growth and nutrient uptake for a longer period during the growing season (Chapin *et al.*, 1988). This increased heat flux and soil warming could also enhance microbial activity and thus nitrogen mineralization (Chapin *et al.*, 1988; Hastings *et al.*, 1989). Therefore, productivity and nutrient cycling rates are suggested to be greater in tundra landscape positions with high water content and drainage, which, as described above, are the main sites of shrub expansion. In addition, more snow is captured in channels and on hill slopes (with aspects and slopes that lead to snow deposition) compared to plateaux due to the distribution of snow by prevailing winds (P. Marsh, unpublished data). This may result in increased nitrogen mineralization in shrub patches through warmer subnivean temperatures as hypothesized by Sturm *et al.* (2001b, 2005b) and higher water and nutrient deposition in these areas via snowmelt (Bowman, 1992).

Despite clear evidence of resource availability as a driver of shrub distribution and expansion on the low arctic tundra, the associations between tundra shrub function, distribution, and abiotic limitations remain understudied. Many studies discuss the potential implications of shrub expansion, such as increased evapotranspirative water loss and the subsequent increase in regional warming (e.g., Swann *et al.*, 2010; Bonfils *et al.*,

2012) but direct measurements of shrub function are limited. An excellent approach to understanding the causal mechanisms of plant distribution and function is using plant functional traits because they allow us to understand trade-offs that determine ecological strategies and identify traits of plants that are responsible for those trade-offs (Reich, 2014). Ecologists have recently been utilizing an integrative approach to understand plant water transport by incorporating the measurement of several leaf and stem traits (Apgaua *et al.*, 2015; Worbes *et al.*, 2013). Water transport can be quantified through measurements of stem sap flow which is an indication of transpiration and thus productivity (Swanson, 1994). Leaf and stem functional traits encompass morphological and physiological features that regulate the ecological functioning of an individual (Pérez-Harguindeguy *et al.*, 2013). *In situ* measurements of functional traits can capture both local adaptation and plastic responses to variation in resource availability (Willson *et al.*, 2008; Paquette *et al.*, 2015) and thus are useful for understanding spatial heterogeneity in plant distribution and function along resource gradients (McGill *et al.*, 2006; Westoby & Wright, 2006).

The aim of this study was to improve our understanding of tundra shrub function by answering the following questions: 1) How much water do tundra shrubs use?; 2) How do topography and associated gradients in water and nutrient availability influence tundra shrub water use?; and 3) How variable are functional traits among individual shrubs and is this variability attributable to shrub location along topographic and/or resource gradients?

To address these questions, we measured sap flow, stem water potential, and a range of foliar and whole-plant functional traits of green alder (*Alnus viridis* ssp.

fruticosa) shrubs during the growing seasons of 2015 and 2016 on the low arctic tundra of the Northwest Territories. We scaled estimates of stem sap flow to green alder patch transpiration to support the incorporation of shrub water use estimates into models predicting the magnitude and impacts of tundra shrubbing on evapotranspiration. To understand variation in resource availability, we quantified water and nutrient availability along toposequences within green alder patches. Green alder is one of the tallest shrub species undergoing expansion (ranging from 1-4 m in height) and therefore may have the greatest impact on tundra ecosystems in terms of canopy size effects (e.g., shading, albedo, litter input, and snow capture) and water use. Green alder has the capacity to access atmospheric nitrogen as a result of a symbiotic relationship with the nitrogen-fixing actinomycete *Frankia* (Benecke, 1970), and thus may have a different functional response to abiotic limitations compared to other shrub species that are more commonly studied, such as *Betula* and *Salix* spp. Understanding the drivers of tundra shrub function is critical for understanding feedbacks of changing resource availability on shrub function and how shrubs may respond to future warming.

2.3 Methods

2.3.1 Study site

Trail Valley Creek (TVC; 68º44'N, 133º30'W) is located approximately 50 km north-northeast of Inuvik, Northwest Territories, Canada (Marsh & Pomeroy, 1999). The TVC watershed is 57 km^2 in area, underlain by continuous permafrost, and characterized by rolling hills, deeply incised river valleys, and small lakes (Pomeroy *et al.*, 1997; Marsh *et al.*, 2008). Situated at the northern edge of the boreal forest, TVC is part of the forest-tundra ecotone, with graminoids, lichens, mosses, and low-growing woody

vegetation (e.g., *Vaccinium uliginosum*, *Rhododendron groenlandicum*) dominating the upland vegetation. There are sparse stands of white spruce (*Picea glauca*) and black spruce (*P. mariana*) throughout the southern part of the basin. Moist hill slopes, valley bottoms, and drainage channels are dominated by green alder, willow (*Salix glauca* and *S. pulchra*), and dwarf birch (*Betula glandulosa*). The soils are organic cryosols consisting of an upper peat layer (0.5 cm to 34 cm) underlain by a mineral, silty clay soil (C. Wallace, unpublished data). The microtopography of TVC consists of mineral earth hummocks created by frost heave and cryoturbation and peat-dominated interhummocks.

The climate is characterized by short summers with a mean daily temperature of 9.3°C (May-August, 1981-2006), long, cold winters with an average daily temperature of -17°C (September-April, 1981-2006) and a mean annual air temperature of -8.2°C (1981-2006; Environment and Climate Change Canada (ECCC), 2011). The mean annual rainfall and snowfall is 114.5 mm and 158.6 cm, respectively (1981-2003; ECCC, 2011). The mean air temperatures during the study periods were 11.2°C for 2015 (study period: June 11-August 22; range: 0.2°C to 27.2°C) and 11.7°C for 2016 (study period: June 6-August 19; range: -2.5°C to 30.1°C; P. Marsh, unpublished data). Total rainfall during the study periods was 67.4 mm and 85.2 mm for 2015 and 2016, respectively (P. Marsh, unpublished data).

2.3.2 Green alder patch selection

Green alder patches were selected using high-resolution orthoimagery collected during the summer of 2004 (GNWT Centre for Geomatics, Mackenzie Valley OrthoPhoto Cached Mosaic Service, copyright material used with the permission of the GNWT). Patches were defined from imagery as clusters of green alders on slopes

surrounded by ‘open’ tundra. Patches were on approximately south-facing slopes, spanned continuously from the plateau at the top of a hill, down to the bottom of the slope or drainage channel, and they were within 2 km of the TVC research station due to logistical considerations. Eight patches were selected for the 2015 growing season and three of these patches were more intensively studied during the 2016 growing season. Patch slopes ranged from 1.4° to 5.7° and ranged from 44 m to 175 m in length from top to bottom (or drainage channel, if present; see below).

2.3.3 Green alder selection

Within each patch, a single transect was established from the top plateau of the patch downslope to the bottom of the hill or drainage channel. Along this transect, the nearest healthy green alder that had stems that reached 4-6 cm in basal diameter was selected at each of the following topographic positions: a) the plateau at the top of the hill, b) the middle of the hill slope, c) the bottom of the hill slope, and, when present, d) a drainage channel (Fig. 2.1). Topographic positions a) through c) were determined using the length and slope information of each patch. Drainage channels were defined as areas of standing or flowing water extending out from the bottom of a patch. Twenty-seven individuals were studied during the 2015 growing season and 28 individuals during the 2016 growing season (Table S1; Fig. S1).

2.3.4 Sap flow

We measured sap flow of all study shrubs. Sap flow was measured continuously from early June to late August of each year using automated Heat Ratio Method (HRM) sap flow meters (SFM1 Sap Flow Meters, ICT International, Armidale, NSW, AU). Sap flow meters were set to make measurements every 30 minutes in 2015 and every 15

minutes in 2016. Meters were installed at the base of one 4-6 cm diameter stem per shrub (hereafter referred to as 'instrumented shrubs') to avoid size-related biases in sapwood area and sap flow estimates (see below). The HRM sap flow meters have two temperature needles that are inserted into the xylem tissue to measure a temperature pulse from a heat pulse needle inserted equidistant between the upstream and downstream temperature needles (Burgess *et al.*, 2001). A short pulse of heat is used as a tracer in the sap during each measurement interval (Smith & Allen, 1996; 40 J pulses) and the ratio of the difference in temperature between the two temperature needles provides the sap velocity (Burgess *et al.*, 2001) calculated as (Marshall, 1958):

$$V_h = \frac{k}{x} \, ln\left(\frac{v_1}{v_2}\right) 3600 \qquad (1)$$

where k is the thermal diffusivity of fresh wood (2.5×10^{-3} $cm^2 \cdot s^{-1}$), x is the distance between the heat pulse needle and either temperature needle (0.6 cm), and v_1 and v_2 are increases in temperature (from initial temperatures; °C) at the two temperature needles equidistant from the heat pulse needle. Multiplying by 3600 converts V_h to $cm \cdot h^{-1}$. Volumetric sap flow ($cm^3 \cdot h^{-1}$) was derived by multiplying V_h by the cross-sectional area of conducting sapwood (Burgess *et al.*, 2001). To quantify sapwood area, a stem cross-section was removed from the location of instrumentation on each instrumented shrub when meters were uninstalled each year. The sapwood-heartwood boundary of green alders is indistinguishable and so this boundary was determined in the field during the 2016 growing season by observing differences in stain uptake (over-the-counter betadine solution) in fresh stem cross-sections. Measurements of stem diameter, bark thickness, sapwood thickness, and heartwood diameter at four points around each stem cross-section were used to compute sapwood area. Sapwood area was estimated for stem cross-sections

collected during the 2015 growing season using a linear regression between stem diameter and sapwood thickness for the 2016 stem cross-sections (Fig. S2; $R^2 = 0.51$, $p < 0.001$). ICT HRM meters have two thermistors along each needle (7.5 mm, 22.5 mm); due to the relatively small diameter (4.21 cm ± 0.08 cm standard error) and therefore small sapwood thickness (0.98 cm ± 0.04 cm) of the instrumented stems, we used data from the outer thermistors for sap flow calculations since the inner thermistors were often installed in heartwood. Conversion of sap velocities to mass flows was performed using Sap Flow Tool software (v. 1.5.0 beta 1, ICT International). We confirmed that sapwood area did not differ among topographic positions using an ANOVA (2015: $F_{3,19} = 0.788$, $p = 0.515$; 2016: $F_{3,23} = 0.283$, $p = 0.837$) as topographic differences in sapwood area could drive topographic differences in sap flow.

2.3.5 Upscaling stem-level sap velocity to shrub patch water flux

We scaled single stem V_h estimates ($cm \cdot day^{-1}$) of shrubs to green alder patch water fluxes ($mm \cdot day^{-1}$) to support comparison to literature values of tundra evapotranspiration. V_h was converted to sap flow density (J_s; $kgH_2O \cdot m^{-2}$ sapwood$\cdot day^{-1}$) by multiplying V_h by the density of water, assuming one unit of sapwood area and water density was equal to 1000 $kg \cdot m^{-3}$ (note: $kgH_2O\ m^{-2} = mm$). Green alder patch transpiration was calculated using the following equation:

$$T_{patch} = J_s \left(\frac{(N_{shrubs})(N_{stems})(SA)}{PA} \right) \quad (2)$$

where N_{shrubs} is the number of green alders in a patch, N_{stems} is the mean number of stems per green alder, SA is the mean sapwood area per stem, and PA is the area of a patch. N_{shrubs} and PA were obtained from green alder patch maps of 10 patches in the TVC research basin (C. Wallace, unpublished data; mean number of shrubs per patch = 74 ±

11). N_{stems} was determined by averaging the number of green alder stems in 20 photos of instrumented shrubs taken during the 2015 and 2016 growing seasons (mean number of stems per shrub = 18 ± 2.5). *SA* was calculated by averaging sapwood area of all instrumented stems across both study years (mean sapwood area = 9.48 cm^2 ± 0.48 cm^2). We made the assumption that all shrubs across patches were similar in size and had a similar number of stems and sapwood area as instrumented shrubs.

2.3.6 Stem water potential

To investigate variation in shrub water status among topographic positions, we measured midday stem water potential (Ψ_{stem}) using a pressure chamber (Model 1000 Pressure Chamber Instruments, PMS Instrument Company, Albany, NY, USA). Midday measurements provide an estimate of maximum water stress (Williams & Araujo, 2002). To avoid destructive sampling of instrumented shrubs, non-instrumented shrubs at one patch proximal to camp were haphazardly selected such that 3-4 individuals were measured in each of the four described topographic positions (Table S2). Shrubs selected for Ψ_{stem} measurements were similar in apparent health and size to instrumented shrubs. At each shrub selected for Ψ_{stem} measurements, three stems less than 3 mm in diameter (so that stems were contiguous with the gasket in the pressure chamber) with 4-6 green, healthy leaves were haphazardly selected, removed with a razor blade, and measured according to instrument protocols (Model 1000 Pressure Chamber Instrument Operating Instructions, PMS Instrument Company). Ψ_{stem} was measured on sunny days that did not have rainfall 24 hours prior. Ψ_{stem} was measured on June 18, July 26, and August 21 in 2015 to capture seasonal variation in water status and on August 9 in 2016 (only one measurement period due to logistical reasons).

2.3.7 Frost table depth and soil moisture

At each instrumented shrub, we established a 2 m transect perpendicular to the patch slope such that 1 m extended out from the centre of each shrub. Frost table depth and soil moisture measurements were made at approximately 20, 100, and 180 cm distances along each transect to capture variability in these abiotic properties beneath green alder canopies (subsamples were pooled in statistical analyses). Frost table depth was measured by probing the soil (depth to refusal) with a 2 m graduated steel rod. In 2015, soil moisture was measured using a 5 cm pronged probe (Frequency Domain Reflectometry (FDR) Soil Moisture POGO, Stevens Water Monitoring Systems Inc., Portland, OR, USA). In 2016, soil moisture was measured using the same probe when the frost table was shallower than 20 cm combined with a 20 cm probe (FieldScout Time Domain Reflectometry (TDR) 300 Soil Moisture Meter, Spectrum Technologies Inc., Aurora, IL, USA) when the frost table was deeper than 20 cm to characterize variability in soil moisture with depth. Soil moisture values were calibrated for TVC-specific soils using generalized calibration equations applicable in both mineral and organic soils developed using gravimetric soil cores of known volume collected during the summers of 2014 and 2015. The developed calibrations for the FDR and TDR probes yielded an accuracy of 0.5 $m^3 \cdot m^{-3}$ when used in both mineral and organic soils (Wrona, 2016). Paired frost table depth and soil moisture measurements were made on June 30-July 3 and August 19-22 in 2015 and on June 28-29, July 13-19, and August 6 in 2016. Soil moisture measurements were made on days with no rainfall 24 hours prior.

2.3.8 Soil inorganic nutrients

To characterize soil inorganic nutrient availability, we installed four Plant Root Simulator (PRS) Probes (Western Ag Innovations, Saskatoon, SK, CA) in early June of 2016 at approximately 20 cm and 180 cm along the 2 m transect that traversed each instrumented shrub. The four PRS probes at each instrumented shrub consisted of two cation and two anion probes inserted into the top 10 cm of the soil surface. Although the PRS probes measure the availability of a suite of soil ions, the soil ions of interest in this study were ammonium (NH_4^+), nitrate (NO_3^-), phosphorous (P; $H_2PO_4^-$ and HPO_4^{-2}), and potassium (K^+) as they represent the primary macronutrients used by plants. The PRS probes were removed mid-August (mean burial length = 72 days), thoroughly washed with deionized water, packaged in individual plastic bags, and shipped in a cooler to Western Ag Innovations for analysis.

2.3.9 Functional traits

Since leaf N and soil nutrient supply are generally known to be strongly positively related (e.g., Ordoñez *et al.*, 2009), we further characterized available soil nitrogen (soil N) through measurement of leaf nitrogen concentration (leaf N) for all instrumented shrubs in both study years. Leaf N and photosynthetic capacity are also known to be strongly positively related because leaf N is integral in the proteins required for photosynthesis, especially RuBisCo (e.g., Wright *et al.*, 2004), thus leaf N was also used as a proxy of productivity. Leaf carbon was measured to calculate leaf C:N, which is a measure of leaf toughness (i.e., decomposability; Enriquez *et al.*, 1993). Five healthy, green leaves from one stem on each instrumented shrub were haphazardly selected for harvest in mid-August 2015 and mid-July 2016. Leaves were placed in coin envelopes

and air dried. All dried leaf samples were ground for two minutes using a ball mill, weighed using a microbalance (SE2 Ultra-microbalance, Sartorius, Bohemia, NY, USA), and encapsulated in tin capsules. 2015 leaf N was analyzed using an elemental analyzer (2400 CHNS Analyzer, PerkinElmer, Guelph, ON, CA). To ensure accuracy, acetanilide check standards were used at the beginning, middle, and end of the analysis and compared to expected values of standard weight percent theories for N. Comparisons of check standards to expected values yielded an average relative error of 0.003 $\%\cdot\%^{-1}$ for N. 2016 leaf samples were sent to the University of California Davis Stable Isotope Facility (UCD SIF; Davis, CA, USA) for analysis using an elemental analyzer interfaced to a continuous flow isotope ratio mass spectrometer. UCD SIF's procedure for checking measured mass values against expected mass values for elemental totals yielded an average relative error of 0.009 $\mu g\cdot\mu g^{-1}$ for N and 0.004 $\mu g\cdot\mu g^{-1}$ for C. C:N was calculated by dividing leaf C by leaf N.

We measured leaf mass per area (LMA) to characterize leaf thickness and density (Niinemets, 2001). Following removal of sap flow meters, all leaves were removed from instrumented stems to measure total stem leaf area. Due to the large number of leaves, fresh leaf scans for all instrumented stems was not feasible. To address this, we developed a relationship between fresh leaf area and dry leaf area using a subsample of 400 fresh leaves which were scanned in 25 batches and their batch areas measured. These leaves were then oven dried for 48 hours at 70°C and re-scanned to determine dry leaf area and the subsequent fresh to dry leaf area relationship (Fig. S3; $R^2 = 0.92$, $p < 0.001$). All remaining leaves were oven-dried, scanned in batches, and the fresh to dry leaf area relationship was used to correct for leaf shrinkage in the large batches. The fresh area of

each batch was summed for each instrumented stem to obtain total stem leaf area. All leaf area measurements were performed using WinFOLIA (v. 2004a, Regent Instruments Inc., Ville de Québec, QC, CA). Leaves were weighed and average shrub canopy LMA was calculated by dividing total stem leaf dry mass by total stem leaf fresh area.

To investigate variation in water use strategies among topographic positions, we measured leaf $\delta^{13}C$ and leaf area to sapwood area ratio (LA:SA) of instrumented shrubs. Stomatal closure (which occurs under water limitations) results in greater proportional uptake of the heavier ^{13}C isotope caused by reduced discrimination between isotopes during drawdown of ^{12}C in the internal CO_2 (Farquhar *et al.*, 1995). As a consequence, isotopic signature provides an indication of water use efficiency integrated over the leaf lifetime (Farquhar *et al.*, 1989). The same leaf samples that were sent to UCD SIF for leaf N and C analysis were analyzed to determine their $^{13}C/^{12}C$ ratios. The ratios were expressed as $\delta^{13}C$ against a Vienna PeeDee Belemnite standard, where:

$$\delta^{13}C = [R \text{ sample}/R \text{ standard}) - 1]1000, \text{ where } R = {}^{13}C/{}^{12}C \quad (3)$$

UCD SIF's procedure for checking measured mass values against expected mass values for isotopic totals yielded an average relative error of 0.001 $\mu g \cdot \mu g^{-1}$ for $\delta^{13}C$.

LA:SA represents the balance between transpirational surface area and stem water supply to leaves (Waring *et al.*, 1982). LA:SA provides insight into leaf biomass allocation and hydraulic architecture because water loss through leaves must be compensated by the upward flow of water through the sapwood (Shinozaki *et al.*, 1964a, b), thereby providing an indication of whole-plant water use efficiency. Plants often respond to drought by decreasing their LA:SA to increase their water use efficiency

(Poorter *et al*., 2009). LA:SA was calculated by dividing total stem fresh leaf area by stem sapwood area.

2.3.10 Data analysis

Sap flow data processing

Due to technical issues that resulted in large periods of missing data, we were unable to calculate the total (cumulative) volume of sap used by green alder stems during the 2015 and 2016 growing seasons. Instead, we focused on shorter time frames of available data to characterize seasonal variation in stem sap flow. We divided estimates of daily cumulative stem sap volume into three periods for each study year: early in the season, during peak physiological activity (i.e., maximum sap flow), and late in the season. We determined the approximate day of peak physiological activity of each shrub through visual inspection of seasonal sap flow tracings (see Fig. S4 for an example of a tracing). To characterize shrub water use during peak physiological activity, we averaged daily cumulative sap volume of stems (one stem per individual) across a seven day period surrounding the average day of maximum sap flow (excluding days with rainfall; SF_{peak}). We used a seven day period to characterize SF_{peak} because the day of maximum sap flow varied by a week among shrubs (i.e., not all shrubs experienced maximum sap flow on the same day). We used a similar procedure as above to characterize early and late season sap flow. Specifically, we averaged daily cumulative sap volume across five day periods based on when sap flow meters were installed (early season) and uninstalled (late season). We used five day periods for these early and late season estimates as they reflected the number of days it took to fully install and uninstall all shrubs with sap flow meters (i.e., meters were not installed/removed from shrubs at the same time among

shrubs). Following the above procedures, we determined mean shrub patch transpiration (calculated using Equation 2 and averaged across 10 patches) for early in the season, during peak physiological activity, and late in the season for both study years. The study years were analyzed separately for mean stem sap flow and mean shrub patch transpiration due to different levels of nesting and replication between years.

Quantifying green alder water status

Since Ψ_{stem} measurements were not made on instrumented shrubs, Ψ_{stem} data were analyzed separately. To test for differences in Ψ_{stem} among topographic positions at different points in the growing season, we used a linear mixed effects model with an interaction between topographic position and measurement period ('lme' function in the R package 'nlme'). We used *a priori* contrasts to test for differences in Ψ_{stem} between topographic positions (top vs. middle, bottom, channel; middle vs. bottom, channel; and top vs. bottom) and measurement periods (mid- vs. early season; mid- vs. late season). Topographic position contrasts were used to make pre-planned comparisons based on an expected gradient in abiotic conditions from the top of the slope to the channel, with the expectation that the channel would be the highest resource environment but with potentially waterlogged soils that may decrease water use. Contrasts were therefore made between a) what we hypothesized would be the least ideal position for a shrub (top) and all downslope locations (middle, bottom, and channel), b) the next least ideal position for a shrub (middle) and all downslope locations (bottom, channel), and c) the least ideal position for a shrub (top) and the most ideal position for a shrub (bottom). Measurement period contrasts were set up to make pre-planned comparisons between periods using the middle of the season as a reference (i.e., when shrubs should have the greatest

physiological activity). We used 'individual' as a random effect to account for repeated measures. To compare shrub water status between years differing in rainfall, we compared late season Ψ_{stem} among topographic positions and between study years using an ANOVA with an interaction between topographic position and study year. We used *a priori* contrasts to test for differences in mean late season Ψ_{stem} among topographic positions and study years. Model assumptions of homoscedasticity and normality were verified through visual inspection.

Modelling the relative importance of water availability, nutrient availability, and topography on shrub water use

We tested the relative importance of water availability, nutrient availability, and topography on mean daily cumulative sap volume (SF_{daily}) of shrubs (one instrumented stem per shrub) averaged over seven-day periods that corresponded with the timing of frost table depth and soil moisture measurements (excluding days with rainfall). We used seven day periods as it often took a week to perform abiotic measurements for all shrubs during a round of measurements. Using SF_{daily} as a response variable allowed us to determine which abiotic variables were important drivers of shrub water use. SF_{daily} was modelled through candidate sets of linear mixed effects models (one set of candidate models per growing season; Tables S3 and S4). Candidate models represented biological hypotheses regarding the individual effects of water availability, nutrient availability, topography, and their combined effects on SF_{daily}. Model selection was based on the corrected minimum Akaike information criterion (AIC_c) and associated statistics, as models with lower AIC_c values are more parsimonious when considering both model fit and complexity (Burnham & Anderson, 1998). Prior to creating models, we tested for

collinearity between continuous predictor variables using a Pearson's correlation matrix and excluded collinear variables from models using a cut-off correlation coefficient of r = 0.3 (Tables S5 and S6). We tested for collinearity between continuous predictor variables and topographic position through visual inspection of boxplots. Since no obvious trends were present between the continuous predictor variables and topographic position, topographic position was included as a categorical predictor variable in models to represent topographic-induced variation in SF_{daily} through variables that we did not directly measure, such as variation in vapour pressure deficit that may occur with topographic position or topographically driven soil characteristics (e.g., organic layer thickness). We used *a priori* contrasts to test for differences in SF_{daily} among topographic positions (see above). The random effect term was 'individual' nested within 'patch' to account for our spatially-nested sampling design ('patch') and repeated measures ('individual'). Model assumptions were verified for full models through visual inspection.

Determining gradients in shrub functional traits to explain the topographic pattern in shrub expansion

To investigate how green alder functional traits relate to resource use, we used a principal components analysis (PCA) to reduce functional trait variables (including SF_{peak}) into gradients that explain variation in resource use strategies in multivariate trait space (built-in R function 'prcomp'). We retained a sufficient number of principal components (PCs) so that cumulatively they explained at least 80% of the variation in the data. To determine if topography could be used to help explain variability in resource use strategies, we grouped data points (representing individual shrubs) by topographic

position by overlaying confidence ellipses (95%) onto the PCA. We used an ANOVA to confirm significant differences in PC scores among topographic positions. We verified that all variables had linear relationships with one another through visual inspection of scatterplots.

All continuous predictor variables were standardized using Z-transformation to eliminate scaling issues. All statistical analyses were performed in R v. 3.3.2 (R Development Core Team, 2013).

2.4 Results

2.4.1 Seasonal variation in water use

Peak physiological activity of green alders was approximately June 22-June 28 in 2015 and July 9-15 in 2016. Early season stem sap flow was calculated for June 13-17 and June 9-13 for 2015 and 2016, respectively. Late season stem sap flow was calculated for August 15-19 for 2015 and August 11-15 for 2016. Seasonal variation in mean stem sap flow for each year is shown in Fig. 2.2a. In 2015, early season, peak activity, and late season mean stem sap flow was 691.70 $cm^3 \cdot day^{-1}$ (± 149.56 $cm^3 \cdot day^{-1}$), 1832.13 $cm^3 \cdot day^{-1}$ (± 224.05 $cm^3 \cdot day^{-1}$), and 72.49 $cm^3 \cdot day^{-1}$ (± 15.11 $cm^3 \cdot day^{-1}$), respectively. In 2016, early season, peak activity, and late season mean stem sap flow was 375.62 $cm^3 \cdot day^{-1}$ (± 87.61 $cm^3 \cdot day^{-1}$), 1324.99 $cm^3 \cdot day^{-1}$ (± 170.13 $cm^3 \cdot day^{-1}$), and 436.76 $cm^3 \cdot day^{-1}$ (± 60.50 $cm^3 \cdot day^{-1}$), respectively. Mean stem sap flow was positive throughout the majority of the 2015 and 2016 growing seasons (e.g., Fig. S4), likely due to nearly 24 hours of daylight at the study site. Stem sap flow typically did not fall below 500 $cm^3 \cdot day^{-1}$ during peak physiological activity (e.g., Julian days 171-177 in Fig. S4), indicating that shrubs were actively transpiring throughout the night during periods of maximum sap flow. Mean

stem sap flow generally decreased after peak physiological activity and usually dropped close to zero at night towards the end of August (e.g., Fig. S4) as shrubs responded to decreasing solar radiation at night while simultaneously starting senescence.

Seasonal variation in mean green alder patch water flux for each year is shown in Fig. 2.2b. In 2015, early season, peak activity, and late season mean shrub patch water flux was 0.74 $mm \cdot day^{-1}$ (± 0.06 $mm \cdot day^{-1}$), 2.09 $mm \cdot day^{-1}$ (± 0.18 $mm \cdot day^{-1}$), and 0.09 $mm \cdot day^{-1}$ (± 0.01 $mm \cdot day^{-1}$), respectively. In 2016, early season, peak activity, and late season mean shrub patch water flux was 0.35 $mm \cdot day^{-1}$ (± 0.03 $mm \cdot day^{-1}$), 1.30 $mm \cdot day^{-1}$ (± 0.11 $mm \cdot day^{-1}$), and 0.44 $mm \cdot day^{-1}$ (± 0.04 $mm \cdot day^{-1}$), respectively. The overall (growing season) mean shrub patch water flux (averaged across early, peak, and late periods) was 0.97 $mm \cdot day^{-1}$ (± 0.59 $mm \cdot day^{-1}$) in 2015 and 0.70 $mm \cdot day^{-1}$ (± 0.53 $mm \cdot day^{-1}$) in 2016. Shrub patch water flux ranged from 0.05 $mm \cdot day^{-1}$ to 2.95 $mm \cdot day^{-1}$ in 2015 and 0.18 $mm \cdot day^{-1}$ to 1.84 $mm \cdot day^{-1}$ in 2016.

2.4.2 Topographic and seasonal patterns in water status

In 2015, mean Ψ_{stem} significantly differed across a topographic gradient such that downslope locations had generally higher Ψ_{stem} values (closer to zero) than upslope locations. Mean Ψ_{stem} also significantly differed through the 2015 growing season such that shrubs had higher Ψ_{stem} values earlier in the season relative to mid-season and lower Ψ_{stem} values at the end of the season relative to mid-season. There was no significant interaction between topographic position and measurement period in 2015 (Table 2.1; see Table S7 for the random effects output; Fig. 2.3a). The lowest value of Ψ_{stem} experienced by a shrub (maximum water stress) during the 2015 growing season was -24.0 bars and the highest value (minimum water stress) was -2.8 bars.

Late season mean Ψ_{stem} significantly differed between study years, with shrubs having significantly lower Ψ_{stem} values during August 2015 than August 2016. Green alders on the tops of patch slopes had significantly lower mean late season Ψ_{stem} than downslope locations in 2015 but not in 2016 (Table 2.2; Fig. 2.3b). Mean late season Ψ_{stem} ranged from -24.0 bars to -9.5 bars in 2015 and -11.7 bars to -6.3 bars in 2016.

2.4.3 Abiotic drivers of shrub water use

Variation in SF_{daily} in both study years was best characterized by full models that included all metrics of water availability, nutrient availability, and topography (Tables S8 and S9). Thus, all abiotic variables and topographic position were important in combination for predicting SF_{daily}. Based on the outputs of the AICc-selected models (Tables 2.3 and 2.4), the main abiotic driver of SF_{daily} for both study years was frost table depth (Fig. 2.4; see Tables S10 and S11 for the random effects outputs). The overall (entire growing season) relationship between frost table depth and SF_{daily} was negative for both 2015 and 2016. However, the relationship between frost table depth and SF_{daily} early in the 2015 growing season was positive (Fig. 2.4a). Surprisingly, SF_{daily} did not significantly differ among topographic position contrasts in 2015 or 2016, potentially due to the high variability in SF_{daily} among topographic positions as indicated by the large standard errors in Tables 2.3 and 2.4

2.4.4 Functional trait spectra

Data reduction using PCA resulted in three axes explaining variation in functional traits. These three axes (PCs) cumulatively explained 82.8% of the variation in the functional traits investigated. The amount of variation that each trait explains in a PC is represented through the loadings on the PC. The magnitude and directionality of the

loadings of our three retained PCs (Table S12) indicated that, when plotted against one another, PCs 1 and 2 could be thought of as separate functional trait spectra (Fig. S5a). PC1 explained a gradient in resource use based on leaf traits: leaf N was negatively related to leaf C:N, LMA, and leaf $\delta^{13}C$. PC 2 captured a gradient in leaf and whole-plant water use efficiency: LA:SA and leaf $\delta^{13}C$ were negatively related. SF_{peak} was unimportant in the bi-plot of PC 1 vs. PC 2 (Fig. S5a) as PC 3 was mainly explained by SF_{peak}, meaning that SF_{peak} was unrelated to the plant resource economics gradients explained by PCs 1 and 2. Bi-plots of PC 1 vs. PC 3 and PC 2 vs. PC 3 are shown in Figs. S5b and c, respectively.

Overlaying topographic position onto the bi-plot of PC 1 vs. PC 2 demonstrated that topography could be used to help explain variability in resource use strategies (Fig. 2.5). Shrubs in channels clearly separated out from shrubs on the tops of patches along the leaf functional trait spectrum explained by PC 1. An ANOVA further confirmed that PC 1 scores significantly differed between shrubs at the tops of patches and shrubs in channels (top vs. channel; $F_{3,19} = 8.058$, $p = 0.009$). Shrubs in channels were characterized by higher leaf N and lower leaf C:N, LMA, and leaf $\delta^{13}C$. Conversely, shrubs at the tops of patch slopes were characterized by lower leaf N and higher leaf C:N, LMA, and leaf $\delta^{13}C$.

2.5 Discussion

In the present manuscript, we provide the first empirical data on tall tundra shrub water status and use. Using a range of predictors of shrub water use, we found that frost table depth was a central predictor, with implications for predicting seasonal water use and understanding the effects of warming-induced permafrost thaw on tundra

ecohydrology. Though not central in determining shrub water use, topographic position drove variability in shrub leaf functional traits pertaining to resource use and productivity. Given the rates of shrub proliferation on the low arctic tundra, information on tall shrub water use and the drivers of shrub function are critical for predictive models of ecosystem function.

Unexpectedly, our estimates of mean shrub patch water flux over the growing seasons of 2015 and 2016 are lower than most estimates of growing season evapotranspiration for other tundra vegetation assemblages (e.g., tussock tundra, low shrub tundra; Table 2.5). However, our estimates of shrub patch transpiration are conservative as we only estimated transpiration of green alders and no other shrub species that are dominant in green alder patches (e.g., *Betula glandulosa*, *Vaccinium uliginosum*). Our growing season estimates may also be lower due to the fact that green alder patch water flux was quite low towards the end of both growing seasons (2015 = 0.09 ± 0.001 mm·day^{-1}; 2016 = 0.43 ± 0.04 mm·day^{-1}); it is possible that these larger shrubs are more strongly limited by moisture availability with active layer thaw compared to other types of tundra vegetation. Indeed, our maximum values of patch transpiration during peak water use (2015 = 2.09 mm·day^{-1}; 2016 = 1.30 mm·day^{-1}) are higher than the maximum growing season evapotranspiration of tussock tundra near Eagle Creek, Alaska (1.24 mm·day^{-1}; Stuart *et al*., 1982). Thus, green alders alone may significantly contribute to tall shrub patch water fluxes at TVC during peak water use, but total shrub patch evapotranspiration (i.e., accounting for all vegetation in a shrub patch) is as yet unknown for this site. Ground vegetation community composition differs between shrub patches and tundra at this site (C. Wallace, personal communication) with

implications for fluxes. Further characterizing tall shrub patch evapotranspiration will be essential for understanding the hydrological implications of shrub expansion, which our results suggest will be influential, particularly during peak physiological periods.

The overall significant negative relationship between frost table depth and SF_{daily} for both study years (Fig. 2.4) suggests that thaw depth is the main limiting factor in green alder water use. In permafrost regions, the water table perches on top of the impermeable frost table (Quinton & Baltzer, 2013). Consequently, as the frost table and water table deepen with seasonal thaw, plant access to soil moisture decreases (Patankar *et al.*, 2015; Quinton & Baltzer, 2013). Patankar *et al.* (2015) similarly found a significant negative relationship between frost table depth and black spruce sap flow in a subarctic boreal peatland in the Northwest Territories. Their results indicated 50-60% reductions in sap flow with greater active layer thaw, which they attributed to reduced soil moisture availability as a result of the paired deepening of the frost and water tables. At the same site as Patankar *et al.* (2015), Warren (2015) found that soil moisture at ~10 cm depth was a better predictor of black spruce sap flow than soil moisture at ~5 or ~20 cm depths, providing insight into where black spruce predominantly accesses soil water and how it may respond to deepening frost and water tables. Although we do not have direct estimates of green alder rooting depth at our study site, the overall negative response of green alder SF_{daily} to a deeper frost table is likely due to seasonally drier surface soils in which green alders are rooted. The 2016 growing season received 26.4% more rain than the 2015 growing season and shrubs in August 2016 had significantly higher water potentials than shrubs in August 2015. This further demonstrates how surface water availability impacts shrub water status and use.

Despite an overall (entire season) significant negative relationship, there was a positive relationship between frost table depth and green alder SF_{daily} early in the 2015 growing season (Figure 2.4a). This early season relationship may be a result of increased soil temperatures with ground thaw (in relation to a frozen active layer) while the frost table is still shallow relative to the maximum active layer thickness achieved towards the end of the growing season (Williams *et al.*, 2013). Warmer soil temperatures could enhance root function, soil microbial activity, shrub water use, and overall shrub function (Chapin, 1983; Rustad *et al.*, 2001; Keuper *et al.*, 2012b). Thus, warmer soil temperatures combined with a frost table depth that still permits sufficient surface water availability could explain the positive relationship between frost table depth and green alder SF_{daily} early in the growing season of 2015. Since this early season relationship switches to a neutral relationship with deeper frost tables towards the end of the 2015 growing season, there may be a threshold at which active layer thaw is no longer beneficial for shrub function, resulting in an overall negative relationship. Our results from the 2015 study period suggest that this threshold value is ~40 cm, with frost tables deeper than ~40 cm not permitting sufficient surface water availability. However, this positive early season relationship was not found for the 2016 study period, potentially because the timing of early season measurements coincided with relatively lower vapour pressure deficits and solar radiation, both of which have been shown to be the main micrometeorological drivers of sap flow across many systems (e.g., Granier & Bréda, 1996; Patankar *et al.*, 2015).

It could be argued that the overall negative relationship between frost table depth and green alder SF_{daily} is a result of seasonality rather than water limitation. That is,

SF_{daily} may have decreased with greater active layer thaw simply because end of growing season senescence coincides with the timing of maximum active layer thickness. However, our water potential data support that seasonal thaw causes water limitations. Green alders had significantly lower Ψ_{stem} values in the middle of the season compared to early in the season during the 2015 growing season. The decrease in Ψ_{stem} with the progression of the season implicates decreased surface water availability. Thus, the negative influence of frost table depth on SF_{daily} was likely important during the period in which green alders should have the highest water demand (approximately the middle of the season) and not just during the period of senescence.

Knowing that thaw depth is an important driver of green alder water use provides insight into how tall tundra shrubs may respond to future environmental changes. For instance, if high-latitude climate warming continues as projected (Serreze & Barry, 2011), permafrost thaw is expected to accelerate (Lawrence *et al.*, 2008). Our results suggest that this may result in reduced water availability and decreased function for these large tundra shrubs, unless changes in rooting depth occur. Thus, predictions of future permafrost conditions may be useful in forecasting changes in the function and productivity of tall tundra shrubs and possibly belowground biomass allocation.

Using the conceptual framework of the global leaf economics spectrum coined by Wright *et al.* (2004) and the global 'fast-slow' plant economics spectrum proposed by Reich (2014), we provide evidence of a leaf functional trait spectrum that explains a gradient in fast to slow water and nutrient use strategies of green alders that corresponds with topography. PC 1 explained 43.3% of the variation in the measured functional traits, which resulted in a gradient explaining variation in leaf traits relating to resource use:

productivity or photosynthetic potential (leaf N), investment (C:N and LMA), and water use efficiency ($\delta^{13}C$). Green alders in channels had higher leaf N, lower investment in leaf structure (low LMA and C:N) and less conservative water use, whereas green alders at the tops of slopes were characterized by the opposite. These correlations allow general predictions to be made about the variability in resource use and productivity among the topographic positions of green alder patches.

The negative association between leaf N and LMA can provide insight into several traits that reflect variation in productivity. Leaves with high LMA may have greater internal gaseous diffusion limitations (lower CO_2 drawdown) due to greater mesophyll thickness, resulting in decreased photosynthetic activity and slower growth (Mooney & Gulmon, 1982; Parkhurst, 1994; Terashima *et al.*, 2001). Plants with high LMA have been shown to have greater internal self-shading of chloroplasts (Green *et al.*, 2001). However, resource use efficiency and conservation in plants with high LMA increases survival in lower resource conditions through increased resource savings (Funk & Vitousek, 2007; Reich, 2014). In contrast, plants with low LMA usually intercept more light per gram of foliage and consequently may have higher photosynthetic rates and faster growth (Reich, 2014). Further, plants with low LMA may allocate more N to thylakoids and RuBisCo (increased photosynthetic nitrogen use efficiency) whereas plants with high LMA may allocate more N to non-photosynthetic leaf components (Poorter & Evans, 1998). Since plants require high N investment into photosynthetic leaf components for high photosynthetic rates (Evans, 1989), it is plausible that channel shrubs have comparatively cheap and thin leaves, high photosynthetic rates, and faster growth whereas shrubs at the tops of slopes demonstrate the opposite.

Variation in leaf N and C:N between channel shrubs and shrubs at the tops of slopes may translate into differences in leaf decomposition. Plants with low leaf C:N (high N) generally have higher decomposition rates (e.g., Tian *et al.*, 1992) because they provide a higher quality substrate for decomposers (Swift *et al.*, 1979; Manzoni *et al.*, 2008). Leaves with high N therefore release more N during decomposition due to increased depolymerisation of N-containing polymers by soil microbes (Tian *et al.*, 1992; Schimel & Bennett, 2004). In contrast, leaves with high C:N have slower decomposition rates because they are usually low in N and high in lignin (Taylor *et al.*, 1989). Lignin is difficult to decompose due to its inhibition of enzymatic action (Swain, 1979) and because it physically disrupts the decay of other chemical components in leaf cells (Sivapalan *et al.*, 1989). However, high leaf C:N can be advantageous by increasing leaf longevity (Mooney & Gulmon, 1982; Withington *et al.*, 2006) and deterring of herbivores through decreased palatability and nutritive value (Swain, 1979; McClure, 1980). Ultimately, channel shrubs likely return more N to the soil pool via leaf litter, which may increase their available soil N, potentially resulting in a positive feedback to shrub productivity in channels.

Shrubs at the tops of slopes invested more into water use strategies and leaf construction compared to channel shrubs. Plants with conservative water use may have a lower ability to move, use, and lose water which may correspond with a lower ability to acquire and utilize nutrients (Reich, 2014). Water limitations can result in smaller mesophyll cells with thicker walls (Utrillas & Alegre, 1997) and an overall increased proportion of leaf mass as cell walls (Fredeen *et al.*, 1991). These responses to water stress resulted in more rigid leaves that are less susceptible to wilting with smaller

transpirational surface areas that reduce water requirements under dry conditions (Poorter *et al.*, 2009). In addition, leaves with higher water use efficiencies generally have higher carbon concentrations simply because more carbon is fixed per unit water transpired (Seibt *et al.*, 2008). These water stress-induced changes in leaf structure provide a possible explanation for why shrubs at the tops of slopes had higher LMA, C:N, and leaf water use efficiency compared to channel shrubs.

Surprisingly, leaf ($\delta^{13}C$) and whole-plant water use efficiency (LA:SA) were unrelated to SF_{peak} along PC 2, and this PC was not associated with topography. Similarly, Apgaua *et al.* (2015) found that sap velocity was poorly predicted by ordinated stem and leaf traits relating to water use for seven tropical lowland rainforest tree species in northeast Australia. Apgaua *et al.* (2015) attributed the lack of predictability to high variability in sap flow and functional traits within and between species. Our sap flow data were also highly variable, however, it is also possible that SF_{peak} is less representative of transpiration in this system and is perhaps more demonstrative of water storage. That is, not all water moving through the base of green alder stems (where our sap flow sensors were installed) may be leaving via transpiration; some portion of water may be stored in sapwood to use during periods of high evaporative demand or water stress (Goldstein *et al.*, 1998). Green alders experience a high evaporative demand in a short growing season with nearly full days of sunlight as well as seasonal variation in water availability through active layer thaw. Thus, green alders may use water stored within stem tissues rather than water from the soil reservoir to help with refilling processes due to 24-hour daylight or during periods where decreased surface soil moisture associated with seasonal thaw may limit refilling of cavitated vessels.

Although green alder leaf functional traits were dictated by topography, it is not clear whether topographically-driven differences in water or nutrient availability were the drivers of this relationship. Our analyses did not yield any differences in surface soil moisture or frost table depth between the tops of slopes and channels. This was unexpected as it was quite evident in the field that channels were wetter than upslope locations. It is possible that variation in abiotic conditions across microtopography masked variation at the level of macrotopography. Differences in soil chemistry and water content may dramatically differ between hummocks and interhummocks at TVC due to differences in permafrost configuration and organic matter content. NH_4^+ and NO_3^- supply rates also did not differ between the tops of slopes and channels, yet channel shrubs had significantly higher leaf N than shrubs at the tops of slopes, suggesting greater N availability and uptake in channels. A paired study performed at TVC by Rabley (2017) demonstrated that mean nodule count and average nodule biomass per shrub did not significantly differ between the tops of slopes and channels, implying that N fixation rates should be similar at these two topographic positions if nodules have equivalent function across topographic positions. Thus, the differences in leaf functional traits appear unrelated to nodulation. We hypothesize that differences in leaf N may thus be due to greater organic N availability in channels rather than differences in inorganic N availability or symbiotic N fixation rates. Arctic plants often rely more on organic sources of N (mainly amino acids; Chapin *et al.*, 1993; Kielland, 1994) because inorganic forms are very limited due to low litter inputs and slow decomposition and N cycling rates (Haag, 1974; Schimel & Bennett, 2004). Nitrogenase activity on the tundra may be limited by low temperatures (Winship & Tjepkema, 1985); green alders at TVC may

therefore rely more on organic N sources rather than N fixed by *Frankia* relative to the high N contribution of *Frankia* to *Alnus* spp. at non-tundra sites (70-100%; Hurd *et al.*, 2001; Myrold & Huss-Danell, 2003). Since several studies argue that tundra shrub productivity is nutrient- rather than water-limited (Chapin *et al.*, 1995; Keuper *et al.*, 2012a), measurements of dissolved organic N availability and uptake across the toposequence of shrub patches would be valuable to determine how organic N availability influences shrub productivity across the landscape.

2.6 Acknowledgements

Funding for this study was provided by ArcticNet, the Natural Sciences and Engineering Research Council of Canada, Canadian Northern Studies Trust, Wilfrid Laurier University (Laurier), the Polar Continental Shelf Program, Polar Knowledge Canada, Canada Foundation for Innovation, Ontario Ministry of Research and Innovation, and the Northern Scientific Training Program. We are grateful to C. Wallace for all of his logistical support, field assistance, guidance, and help with ArcGIS. We would like to thank J. Rabley, T. Giguere, and E. Way-Nee for their help with field data collection. N. Tran provided excellent technical support for sap flow data processing. We would like to thank P. Marsh and K. Stevens for input regarding study design. A. Berg provided soil moisture equipment and E. Wrona provided soil moisture calibrations. We thank N. Day for her helpful suggestions regarding statistical analyses. We acknowledge logistical support provided by the Government of the Northwest Territories – Laurier Partnership. We thank the Aurora Research Institute for their assistance in obtaining a research license (license number 15609).

2.7 References

Apgaua DMG, Ishida FY, Tng DYP, Laidlaw MJ (2015) Functional traits and water transport strategies in lowland tropical rainforest trees. *PLoS ONE*, **10**, 1–19.

Aubin I, Munson AD, Cardou F et al. (2016) Traits to stay, traits to move: A review of functional traits to assess sensitivity and adaptive capacity of temperate and boreal trees to climate change. *Environmental Reviews*, **24**, 164–186.

Benecke U (1970) Nitrogen fixation by *Alnus viridis*. *Plant and Soil*, **33**, 30–48.

Berg B, Staaf H (1980) Decomposition rate and chemical changes of Scots pine needle litter. II. Influence of chemical composition. *Ecological Bulletins*, **32**, 373–390.

Blok D, Heijmans MMPD, Schaepman-Strub G, van Ruijven J, Parmentier FJW, Maximov TC, Berendse F (2011) The cooling capacity of mosses: Controls on water and energy fluxes in a Siberian tundra site. *Ecosystems*, **14**, 1055-1065.

Bolton JK, Brown RH (1980) Photosynthesis of grass species differing in carbon dioxide fixation pathways. *Plant Physiology*, **66**, 97–100.

Bonfils CJW, Phillips TJ, Lawrence DM, Cameron-Smith P, Riley WJ, Subin ZM (2012) On the influence of shrub height and expansion on northern high latitude climate. *Environmental Research Letters*, **7**, 1-9. DOI: 10.1088/1748-9326/7/1/015503.

Bowman WD (1992) Inputs and storage of nitrogen in winter snowpack in an alpine ecosystem. *Arctic and Alpine Research*, **24**, 211–215.

Bühlmann T, Körner C, Hiltbrunner E (2016) Shrub expansion of *Alnus viridis* drives former montane grassland into nitrogen saturation. *Ecosystems*, **19**, 968–985.

Burgess SS, Adams MA, Turner NC, Beverly CR, Ong CK, Khan AA, Bleby TM (2001) An improved heat pulse method to measure low and reverse rates of sap flow in woody plants. *Tree Physiology*, **21**, 589–598.

Burnham KP, Anderson DR (1998) Model selection and inference: A practical information theoretic approach. New York, NY: Springer-Verlag.

Chapin FS (1980) The mineral nutrition of wild plants. *Annual Review of Ecology and Systematics*, **11**, 233–260.

Chapin FS, Fetcher N, Kielland K, Everett KR, Linkins AE (1988) Productivity and nutrient cycling of Alaskan tundra: Enhancement by flowing soil water. *Ecology*, **69**, 693–702.

Chapin FS, Moilanen L, Kielland K (1993) Preferential use of organic nitrogen for growth by a non-mycorrhizal arctic sedge. *Nature*, **361**, 150–153.

Chapin FS, Shaver GR, Giblin A, Nadelhoffer K, Laundre J (1995) Responses of arctic tundra to experimental and observed changes in climate. *Ecology*, **76**, 694–711.

Chapin FS, Sturm M, Serreze MC et al. (2005) Role of land-surface changes in arctic

summer warming. *Science*, **310**, 657–660.

Cornwell WK, Cornelissen JHC, Amatangelo K et al. (2008) Plant species traits are the predominant control on litter decomposition rates within biomes worldwide. *Ecology Letters*, **11**, 1065–1071.

Coulson JC, Butterfield J (1978) An investigation of the biotic factors determining the rates of plant decomposition on blanket bog. *Journal of Ecology*, **66**, 631–650.

Elmendorf SC, Henry GHR, Hollister RD et al. (2012) Plot-scale evidence of tundra vegetation change and links to recent summer warming. *Nature Climate Change*, **2**, 453–457.

Enriquez S, Duarte C, Sand-Jensen K (1993) Patterns in decomposition rates among photosynthetic organisms: The importance of detritus C:N:P content. *Oecologia*, **94**, 457–471.

Environment and Climate Change Canada (2011) Canadian Climate Normals 1981-2010. Available at http://climate.weather.gc.ca/climate_normals/results_1981_2010_e.html (accessed on 7 April 2016).

Epstein HE, Beringer J, Gould WA et al. (2004) The nature of spatial transitions in the Arctic. *Journal of Biogeography*, **31**, 1917–1933.

Evans JR (1989) Photosynthesis and nitrogen relationships in leaves of C3 plants. *Oecologia*, **78**, 9–19.

Farquhar GD, O'Leary MH, Berry J (1982) On the relationship between carbon isotope discrimination and the intercellular carbon dioxide concentration in leaves. *Australian Journal of Plant Physiology*, **9**, 121–137.

Farquhar GD, Ehleringer JR, Hubick KT (1989) Carbon isotope discrimination and photosynthesis. *Annual Review of Plant Physiology and Plant Molecular Biology*, **40**, 503–537.

Forbes BC, Fauria MM, Zetterberg P (2010) Russian Arctic warming and "greening" are closely tracked by tundra shrub willows. *Global Change Biology*, **16**, 1542–1554.

Fraser RH, Lantz TC, Olthof I, Kokelj SV, Sims RA (2014) Warming-induced shrub expansion and lichen decline in the western Canadian Arctic. *Ecosystems*, **17**, 1151–1168.

Fredeen AL, Gamon JA, Field CB (1991) Responses of photosynthesis and carbohydrate-partitioning to limitations in nitrogen and water availability in field-grown sunflower. *Plant, Cell and Environment*, **14**, 963–970.

Funk JL, Vitousek PM (2007) Resource-use efficiency and plant invasion in low-resource systems. *Nature*, **446**, 1079–1081.

Goldstein G, Andrade JL, Meinzer FC, Holbrook NM, Cavelier J, Jackson P, Celis A (1998) Stem water storage and diurnal patterns of water use in tropical forest canopy

trees. *Environment*, **21**, 397–406.

Granier A, Bréda N (1996) Modelling canopy conductance and stand transpiration of an oak forest from sap flow measurements. *October*, **53**, 537–546.

Green DS, Kruger EL (2001) Light-mediated constraints on leaf function correlate with leaf structure among deciduous and evergreen tree species. *Tree Physiology*, **21**, 1341–1346.

Gulmon SL, Chu CC (1981) The effects of light and nitrogen on photosynthesis, leaf characteristics, and dry matter allocation in the chaparral shrub, *Diplacus aurantiacus*. *Oecologia*, **49**, 207–212.

Haag RW (1974) Nutrient limitations to plant production in two tundra communities. *Canadian Journal of Botany*, **52**, 103–116.

Hastings SJ, Luchessa SA, Oechel WC, Tenhunen JD (1989) Standing biomass and production in water drainages of the foothills of the Philip Smith Mountains, Alaska. *Holarctic Ecology*, **12**, 304–311.

Hinzman LD, Bettez ND, Bolton WR et al. (2005) Evidence and implications of recent climate change in northern Alaska and other arctic regions. *Climatic Change*, **72**, 251–298.

Hurd T, Raynal D, Schwintzer C (2001) Symbiotic N_2 fixation of *Alnus incana* ssp. *rugosa* in shrub wetlands of the Adirondack Mountains, New York, USA. *Oecologia*, **126**, 94–103.

Keuper F, Parmentier FJW, Blok D et al. (2012a) Tundra in the rain: Differential vegetation responses to three years of experimentally doubled summer precipitation in Siberian shrub and Swedish bog tundra. *Ambio*, **41**, 269–280.

Keuper F, van Bodegom PM, Dorrepaal E, Weedon JT, van Hal J, van Logtestijn RSP, Aerts R (2012b) A frozen feast: Thawing permafrost increases plant-available nitrogen in subarctic peatlands. *Global Change Biology*, **18**, 1998–2007.

Kielland K (1994) Amino acid absorption by arctic plants: Implications for plant nutrition and nitrogen cycling. *Ecology*, **75**, 2373–2383.

Lafleur P, Humphreys ER (2007) Spring warming and carbon dioxide exchange over low arctic tundra in central Canada. *Global Change Biology*, **14**, 740-756.

Lantz TC, Marsh P, Kokelj SV (2013) Recent shrub proliferation in the Mackenzie Delta Uplands and microclimatic implications. *Ecosystems*, **16**, 47–59.

Lawrence DM, Swenson SC (2011) Permafrost response to increasing arctic shrub abundance depends on the relative influence of shrubs on local soil cooling versus large-scale climate warming. *Environmental Research Letters*, **6**, 1-8. DOI: 10.1088/1748-9326/6/4/045504.

Lawrence DM, Slater AG, Tomas RA, Holland MM, Deser C (2008) Accelerated arctic

land warming and permafrost degradation during rapid sea ice loss. *Geophysical Research Letters*, **35**, 2–7.

Loranty MM, Goetz SJ (2012) Shrub expansion and climate feedbacks in arctic tundra. *Environmental Research Letters*, **7**, 1-3. DOI: 10.1088/1748-9326/7/1/011005.

Loranty MM, Goetz SJ, Beck PSA (2011) Tundra vegetation effects on pan-Arctic albedo. *Environmental Research Letters*, **6**, 1-7. DOI: 10.1088/1748-9326/6/2/029601.

Manzoni S, Jackson RB, Trofymow JA, Porporato A (2008) The global stoichiometry of litter nitrogen mineralization. *Science*, **321**, 684-686.

Marsh P, Pomeroy JW (1999) Spatial and temporal variations in snowmelt runoff chemistry, Northwest Territories, Canada. *Water Resources Research*, **35**, 1559–1567.

Marshall DC (1958) Measurement of sap flow in conifers by heat transport. *Plant Physiology*, **33**, 385–396.

Matthes-Sears U, Matthes-Sears WC, Hastings SJ, Oechel WC (1988) The effects of topography and nutrient status on the biomass, vegetative characteristics, and gas exchange of two deciduous shrubs on an arctic tundra slope. *Arctic and Alpine Research*, **20**, 342–351.

McClure MS (1980) Foliar nitrogen: A basis for host suitability for elongate hemlock scale, *Fiorinia externa* (Homoptera: Diaspididae). *Ecology*, **61**, 72–79.

McGill BJ, Enquist BJ, Weiher E, Westoby M (2006) Rebuilding community ecology from functional traits. *Trends in Ecology and Evolution*, **21**, 178–185.

McNulty SG, Swank WT (1995) Wood $\delta^{13}C$ as a measure of annual basal area growth and soil water stress in a *Pinus strobus* forest. *Ecology*, **76**, 1581–1586.

Mooney HA, Gulmon SL (1982) Constraints on leaf structure and function in relation to herbivory. *BioScience*, **32**, 198–206.

Mooney HA, Ferrar PJ, Slayter RO (1978) Photosynthetic capacity and carbon allocation patterns in diverse growth forms of *Eucalyptus*. *Oecologia*, **36**, 103–111.

Muster S, Langer M, Heim B, Westermann S, Boike J (2012) Subpixel heterogeneity of ice-wedge polygonal tundra: A multi-scale analysis of land cover and evapotranspiration in the Lena River Delta, Siberia. *Tellus B: Chemical and Physical Meteorlogy*, **64**, 1-19. DOI: 10.3402/tellusb.v64i0.17301.

Myers-Smith IH, Hik DS (2013) Shrub canopies influence soil temperatures but not nutrient dynamics: An experimental test of tundra snow-shrub interactions. *Ecology and Evolution*, **3**, 3683–3700.

Myers-Smith IH, Forbes BC, Wilmking M et al. (2011) Shrub expansion in tundra ecosystems: Dynamics, impacts and research priorities. *Environmental Research Letters*, **6**, 1–15.

Myers-Smith IH, Elmendorf SC, Beck PSA et al. (2015) Climate sensitivity of shrub growth across the tundra biome. *Nature Climate Change*, **5**, 887–891.

Myrold DD, Huss-Danell K (2003) Alder and lupine enhance nitrogen cycling in a degraded forest soil in northern Sweden. *Plant and Soil*, **254**, 47–56.

Naito AT, Cairns DM (2011) Relationships between arctic shrub dynamics and topographically derived hydrologic characteristics. *Environmental Research Letters*, **6**, 1-8. DOI:10.1088/1748-9326/6/4/045506.

Niinemets U (2001) Global-scale climatic controls of leaf dry mass per area, density, and thickness in trees and shrubs. *Ecology*, **82**, 453–469.

Ordoñez JC, Van Bodegom PM, Witte JPM, Wright IJ, Reich PB, Aerts R (2009) A global study of relationships between leaf traits, climate and soil measures of nutrient fertility. *Global Ecology and Biogeography*, **18**, 137–149.

Ostendorf B, Reynolds JF (1993) Relationships between a terrain-based hydrologic model and patch-scale vegetation patterns in an arctic tundra landscape. *Landscape Ecology*, **8**, 229–237.

Pajunen AM, Oksanen J, Virtanen R (2011) Impact of shrub canopies on understorey vegetation in western Eurasian tundra. *Journal of Vegetation Science,* **22**, 837–846.

Paquette A, Joly S, Messier C (2015) Explaining forest productivity using tree functional traits and phylogenetic information: Two sides of the same coin over evolutionary scale? *Ecology and Evolution*, **5**, 1774–1783.

Parkhurst DF (1994) Diffusion of CO_2 and other gases inside leaves. *New Phytologist*, **126**, 449–479.

Patankar R, Quinton WL, Hayashi M, Baltzer JL (2015) Sap flow responses to seasonal thaw and permafrost degradation in a subarctic boreal peatland. *Trees*, **29**, 129–142.

Pearson RG, Phillips SJ, Loranty MM, Beck PSA, Damoulas T, Knight SJ, Goetz SJ (2013) Shifts in arctic vegetation and associated feedbacks under climate change. *Nature Climate Change*, **3**, 673–677.

Pérez-Harguindeguy N, Díaz S, Garnier E et al. (2013) New handbook for standardised measurement of plant functional traits worldwide. *Australian Journal of Botany*, **61**, 167–234.

Pomeroy JW, Marsh P, Gray DM (1997) Application of a distributed blowing snow model to the Arctic. *Hydrological Processes*, **11**, 1451–1464.

Poorter H, Evans JR (1998) Photosynthetic nitrogen-use efficiency of species that differ inherently in specific leaf area. *Oecologia*, **116**, 26–37.

Poorter H, Niinemets Ü, Poorter L, Wright IJ, Villar R (2009) Causes and consequences of variation in leaf mass per area (LMA): A meta-analysis. *New Phytologist*, **182**, 565–588.

Quinton WL, Baltzer JL (2013) The active-layer hydrology of a peat plateau with

thawing permafrost (Scotty Creek, Canada). *Hydrogeology Journal*, **21**, 201–220.

R Development Core Team (2013) R: A language and environment for statistical computing. R Foundation for Statistical Computing, Vienna, Austria. ISBN 3-900051-07-0, URL http://www.R-project.org.

Rabley JM (2017) *The influence of topographic gradients and environmental drivers on the nodulation rate of* Alnus viridis *at a low arctic site* (unpublished undergraduate thesis). Wilfrid Laurier University, Waterloo, Canada.

Reich PB (2014) The world-wide "fast-slow" plant economics spectrum: A traits manifesto. *Journal of Ecology*, **102**, 275–301.

Schimel JP, Bennett J (2004) Nitrogen mineralization: Challenges of a changing paradigm. *Ecology*, **85**, 591–602.

Schuldt B, Leuschner C, Horna V, Moser G, Köhler M, Van Straaten O, Barus H (2011) Change in hydraulic properties and leaf traits in a tall rainforest tree species subjected to long-term throughfall exclusion in the perhumid tropics. *Biogeosciences*, **8**, 2179–2194.

Seibt U, Rajabi A, Griffiths H, Berry JA (2008) Carbon isotopes and water use efficiency: Sense and sensitivity. *Oecologia*, **155**, 441–454.

Serreze MC, Barry RG (2011) Processes and impacts of arctic amplification: A research synthesis. *Global and Planetary Change*, **77**, 85–96.

Shaver GR, Chapin FS (1980) Response to fertilization by various plant growth forms in an Alaskan tundra: Nutrient accumulation and growth. *Ecology*, **61**, 662–675.

Shinozaki K, Yoda K, Hozumi K, Kira T (1964a) A quantitative analysis of plant form: The pipe model theory. I. Basic analyses. *Japanese Journal of Ecology*, **14,** 97-105.

Shinozaki K, Yoda K, Hozumi K, Kira T (1964b) A quantitative analysis of plant form: The pipe model theory. II. Further evidence of the theory and its application in forest ecology. *Japanese Journal of Ecology*, **14**, 133-139.

Sivapalan K, Fernando V, Thenabadu MW (1985) N-mineralization in polyphenol-rich plant residues and their effect on nitrification of applied ammonium sulphate. *Soil Biology and Biochemistry*, **17**, 547–551.

Smith DM, Allen SJ (1996) Measurement of sap flow in plant stems. *Journal of Experimental Botany*, **47**, 1833–1844.

Stuart L, Oberbauer S, Miller PC (1982) Evapotranspiration measurements in *Eriophorum vaginatum* tussock tundra in Alaska. *Holarctic Ecology*, **5**, 145-149

Sturm M, Racine C, Tape KD (2001a) Increasing shrub abundance in the Arctic. *Nature*, **411**, 546–547.

Sturm M, McFadden JP, Liston GE, Chapin FS, Racine CH, Holmgren J (2001b) Snow–shrub interactions in arctic tundra: A hypothesis with climatic implications. *Journal*

of Climate, **14**, 336–344.

Sturm M, Schimel J, Michaelson G et al. (2005a) Winter biological processes could help convert arctic tundra to shrubland. *BioScience*, **55**, 17.

Swain, T (1979) Tannins and lignins. In Herbivores: Their interactions with secondary plant metabolites (Rosenthal GA & Janzen DH). pp. 657-822. New York, NY: Academic Press.

Swann AL, Fung IY, Levis S, Bonan GB, Doney SC (2010) Changes in arctic vegetation amplify high-latitude warming through the greenhouse effect. *Proceedings of the National Academy of Sciences*, **107**, 1295–1300.

Swanson RH (1994) Significant historical developments in thermal methods for measuring sap flow in trees. *Agricultural and Forest Meteorology*, **72**, 113–132.

Swift MJ, Heal OW, Anderson JM (1979) Decomposition in terrestrial ecosystems. Studies in ecology. Volume 5. Berkeley, CA: University of California Press.

Tape KD, Sturm M, Racine C (2006) The evidence for shrub expansion in northern Alaska and the pan-Arctic. *Global Change Biology*, **12**, 686–702.

Tape KD, Hallinger M, Welker JM, Ruess RW (2012) Landscape heterogeneity of shrub expansion in arctic Alaska. *Ecosystems*, **15**, 711–724.

Taylor BR, Parkinson D, Parsons WFJ (1989) Nitrogen and lignin content as predictors of litter decay rates: A microcosm test. *Ecology*, **70**, 97–104.

Terashima I, Miyazawa S, Hanba YT (2001) Why are sun leaves thicker than shade leaves? — Consideration based on analyses of CO_2 diffusion in the leaf. *Journal of Plant Research*, **114**, 93–105.

Tian G, Kang BT, Brussaard L (1992) Biological effects of plant residues with contrasting chemical compositions under humid tropical conditions - Decomposition and nutrient release. *Soil Biology and Biochemistry*, **24**, 1051–1060.

Tobner CM, Paquette A, Messier C (2013) Interspecific coordination and intraspecific plasticity of fine root traits in North American temperate tree species. *Frontiers in Plant Science*, **4**, 1–11.

Utrillas MJ, Alegre L (1997) Impact of water stress on leaf anatomy and ultrastructure in *Cynodon dactylon* (L.) Pers. under natural conditions. *International Journal of Plant Sciences*, **158**, 313–324.

Vourlitis GL, Oechel WC (1999) Eddy covariance measurements of CO_2 and energy fluxes of an Alaskan tussock tundra ecosystem. *Ecology*, **80**, 686-701.

Wahren CHA, Walker MD, Bret-Harte MS (2005) Vegetation responses in Alaskan arctic tundra after 8 years of a summer warming and winter snow manipulation experiment. *Global Change Biology*, **11**, 537–552.

Walker MD, Wahren CHA (2006) Plant community responses to experimental warming

across the tundra biome. *Proceedings of the National Academy of Sciences*, **103**, 1342–1346.

Waring RH, Schroeder PE, Oren R (1982) Application of the pipe model theory to predict canopy leaf area. *Canadian Journal of Forest Research*, **12**, 556–560.

Warren RK (2015) *Examining the spatial distribution of soil moisture and its relationship to vegetation and permafrost dynamics in a subarctic permafrost peatland* (unpublished Master's thesis). University of Guelph, Guelph, Canada.

Westoby M, Wright IJ (2006) Land-plant ecology on the basis of functional traits. *Trends in Ecology and Evolution*, **21**, 261–268.

Williams LE, Araujo FJ (2002) Correlations among predawn leaf, midday leaf, and midday stem water potential and their correlations with other measures of soil and plant water status in *Vitis vinifera*. *Journal of the American Society for Horticultural Science*, **127**, 448–454.

Williams TJ, Quinton WL, Baltzer JL (2013) Linear disturbances on discontinuous permafrost: Implications for thaw-induced changes to land cover and drainage patterns. *Environmental Research Letters*, **8**, 25006.

Willson CJ, Manos PS, Jackson RB (2008) Hydraulic traits are influenced by phylogenetic history in the drought-resistant, invasive genus *Juniperus* (Cupressaceae). *American Journal of Botany*, **95**, 299–314.

Winship L, Tjepkema J (1985) Nitrogen fixation and respiration by root nodules of *Alnus rubra* Bong.: Effects of temperature and oxygen concentration. *Plant and Soil*, **87**, 91–107.

Withington JM, Reich PB, Oleksyn J, Eissenstat DM (2006) Comparisons of structure and life span in roots and leaves among temperate trees. *Ecological Monographs*, **76**, 381–397.

Worbes M, Blanchart S, Fichtler E (2013) Relations between water balance, wood traits and phenological behavior of tree species from a tropical dry forest in Costa Rica - A multifactorial study. *Tree Physiology*, **33**, 527–536.

Wright IJ, Reich PB, Westoby M et al. (2004) The worldwide leaf economics spectrum. *Nature*, **428**, 821–827.

Wrona E (2016) *Evaluation of novel remote sensing techniques for soil moisture monitoring in the western Canadian Arctic* (unpublished Master's thesis). University of Guelph, Guelph, Canada.

2.8 Tables and figures

Table 2.1: Output of a linear mixed effects model used to test for differences in mean stem water potential (Ψ_{stem}) of green alders among topographic positions (top, middle, bottom, channel; see Fig. 2.1 for depiction of these positions) and measurement periods (early, mid-, and late season) as well as among topographic positions during different measurement periods (interaction between topographic position and measurement period) for the 2015 growing season. Measurement periods were as follows: June 18 (early season), July 26 (mid-season), and August 21 (late season). We used *a priori* contrasts to test for differences in mean Ψ_{stem} among topographic positions and measurement periods. We used 'individual' as a random effect to account for repeated measures. Significant p-values (<0.05) are bolded. Random effects information can be found in Table S7.

	Estimate	Standard error	df	t-value	p-value
Top vs. middle, bottom, channel	-2.0	0.537	8	-3.664	**0.006**
Middle vs. bottom, channel	-1.4	0.458	8	-3.058	**0.016**
Top vs. bottom	-3.0	1.375	8	-2.195	0.059
Early vs. mid-season	4.6	0.642	16	7.183	**2.18×10^{-6}**
Mid- vs. late season	4.8	0.642	16	7.399	**1.50×10^{-6}**
(Top vs. middle, bottom, channel)*(early vs. mid-season)	-1.4	0.710	16	-1.913	0.074
(Middle vs. bottom, channel)*(mid- vs. early season)	-0.5	0.605	16	-0.846	0.410
(Top vs. bottom)*(mid- vs. early season)	-2.0	1.816	16	-1.112	0.283
(Top vs. middle, bottom, channel)*(mid- vs. late season)	-1.5	0.710	16	-2.066	0.056
(Middle vs. bottom, channel)*(mid- vs. late season)	-1.0	0.605	16	-1.611	0.127
(Top vs. bottom)*(mid- vs. late season)	-1.4	1.816	16	-0.755	0.461

Table 2.2: Output of a two-way ANOVA ($F_{7,20}$ = 11.5, p = 8.40 x 10^{-6}) used to compare late season (August 21 and 9 in 2015 and 2016, respectively) stem water potential (Ψ_{stem}) of green alders as a function of topographic position (top, middle, bottom, channel; see Fig. 2.1 for depiction of these positions), study year (2015 vs. 2016), and their interaction. We used *a priori* contrasts to test for differences in mean late season Ψ_{stem} between topographic positions and study years. Significant p-values (<0.05) are bolded.

	Estimate	Standard error	t-value	p-value
Top vs. middle, bottom, channel	-3.4	0.700	0.700	**8.43×10^{-5}**
Middle vs. bottom, channel	-0.4	-0.597	0.714	0.483
Top vs. bottom	-4.4	1.790	-2.453	**0.024**
Year	-5.5	0.837	-6.555	**2.19×10^{-6}**
(Top vs. middle, bottom, channel)*year	-2.8	0.925	-3.067	**0.006**
(Middle vs. bottom, channel)*year	-0.2	0.789	-0.340	0.737
(Top vs. bottom)*year	-2.8	2.367	-1.203	0.243

Table 2.3: Output of the AIC_c-selected linear mixed effects model predicting green alder sap flow (SF_{daily}) during the 2015 growing season. We used the output of the best model to determine which specific abiotic variable(s) (in combination with the other variables in the selected model) best predicted SF_{daily}. We used *a priori* contrasts to test for differences in SF_{daily} among topographic positions (top, middle, bottom, channel; see Fig. 2.1 for depiction of these positions). Leaf N represents percent nitrogen in shrub leaves. Significant p-values (<0.05) are bolded. Random effects information can be found in Table S10.

	Estimate	Standard error	df	t-value	p-value
Top vs. middle, bottom, channel	-243.21	124.74	8	-1.877	0.097
Middle vs. bottom, channel	87.07	162.31	8	0.536	0.606
Top vs. bottom	382.28	306.60	8	1.247	0.248
Soil moisture (5 cm)	-101.64	165.49	12	-0.614	0.551
Leaf N	-66.58	118.91	8	-0.560	0.591
Frost table depth	-441.94	125.74	12	-3.515	**0.004**
(Top vs. middle, bottom, channel)*soil moisture	150.10	177.53	12	0.845	0.414
(Middle vs. bottom, channel)*soil moisture	24.53	110.51	12	0.221	0.828
(Top vs. bottom)*soil moisture	-208.95	453.40	12	-0.461	0.653

Table 2.4: Output of the AIC_c-selected linear mixed effects model predicting mean daily green alder sap flow (SF_{daily}) during the 2016 growing season. We used the output of the best model to determine which specific abiotic variable(s) (in combination with the other variables in the selected model) best predicted SF_{daily}. We used *a priori* contrasts to test for differences in SF_{daily} among topographic positions (top, middle, bottom, channel; see Fig. 2.1 for depiction of these positions). Leaf N represents percent nitrogen in shrub leaves. NH_4^+ (ammonium), NO_3^- (nitrate), and P (dihydrogen phosphate and hydrogen phosphate) represent ion supply rate in the soil beneath shrubs during the growing season. Significant p-values (<0.05) are bolded. Random effects information can be found in Table S11.

	Estimate	Standard error	df	t-value	p-value
Top vs. middle, bottom, channel	285.5522	166.3510	15.78	1.717	0.106
Middle vs. bottom, channel	-204.1548	150.9526	13.81	-1.352	0.190
Top vs. bottom	-798.8048	412.4377	16.12	-1.937	0.071
Soil moisture (20 cm)	-10.7804	107.3773	40.76	-0.100	0.921
Frost table depth	-192.2145	62.7565	32.84	-3.063	**0.005**
Leaf N	-264.1198	131.1754	11.70	-2.013	0.068
NH_4^+	-183.2630	129.7910	12.74	-1.412	0.182
NO_3^-	130.6901	143.5322	12.67	0.911	0.380
P	-146.9721	161.6820	11.83	-0.909	0.382
(Top vs. middle, bottom, channel)*soil moisture	-59.3875	137.0610	39.76	-0.433	0.667
(Middle vs. bottom, channel)*soil moisture	-39.6497	101.5875	33.14	-0.390	0.699
(Top vs. bottom)*soil moisture	-0.1858	376.5388	41.24	0.000	0.999

Table 2.5: Compilation of a series of studies investigating evapotranspiration (ET) rates ($mm \cdot day^{-1}$) of different tundra vegetation assemblages on the arctic tundra to facilitate qualitative comparison of our estimates of mean green alder patch transpiration to tundra ET values in the literature. The 'Mean ET' column shows the average ET value for the growing season investigated in the compared studies. We calculated green alder patch water flux for early in the growing season (E), during peak water use (P), and late in the growing season (L).

Study	Site	Vegetation assemblage	Mean ET	Duration of measurements	Measurement technique
Current study	Trail Valley Creek, Northwest Territories	Tall shrub patches dominated by green alder (*Alnus viridis*).	2015 – E: 0.74, P: 2.09, L: 0.09 2016 – E: 0.35, P: 1.30, L: 0.44	Five day periods during early June and late August and seven day periods during peak water use (~ middle of growing season) of 2015 and 2016	Scaled green alder stem sap flow to green alder patch transpiration
Muster *et al*., 2012	Samoylov Island, Siberia	Elevated polygon rims of dry tundra (dominated by *Hylocomium splendens* and *Dryas punctate*).	1.2	Late July to mid-September of 2008	Lysimeters and eddy covariance
Muster *et al*., 2012	Samoylov Island, Siberia	Low-lying centres of wet tundra on polygons (dominated by mosses).	1.3	Late July to mid-September of 2008	Lysimeters and eddy covariance
Blok *et al*., 2011	Kytalyk Nature Reserve, Siberia	Mosses and graminoids collected from wet sedge tundra.	1.5	Late July to early August of 2009	Lysimeters

Lafleur and Humphreys, 2007	Daring Lake, Northwest Territories	Mix of mesic heath tundra (dominated by low shrubs and lichen) and moist shrub tundra (dominated by low shrubs and sedges).	2004 – 1.2 2005 – 1.4 2006 – 1.7	Mid-May to late August of 2004-2006	Eddy covariance
Vourlitis and Oechel, 1999	Happy Valley, Alaska	Moist tussock tundra.	1994 – 1.5 1995 – 1.6	Early June to late August of 1994 and late May to early September of 1995	Eddy covariance
Stuart *et al.*, 1982	Eagle Creek, Alaska	Moist tussock tundra.	0.8	During 10, 24-hour periods from late June to mid-August of 1978	Leaf porometry
Stuart *et al.*, 1982	Eagle Creek, Alaska	Inter-tussock tundra (dominated by mosses and low shrubs).	1.3	During 10, 24-hour periods from late June to mid-August of 1978	Leaf porometry

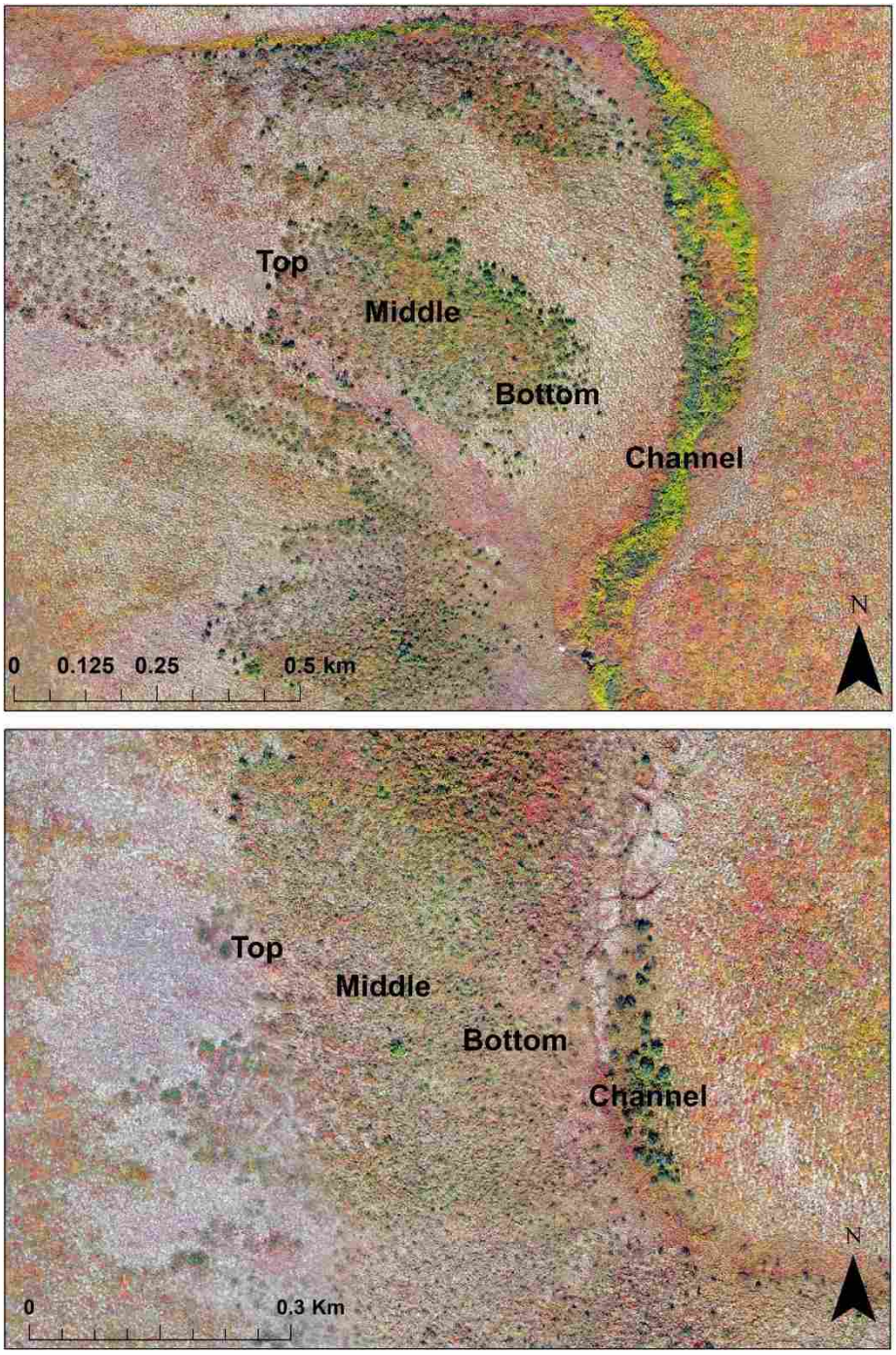

Fig. 2.1: Drone aerial images of shrub patches dominated by green alder in the Trail Valley Creek research basin used for the 2015 and 2016 growing seasons. The four topographic positions investigated per patch are labelled. Images were taken in August of 2015. Images courtesy of P. Marsh. Colour version available online.

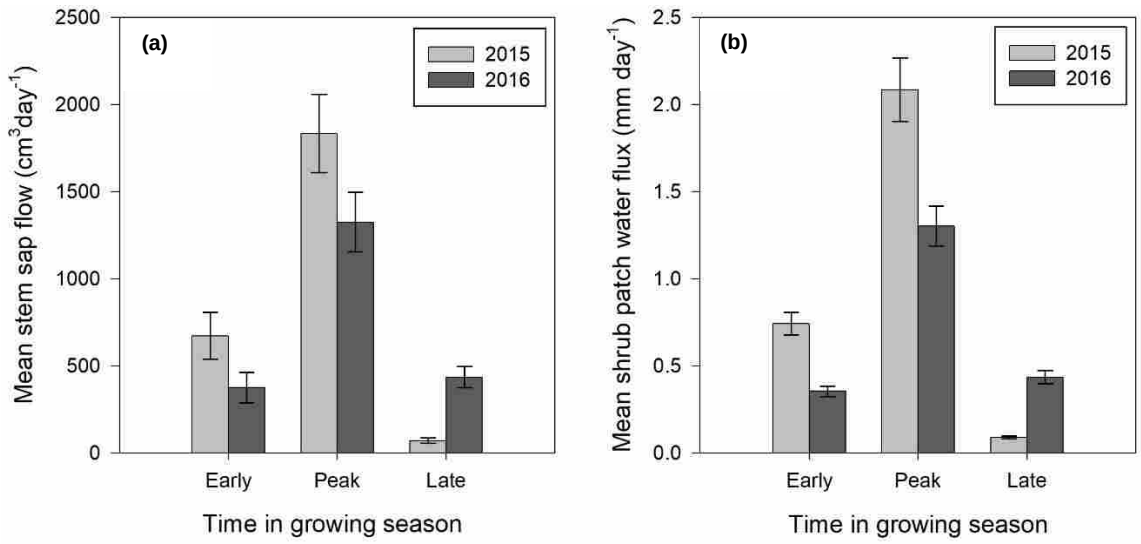

Fig. 2.2: (a) Mean sap flow (± standard error) of green alder stems early in the growing season, during peak physiological activity (i.e., maximum sap flow; approximately the middle of the growing season), and late in the growing seasons of 2015 and 2016. Stem sap flow was measured on one stem per shrub. Mean stem sap flow during peak physiological activity was calculated by averaging daily cumulative stem sap volume of individuals across a seven-day period surrounding the average day of maximum sap flow (excluding days with rainfall). Peak physiological activity of green alders was approximately June 22-June 28 in 2015 and July 9-15 in 2016. We used a similar procedure as above to characterize early and late season sap flow: we averaged daily cumulative sap volume across five-day periods based on when sap flow meters were installed (early season) and uninstalled (late season). Early season stem sap flow was calculated for June 13-17 and June 9-13 for 2015 and 2016, respectively. Late season stem sap flow was calculated for August 15-19 for 2015 and August 11-15 for 2016. Sample sizes are as follows: 2015 early, peak, and late = 9, 19, and 20, respectively; 2016 = 15, 23, and 11. (b) Mean green alder patch water flux (± standard error) during the same time periods as (a) calculated using the number of green alders per patch in 10 different patches and the area of the patches (C. Wallace, unpublished data; mean number of shrubs per patch = 74 ± 11). We assumed all shrubs were similar in size as sap flow meter-instrumented shrubs and had the same number of stems (n = 18) and that each stem had the same sapwood area (9.48 cm^2).

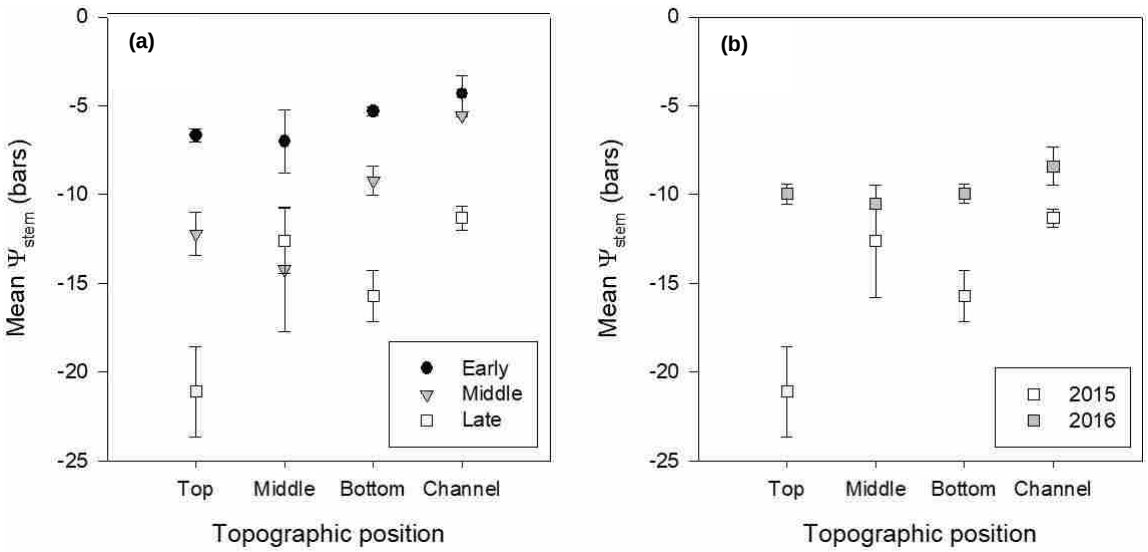

Fig. 2.3: (a) Scatterplot showing mean stem water potential (Ψ_{stem}) of green alders (± standard error) measured early in the growing season (June 18), mid-season (July 26), and late in the growing season (August 21) of 2015. Mean Ψ_{stem} significantly differed across a topographic gradient such that downslope locations generally had higher Ψ_{stem} values than upslope locations. Mean Ψ_{stem} also significantly differed across a seasonal gradient such that green alders had higher Ψ_{stem} values earlier in the season relative to mid-season and lower Ψ_{stem} values at the end of the season relative to mid-season. There was no significant interactive effect between topographic position and study year (Table 2.1). (b) Scatterplot showing mean late season Ψ_{stem} of green alders during the 2015 (August 21) and 2016 (August 9) study years. Mean late season Ψ_{stem} significantly differed between study years. Green alders located on the top of the patch slope had significantly lower late season Ψ_{stem} values than downslope locations in 2015 but not in 2016 (Table 2.2).

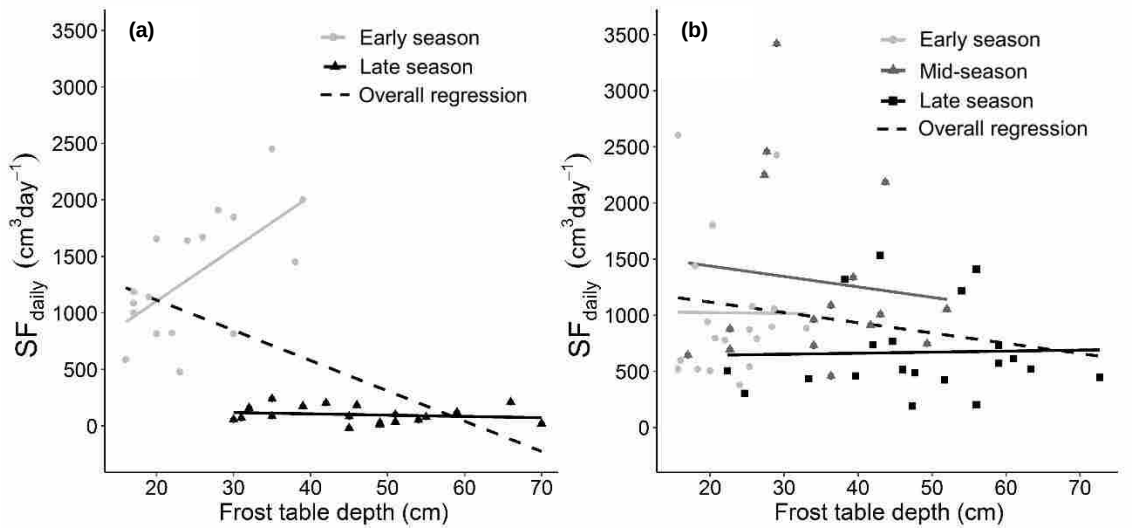

Fig. 2.4: Scatterplots of the relationship between frost table depth and green alder sap flow (mean daily cumulative sap volume during abiotic measurements; SF_{daily}) during the 2015 (a) and 2016 (b) growing seasons. The two abiotic measurement periods during the 2015 growing season were: June 30-July 3 (early season) and August 19-22 (late season). The three abiotic measurement periods during the 2016 growing season were: June 28-29 (early season), July 13-19 (mid-season), and August 6 (late season). The dashed lines represent the overall regression between frost table depth and SF_{daily} (across early, mid-, and late season measurements). Based on the outputs of the AICc-selected linear mixed effect models used to assess the relative importance of water availability, nutrient availability, and topography on green alder sap flow during the 2015 and 2016 growing seasons (Tables 2.3 and 2.4, respectively), the main abiotic driver of green alder SF_{daily} for both study years was frost table depth (2015: $p = 0.004$; 2016: $p = 0.005$).

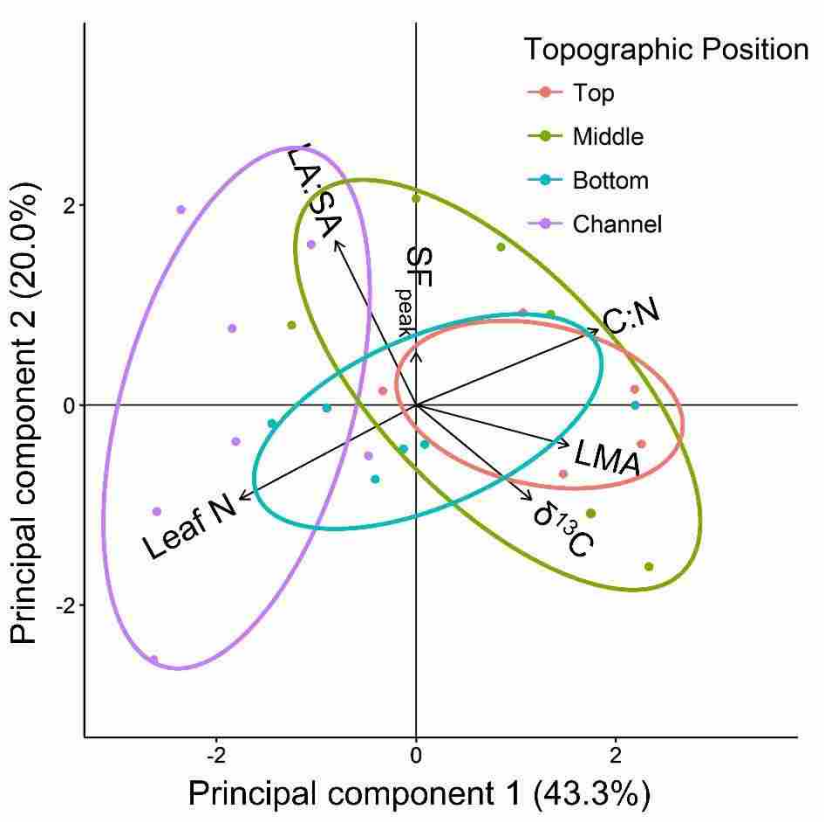

Fig. 2.5: Bi-plot of principal component 1 against principal component 2 from a principal components analysis (PCA) used to reduce functional traits of green alders into gradients that explain variation in resource use strategies in multivariate trait space. Principal component 1 was driven by topography (ANOVA; *a priori* contrast: top vs. channel; $F_{3,19}$ = 8.058, p = 0.009), with channel shrubs clearly separating out from those at the tops of patches. Green alders in channels were characteristic of higher leaf N (leaf nitrogen concentration) and lower C:N (leaf carbon to nitrogen ratio), LMA (leaf mass per area), and leaf $\delta^{13}C$ (integrated water use efficiency). Shrubs at the top of the patches were characterized by the opposite suite of traits. Mean daily cumulative sap volume during peak physiological activity (SF_{peak}) was unimportant in this bi-plot as indicated by its small arrow. LA:SA (leaf area to sapwood area ratio) represents whole-plant water use efficiency. The amount of variation explained by each principal component is indicated on each axis. Colour version available online.

2.9 Supplemental information

Table S1: 2015 and 2016 sample sizes for the number of green alder patches investigated, the number of topographic positions per patch (consistent across all patches), the number of green alders per topographic position (top, middle, bottom, channel; see Fig. 2.1 for depiction of these positions) and the total number of green alders studied. These sample sizes correspond with all measurements excluding stem water potential (see Table S2).

	2015	**2016**
Number of patches	8	3
Number of topographic positions per patch	4	4
Number of green alders per topographic position	6 per top, middle, and bottom; 3 per channel	7
Total number of green alders	27	28

Table S2: 2015 and 2016 sample sizes for the number of green alder patches investigated, the number of topographic positions per patch (consistent across all patches), the number of green alders per topographic position (top, middle, bottom, channel; see Fig. 2.1 for depiction of these positions), and the total number of green alders measured for stem water potential. All stem water potential measurements were performed at the patch closest to the Trail Valley Creek research station for logistical ease.

	2015	**2016**
Number of patches	1	1
Number of topographic positions per patch	4	4
Number of green alders per topographic position	3	4
Total number of green alders	12	16

Table S3: List of candidate linear mixed effects models used to assess the relative importance of water availability, nutrient availability, and topography on green alder water use (mean daily sap flow during abiotic measurements) during the 2015 growing season. The random effect term was 'individual' nested within 'patch' to account for our spatially-nested sampling design ('patch') and repeated measures ('individual').

Model name	Predictor variables used	Effects represented
M0 Null	None	None
M1 Soil moisture	Soil moisture measured at a 5 cm depth.	Surface water availability.
M2 Soil N	Leaf nitrogen concentration	Soil nitrogen (organic and inorganic) availability.
M3 Frost table depth	Frost table depth	Depth of the water table and rooting depth.
M4 Topography	*A priori* contrasts between topographic positions: top vs. middle, bottom, channel; middle vs. bottom, channel; top vs. bottom.	Influence of topography through variables that we were not able to directly measure.
M5 Topography*Soil moisture	Interaction between M1 and M3.	Influence of surface water availability at different topographic positions.
M6 All 'water' variables	M3 + M5	Influence of water availability.
M7 All 'nutrient' variables	M2 + M3 + M4	Influence of nutrient availability.
M8 Full model	M2 + M3 + M5	Combined influence of water availability and nutrient availability.

Table S4: List of candidate linear mixed effects models used to assess the relative importance of water availability, nutrient availability, and topography on green alder water use (mean daily sap flow during abiotic measurements) during the 2016 growing season. The random effect term was 'individual' nested within 'patch' to account for our spatially-nested sampling design ('patch') and repeated measures ('individual').

Model name	Predictor variables used	Effects represented
M0 Null	None	None
M1 Soil moisture	Soil moisture measured at a 20 cm depth.	Surface water availability.
M2 Soil N	Leaf nitrogen concentration	Soil nitrogen (organic and inorganic) availability.
M3 Soil inorganic nutrients	Ammonium (NH_4^+), nitrate (NO_3^-), dihydrogen phosphate, and hydrogen phosphate (P) supply rates.	Soil inorganic nutrient availability.
M4 Frost table depth	Frost table depth	Depth of the water table and rooting depth.
M5 Topography	*A priori* contrasts between topographic positions: top vs. middle, bottom, channel; middle vs. bottom, channel; top vs. bottom.	Influence of topography through variables that we were not able to directly measure.
M6 Topography*Soil moisture	Interaction between M1 and M5.	Influence of surface water availability at different topographic positions.
M7 All 'water' variables	M4 + M6	Influence of water availability.
M8 All 'nutrient' variables	M2 + M3 + M4 + M5	Influence of nutrient availability.
M9 Full model	M2 + M3 + M4 + M6	Combined influence of water availability and nutrient availability.

Table S5: Pearson's correlation matrix to test for collinearity between continuous predictors for the 2015 growing season. Leaf N represents percent nitrogen in green alder leaves. We excluded collinear variables from models using a cut-off correlation coefficient of r = 0.3.

	Frost table depth	Soil moisture (5 cm)	Leaf N
Frost table depth	1.00		
Soil moisture (5 cm)	0.26	1.00	
Leaf N	0.09	-0.20	1.00

Table S6: Pearson's correlation matrix to test for collinearity between continuous predictors for the 2016 growing season. Leaf N represents percent nitrogen in green alder leaves. NH_4^+ (ammonium), NO_3^- (nitrate), P (dihydrogen phosphate and hydrogen phosphate), and K^+ (potassium) represent ion supply rate in the soil beneath green alders during the growing season. We excluded collinear variables from models using a cut-off correlation coefficient of r = 0.3 (variables with r > 0.3 are bolded). Based on this correlation matrix, soil moisture (5 cm) and K^+ were excluded from models.

	Frost table depth	Soil moisture (5 cm)	Soil moisture (20 cm)	NO_3^-	NH_4^+	P	K^+	Leaf N
Frost table depth	1.00							
Soil moisture (5 cm)	0.01	1.00						
Soil moisture (20 cm)	-0.24	**0.41**	1.00					
NO3$^-$	-0.12	**0.37**	0.18	1.00				
NH4$^+$	-0.17	-0.13	-0.02	0.23	1.00			
P	0.18	0.07	-0.17	0.02	0.19	1.00		
K	0.15	-0.20	**-0.42**	-0.26	-0.06	0.28	1.00	
Leaf N	0.18	-0.04	-0.09	-0.04	-0.05	-0.15	-0.07	1.00

Table S7: Random effects output for a linear mixed effects model used to test for differences in mean stem water potential (Ψ_{stem}) of green alders among topographic positions and measurement periods (early, mid-, and late season) as well as among topographic positions (top, middle, bottom, channel; see Fig. 2.1 for depiction of these positions) during different measurement periods (interactive effect). 'Individual' was used as a random effect to account for repeated measures.

	Variance	Standard deviation
Individual	0.363	0.602
Residual	7.418	2.724

Table S8: AIC_c-based rankings from best to worst for nine candidate linear mixed effects models predicting green alder sap flow (SF_{daily}) during the 2015 growing season. Model rankings were based on AIC_c (corrected Akaike's information criterion) values and the associated statistics (Burnham and Anderson, 1998). The associated statistics shown are the difference between each model and the minimum AIC_c model (Δi), the number of parameters per model (K), the log-likelihood values (LogLik), the Akaike weights (w_i), the amount of variation in SF_{daily} that the fixed effects of each model accounted for (pseudo marginal R^2; R^2_m), and the total amount of variation in SF_{daily} that each model accounted for (pseudo conditional R^2; R^2_c; fixed effects and random effects combined). The random effect term was 'individual' nested within 'patch' to account for our spatially-nested sampling design ('patch') and repeated measures ('individual').

Model	K	AIC_c	Δi	LogLik	w_i	R^2_m	R^2_c
M8 Full model	13	484.55	0.00	-221.00	0.97	0.344	0.344
M6 All 'water' variables	12	491.25	6.69	-226.84	0.03	0.352	0.370
M5 Topography*soil moisture	11	508.89	24.34	-237.95	0.00	0.106	0.106
M7 All 'nutrient' variables	9	517.05	32.50	-246.07	0.00	0.329	0.333
M4 Topography	7	546.08	61.53	-264.04	0.00	0.022	0.022
M3 Frost table depth	5	553.09	68.54	-270.55	0.00	0.284	0.284
M1 Soil moisture	5	563.65	79.10	-275.82	0.00	0.031	0.031
M2 Soil N	5	564.73	80.17	-276.36	0.00	0.000	0.000
M0 Null	4	573.50	88.95	-282.11	0.00	0.000	0.000

Table S9: AIC_c-based rankings from best to worst for 10 candidate linear mixed effects models predicting green alder sap flow (SF_{daily}) during the 2016 growing season. Model rankings were based on AIC_c (corrected Akaike's information criterion) values and the associated statistics (Burnham and Anderson, 1998). The associated statistics shown are the difference between each model and the minimum AIC_c model (Δi), the number of parameters per model (K), the log-likelihood values (LogLik), the Akaike weights (w_i), the amount of variation in SF_{daily} that the fixed effects of each model accounted for (pseudo marginal R^2; R^2_m), and the total amount of variation in SF_{daily} that each model accounted for (pseudo conditional R^2; R^2_c; fixed effects and random effects combined). The random effect term was 'individual' nested within 'patch' to account for repeated measures and our spatially nested sampling design, respectively.

Model	K	AIC_c	Δi	LogLik	w_i	R^2_m	R^2_c
M9 Full model	16	730.61	0.00	-342.15	1.00	0.312	0.782
M8 All 'nutrient' variables	12	762.60	31.99	-365.58	0.00	0.320	0.758
M7 All 'water' variables'	12	768.75	38.14	-368.66	0.00	0.140	0.790
M6 Topography*soil moisture	11	784.92	54.31	-378.39	0.00	0.088	0.696
M5 Topography	7	819.68	89.07	-401.65	0.00	0.084	0.681
M3 Soil inorganic nutrients	7	820.88	90.27	-402.25	0.00	0.070	0.771
M4 Frost table depth	5	833.86	103.25	-411.32	0.00	0.064	0.740
M2 Soil N	5	836.66	106.05	-412.71	0.00	0.140	0.620
M1 Soil moisture	5	841.78	111.17	-415.28	0.00	0.002	0.636
M0 Null	4	850.25	119.64	-420.73	0.00	0.000	0.625

Table S10: Random effects output for the AICc-selected linear mixed effects model predicting green alder sap flow during the 2015 growing season. The random effect term was 'individual' nested within 'patch' to account for our spatially-nested sampling design ('patch') and repeated measures ('individual').

	Variance	Standard deviation
Patch	6.66×10^{-2}	0.258
Patch/individual	3.52×10^{-4}	1.88×10^{-2}
Residual	4.18×10^{5}	646.7

Table S11: Random effects output for the AICc-selected linear mixed effects model predicting green alder sap flow during the 2016 growing season. The random effect term was ‘individual’ nested within ‘patch’ to account for our spatially-nested sampling design (‘patch’) and repeated measures (‘individual’).

	Variance	Standard deviation
Patch	6.57×10^4	487.3
Patch/individual	2.37×10^5	256.3
Residual	1.41×10^5	375.4

Table S12: Loadings of a principal components analysis used to reduce functional traits of green alders into gradients that explain variation in resource use strategies in multivariate trait space. Principal components 1-3 cumulatively explained 82.8% of the variation in the functional trait dataset. The magnitude and directionality of the loadings of our three retained principal components indicate that principal components 1 and 2 can be thought of as separate functional trait spectra. The first principal component explained a gradient in leaf investment and productivity: increasing leaf N (leaf nitrogen concentration) and decreasing C:N (leaf carbon to nitrogen ratio) and LMA (leaf mass per area). The second principal component explained a gradient in water use efficiency: increasing LA:SA (leaf area to sapwood area ratio) and decreasing leaf $\delta^{13}C$ (integrated water use efficiency). The third principal component was mainly explained by mean daily cumulative sap volume during peak physiological activity (SF_{peak}).

	Principal component 1	Principal component 2	Principal component 3
Variation explained (%)	43.3	22.0	17.5
Leaf N	-0.54	-0.40	0.06
C:N	0.56	0.32	-0.19
$\delta^{13}C$	0.35	-0.41	-0.15
LA:SA	-0.25	0.70	-0.18
LMA	0.47	-0.17	0.31
SF_{peak}	-0.00	0.22	0.90

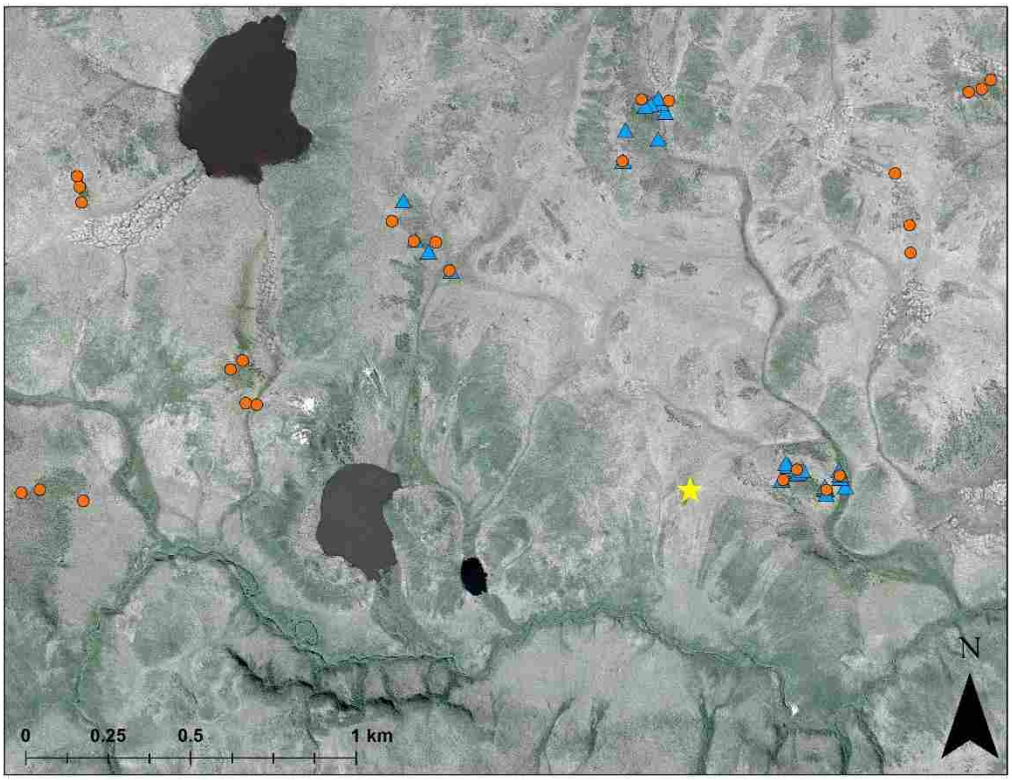

Fig. S1: Map of the lower portion of the Trail Valley Creek research basin indicating the locations of sap flow meter-instrumented shrubs for the 2015 (orange circles) and 2016 (blue triangles) growing seasons. The yellow star indicates the location of the Trail Valley Creek research station base camp. Colour version available online.

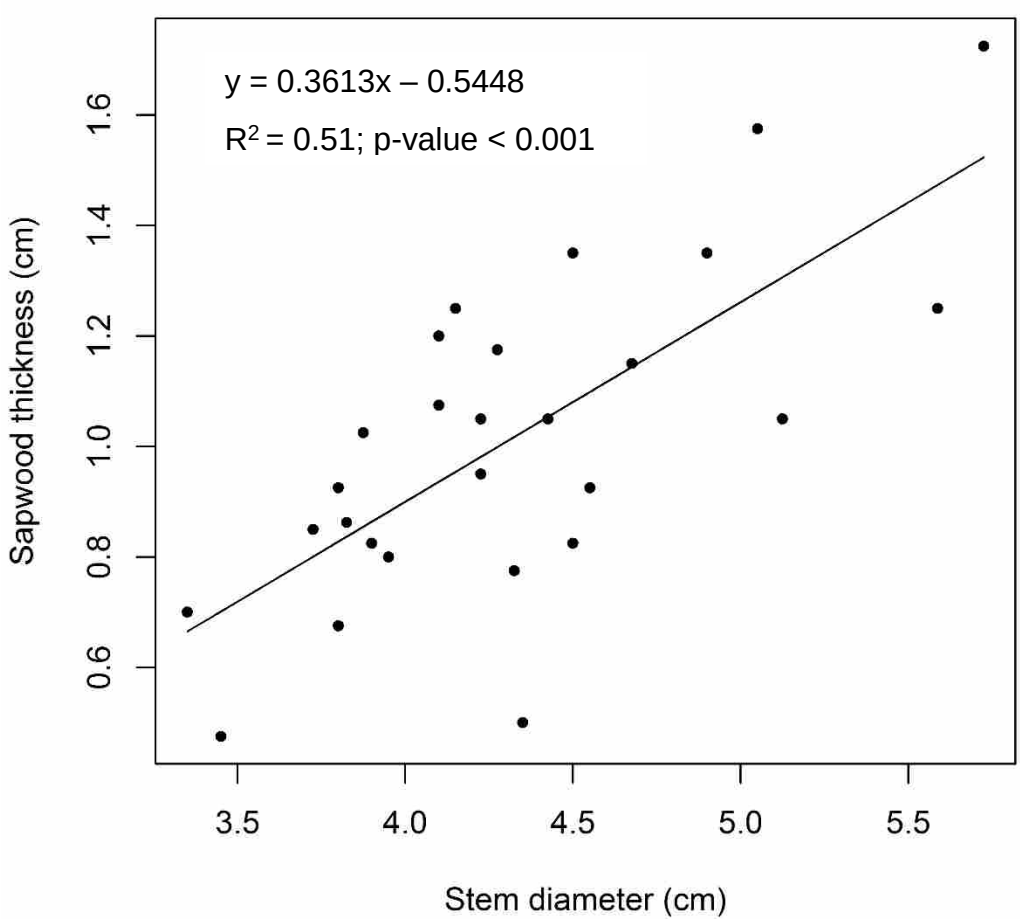

Fig. S2: Linear regression between stem diameter and sapwood thickness for the green alder stem cross-sections collected during the 2016 growing season. The equation of the fitted line and stem diameter information measured during the 2015 growing season were used to estimate sapwood thickness for the stem cross-sections collected during the 2015 growing season.

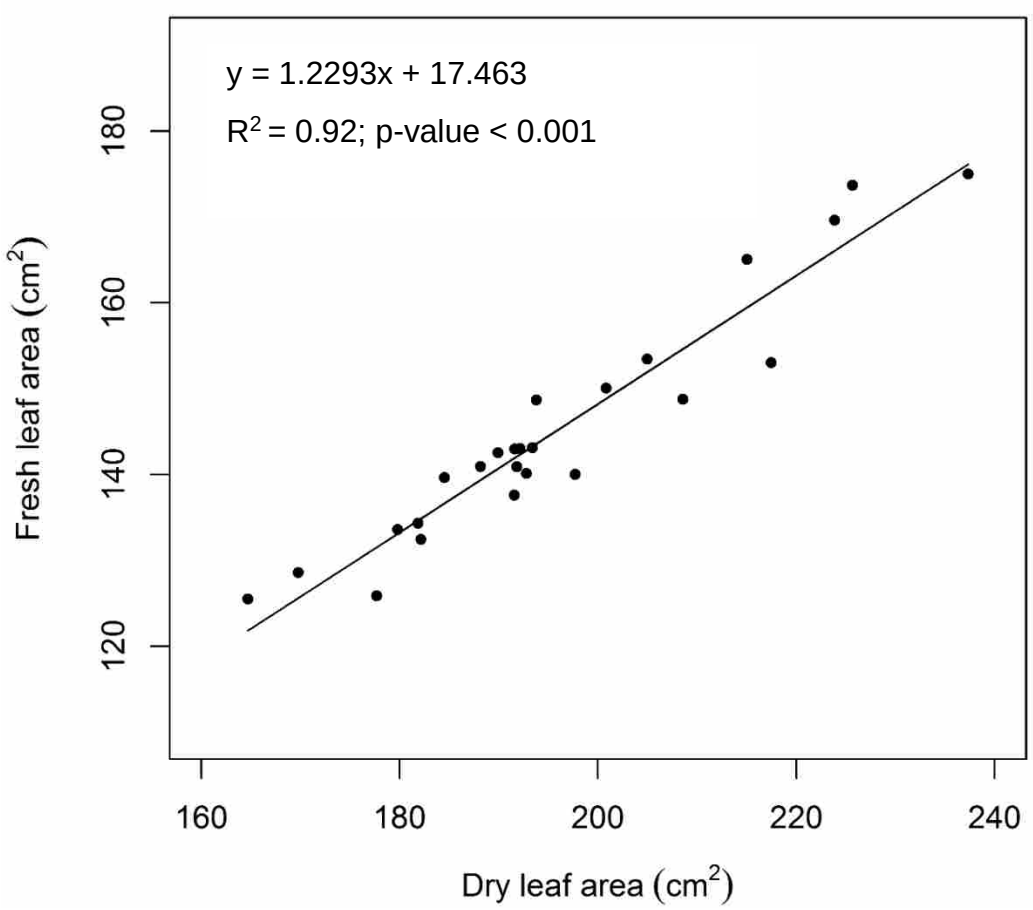

Fig. S3: Linear regression between dry leaf area and fresh leaf area per scanned batch of green alder leaves (n = 25 batches of leaves; 20 leaves per batch; 400 leaves total) for the 2016 growing season. Following removal of sap flow meters, all leaves were removed from instrumented stems to measure total stem leaf area. Due to the large number of leaves, fresh leaf scans for all instrumented stems was not feasible. To address this, we developed a relationship between fresh leaf area and dry leaf area using a subsample of fresh leaves which were scanned in batches and their batch areas measured. These leaves were then oven dried for 48 hours at 70°C and re-scanned to determine dry leaf area and the subsequent fresh to dry leaf area relationship. All remaining leaves were oven-dried, scanned in batches, and the fresh to dry leaf area relationship was used to correct for leaf shrinkage in the large batches. The fresh area of each batch was summed for each instrumented stem to obtain total stem leaf area. All leaf area measurements were performed using WinFOLIA (v. 2004a, Regent Instruments Inc., Ville de Québec, QC, CA).

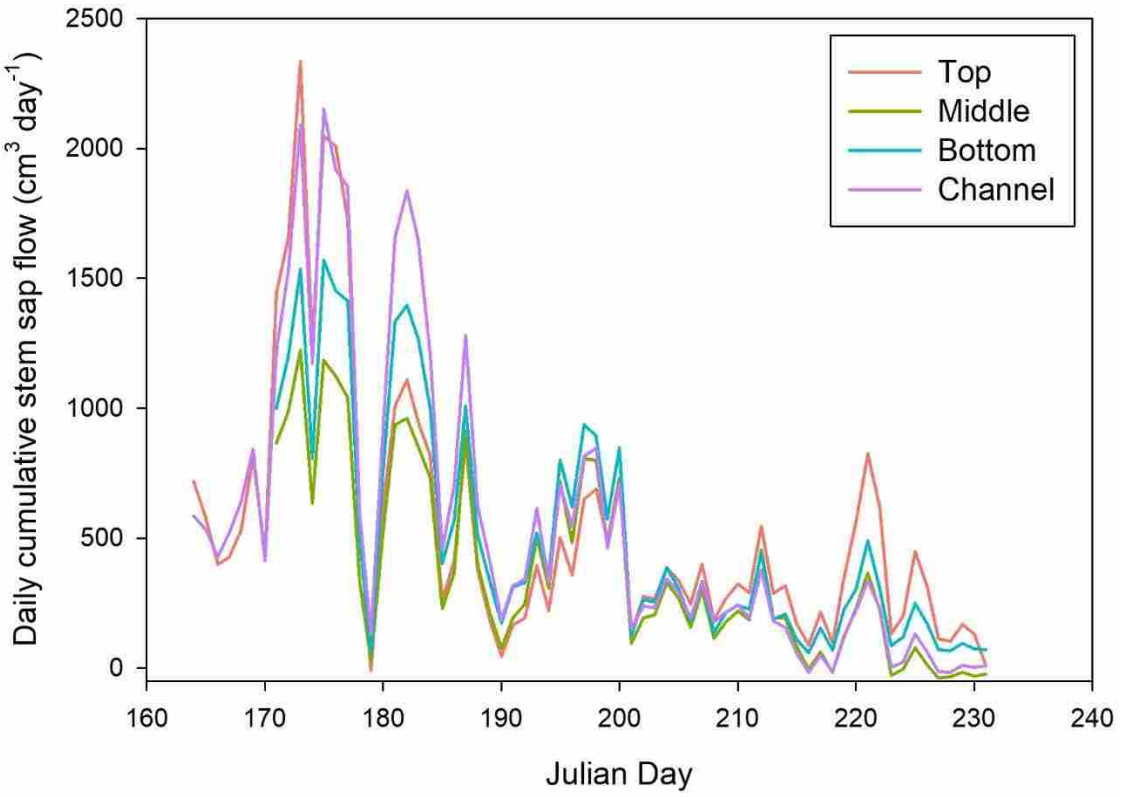

Fig. S4: Continuous tracing of daily cumulative stem sap flow for four shrubs (one per topographic position: top, middle, bottom, and channel) during the 2015 growing season (approximately early June to late August). Despite technical issues that prevented us from calculating the total (cumulative) volume of sap used by green alder stems during the 2015 and 2016 growing seasons, the four shrubs used in this figure had full datasets that are representative of the general seasonal variation in sap flow experienced by our study shrubs in both 2015 and 2016. Colour version available online.

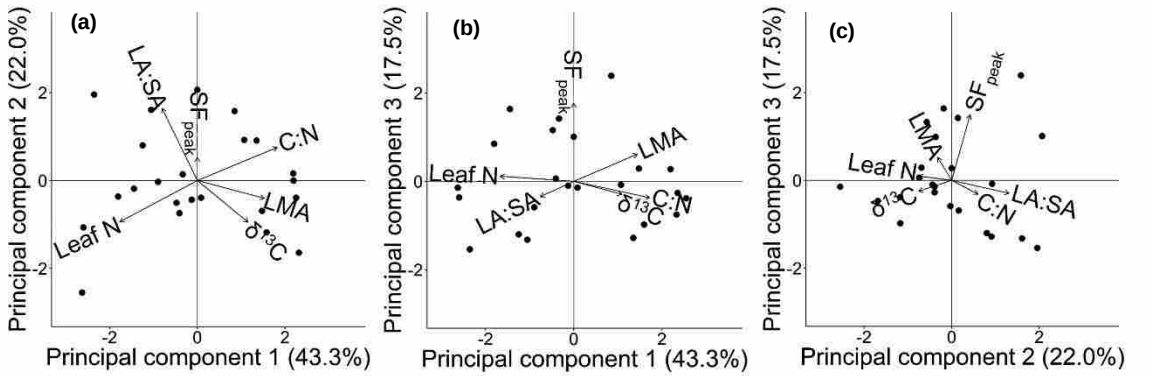

Fig. S5: (a) Bi-plot of principal component 1 against principal component 2 from a principal components analysis used to reduce functional traits of green alders into gradients that explain variation in resource use strategies in multivariate trait space. (b) Bi-plot of principal component 1 against principal component 3. (c) Bi-plot of principal component 2 against principal component 3. The amount of variation explained by each principal component is indicated on each axis. Principal component 1 explained a gradient in productivity, leaf investment, and leaf water use efficiency: decreasing leaf N (leaf nitrogen concentration) and increasing leaf C:N (carbon to nitrogen ratio), LMA (leaf mass per area) and leaf $\delta^{13}C$ (integrated water use efficiency). Principal component 2 explained a gradient in leaf and whole plant water use efficiency: decreasing leaf $\delta^{13}C$ and increasing LA:SA (leaf area to sapwood area ratio). Principal component 3 represented mean daily cumulative sap volume during peak physiological activity (SF_{peak}).

Chapter 3: Summary and general discussion

3.1 Summary of main research findings

The overarching goal of this study was to improve the current understanding of tundra shrub function. The objectives were to 1) characterize tall tundra shrub water use; 2) investigate how topography and associated gradients in water and nutrient availability influence tundra shrub water use; and 3) examine the variability in functional traits among individuals and determine if this variability is attributable to shrub distribution along topographic and resource gradients. We used green alder (*Alnus viridis* ssp. *fruticosa*) as our study species and performed this study during the growing seasons of 2015 and 2016 at Trail Valley Creek (TVC) in the Northwest Territories. The main findings were as follows:

a) On average, green alder stems used 1832.13 cm^3 of water per day (± 224.05 $cm^3 day^{-1}$) and 1324.99 cm^3 of water per day (± 170.13 $cm^3 day^{-1}$) during peak physiological activity (maximum sap flow) in the summers of 2015 and 2016, respectively. Green alders contributed an average of 2.09 $mm \cdot day^{-1}$ (± 0.18 $mm \cdot day^{-1}$) and 1.30 $mm \cdot day^{-1}$ (± 0.11 $mm \cdot day^{-1}$) to tall shrub patch transpiration during peak physiological activity in 2015 and 2016, respectively. The overall (growing season) mean shrub patch water flux was 0.97 $mm \cdot day^{-1}$ (± 0.59 $mm \cdot day^{-1}$) in 2015 and 0.70 $mm \cdot day^{-1}$ (± 0.53 $mm \cdot day^{-1}$) in 2016.
b) Green alder water status significantly varied across topographic and seasonal gradients. Shrubs located in upslope locations (tops and middles of patch slopes) had significantly lower water potentials (more negative) than downslope locations

(bottoms and drainage channels of patches). Shrub water potential decreased from early season to mid-season to late season.

c) The combined effects of topography, water availability, and nutrient availability were important for predicting shrub physiological function, but the most important driver of sap flow was frost table depth. The overall relationship between frost table depth and sap flow was negative.

d) Leaf functional traits were dictated by topography; green alders in channels had higher leaf N, lower investment in leaf structure (low LMA and C:N) and less conservative water use (low $\delta^{13}C$), whereas green alders at the tops of slopes had the opposite.

3.2 Main conclusions

For green alder, active layer thaw is an important driver in water use and underlies water availability. The depth of the frost table plays an important role in controlling surface water availability as the water table sits on top of a seasonally lowering frost table. This relationship may provide insight into how shrub water use and productivity may respond to climate-induced permafrost thaw.

We provide evidence of a leaf functional trait spectrum that explains differences in fast to slow water and nutrient use strategies between shrubs at the tops of patches and in channels. Channel shrubs reflected traits associated with higher resource environments and greater productivity and growth relative to the slower-return strategy of shrubs at the tops of patch slopes. Although resource use strategies involve complex interactions between physiological processes, plant architecture, and abiotic and biotic factors, we

believe that the associations between the traits we measured allow us to identify differences in productivity among shrubs with relevance to their topographic position.

This research will contribute to an improved understanding of the role of resource limitation on tundra shrub function because it provides valuable insight into the abiotic drivers of tundra shrub water use and productivity. Improving our understanding of constraints on shrub distribution will help predict what shrub cover may look like in the future.

3.3 Integration of other research

This work incorporates information from other plant ecology studies performed by Wilfrid Laurier University (WLU) researchers. Cory Wallace, a Ph.D. candidate in Dr. Baltzer's Forest Ecology Research Group (FERG), is investigating the differences in a range of abiotic and biotic conditions between green alder patches and the surrounding open tundra at TVC. Much of Wallace's preliminary field work at TVC guided the research questions investigated in this work as well as the sampling design. Information on the number of green alders per patch and green alder patch area across 10 patches in the TVC research basin obtained by Wallace were used to scale our estimates of stem sap flow to shrub patch transpiration. Wallace's results also provide complementary information to our study. For instance, Wallace's comparisons between green alder patches and open tundra at TVC showed that green alder patches have significantly lower soil water availability than the open tundra (Fig. 3.1a), implying that green alder patches have greater water use and the potential to decrease growing season run-off. Further, Wallace found that surface soil moisture decreases with green alder density (Fig. 3.1b), suggesting that green alder water use has important consequences for local surface

hydrology during the growing season through increased evapotranspirative water loss in areas with more shrubs.

Jenna Rabley, a former undergraduate thesis student in FERG, studied the distribution of N-fixing nodules across the topographic gradient of shrub patches. Rabley's sampling was paired with a subsample of shrubs used in the present study (n = 16) so that we could investigate relationships between topographic position within a shrub patch, nodulation, and shrub function. Rabley found that topographic position was a significant predictor of nodule count per shrub, with shrubs at the bottom of patch slopes having the most nodules. However, average nodule biomass per shrub and total nodule biomass per shrub did not significantly differ among topographic positions. We briefly commented on the potential influence of nodulation on green alder function in Chapter 2 and use this chapter as an opportunity to further explore these relationships as *Frankia* is known to play a substantial role in the N requirements of *Alnus* spp. in other ecosystems (Hurd *et al.*, 2001; Myrold & Huss-Danell, 2003).

We used Rabley's estimates of average and total nodule biomass per shrub and nodule count per shrub to predict the scores of the three principal components (PCs) that we retained in the Principal Components Analysis (PCA) explained in Chapter 2 (refer to Table S12). Predictor variables were visually inspected for normality and square root-transformed when necessary. We applied false discovery rates to p-values from linear regressions that used the same response variables (three adjustments total to account for re-using each of the three PCs as responses to each of the three nodulation metrics) using the Benjamini-Hochberg method (built-in R function 'p.adjust'; Benjamini & Hochberg, 1995). There were no significant relationships between any of the principal components

and nodulation metrics (Table 3.1; Fig. 3.2-3.4). Thus, the relationships between nodulation and tundra shrub function are more complicated than we anticipated.

3.4 Collaboration involved in this work

This work is part of a much larger, long-term, and integrative study aimed at understanding hydrological and ecological changes of high latitude systems under climate change. This project is in multidisciplinary collaboration between FERG researchers and Dr. Philip Marsh (Canada Research Chair in Cold Regions and Water Science, WLU), Dr. Aaron Berg (Canada Research Chair in Hydrology and Remote Sensing, University of Guelph), Dr. Oliver Sonnentag (Canada Research Chair in Atmospheric Biogeosciences at High Latitudes, Université de Montréal), and Dr. Chris Derksen (Research Scientist, Environment and Climate Change Canada). This research team is interested in understanding and predicting the integrated effects of climate on vegetation, snow, permafrost, and lake and stream characteristics. This project is ongoing at TVC and will involve documenting the state of climate, snow, active layer processes, vegetation, and freshwater balance. This broader program aims to carry out detailed ground validation of remote sensing data to understand large-scale variability in permafrost, vegetation, and freshwater characteristics to improve monitoring protocols and predictive tools.

The current work focused on the vegetation aspect of this larger project to develop and improve the current understanding of shrub function at TVC. This work is unique in this context because it provides insight into how tall shrub water use may alter hydrologic conditions through evapotranspiration during the growing season. Limited field measures have been undertaken to understand the moisture and nutrient constraints

on shrub expansion as the climate warms and as such, this work will contribute to the parameterization of new predictive tools. The changes in function of the tundra ecosystem associated with shrub expansion will be incorporated into models that will be important for the assessment, regulatory approvals, management, and development of the north.

3.5 Future work

3.51 Hydrological modelling

Chapter 1 emphasized the need for accurate estimates of tundra shrub water use so that predictive models can be used to predict broad-scale evapotranspiration rates and the associated hydrological impacts. Chapter 2 provided estimates of shrub water use in terms of single stem sap flow as well as scaled green alder patch water flux. Modellers from Dr. Marsh's research group in the Department of Geography at WLU can now incorporate these data into hydrological predictions for the TVC research basin to understand how predicted future increases in shrub cover may alter run-off and basin discharge.

3.52 Further quantification of water and nutrient availability along shrub patch toposequences

As explained in Chapter 2, we found that green alder leaf functional traits were driven by topography, but it is not clear whether this is due to topographically-driven differences in water or nutrient availability. Since leaf traits reflecting both water use ($\delta^{13}C$) and nutrient use (leaf N) significantly differed between the tops of patch slopes and channels, it is likely that both water and nutrient availability are important drivers of shrub functional traits, but we do not know which resource is more important. There are

several different field measures that could be performed to help discern between the effects of water vs. nutrient availability on shrub functional traits since soil moisture, frost table depth, soil inorganic nutrient availability, and nodulation did not significantly differ between the tops of slopes and channels.

As discussed in Chapter 2, quantification of dissolved organic nitrogen (DON) may demonstrate higher organic N availability in channels compared to the tops of slopes, which may explain why channel shrubs had higher leaf N. There are competing hypotheses about which method is best for assessing DON as it is highly influenced by environmental factors (e.g., Jones & Willett, 2006; Ros *et al.*, 2009). However, Mobley *et al.* (2014) measured KCl-extractable DON in surface soils across the US Great Plains and found that a gradient in DON helped explain a gradient in grassland productivity. A similar method should be employed at TVC to understand spatial patterns in DON and whether DON is an important predictor of leaf N and thus shrub productivity.

Characterizing seasonal variability in water table depth and soil/run-off water quality at different topographic positions in patches would be another useful way to quantify water and nutrient availability, respectively. We initially planned to install water wells at the four topographic positions of green alder patches to measure seasonal variation in water table depth and well water quality (using a YSI Pro Plus meter; pH, electrical conductivity, ammonium concentration, and nitrate concentration) but due to logistical issues, we were not able to follow through with this. Wells should be installed along toposequences in green alder patches in future field campaigns to confirm that the water table is shallower in downslope locations. Testing for water quality in these wells would provide additional information regarding soluble inorganic nitrogen concentrations

across topographic gradients as the PRS probes did not yield any topographic differences in NH_4^+ or NO_3^- supply rates, potentially due to high variability in soil conditions with microtopography. This method may also help identify the mechanism for any potential differences in nutrient concentrations between topographic positions (i.e., whether it is due to a surge of nutrients in downslope locations after rain and subsequent run-off events or other reasons).

Hydrologists in Dr. Marsh's research group have measured snow water equivalent along some of the TVC green alder patches that we investigated, and this information could be used to understand how much snow is captured at each topographic position and the amount of water that is deposited via snowmelt. Further, snow samples could be collected from different depths within the snowpack before melt and analyzed to estimate how stored N in snow influences early season growth at each topographic position. Sites with relatively greater snow capture and melt (e.g., bottoms of patch slopes and channels) should receive relatively more N that was deposited in the snow reservoir during the winter (Bowman, 1992). Dr. Marsh's group also has drone aerial images of TVC shrub patches during the melt period which could be used to determine the timing of snow-off for each topographic position. The timing of snow-off has implications for soil moisture and temperature, which may delay shrub leaf out and function, potentially shortening the growing season for shrubs at sites with later melt (Bowman, 1992). Thus, the timing of snow-off may determine topographic patterns in plant ramp-up and early season productivity.

Since frost table depth was a negative driver of sap flow, continuous soil moisture measurements at different depths beneath green alders would be useful for predicting

continuous sap flow data to understand where green alders predominantly access soil water and how shrubs respond to a seasonally deepening frost table. As mentioned in Chapter 2, Warren (2015) used a similar protocol and found that soil moisture at ~10 cm depth was a better predictor of black spruce sap flow compared to soil moisture at ~5 and ~20 cm depths. We did install continuous soil moisture loggers at 5, 10, and 20 cm depths beneath shrubs at one patch at TVC, but due to technical issues, we did not have enough data to test for correlations between continuous soil moisture and sap flow data. The exact rooting depth and distribution of green alder roots is not yet known for TVC. To further understand where alder roots access water and nutrients, green alders should be excavated to quantify the horizontal and vertical spread of roots.

Although Rabley (2017) provided estimates of nodulation rates along the topographic gradient of green alder patches, characterization of N-fixation rates is necessary to understand how *Frankia* contributes to the N requirements of green alders at TVC. Since we did not find a relationship between nodulation and green alder functional traits, the strains of *Frankia* at TVC may be ineffective (Wolters *et al.*, 1997). Thus, green alders at TVC may rely more on N sources from the soil rather than N fixed by *Frankia* relative to the high N contribution of *Frankia* to *Alnus* spp. at non-tundra sites (70-100%; Hurd *et al.*, 2001; Myrold & Huss-Danell, 2003). N-fixation rates are commonly estimated through acetylene reduction activity which uses the ability of the nitrogenase enzyme to reduce triple bounded substrates. More specifically, the measurement uses the nitrogenase-catalyzed reduction of acetylene gas to ethylene, chromatographic isolation of both gases, and then measurement with a hydrogen flame analyzer (Hardy *et al.*, 1968). Such assays should be performed on fresh nodules

collected from TVC to quantify N-fixation rates across the topographic gradient of shrub patches.

Comparing the above additional metrics of water and nutrient availability between topographic positions and using them to predict shrub water use and functional traits may provide greater correlative evidence for which resource is primarily influencing shrub water use and function. In addition, direct evidence could be obtained through controlled, experimental approaches involving water and nutrient additions and inoculation of field-collected *Frankia* while controlling for the effect of topography (i.e., a greenhouse experiment).

3.53 Photosynthetic rates

Most functional trait analyses use direct measures of photosynthetic assimilation rates (e.g., Wright *et al.*, 2004; Reich, 2014), whereas we were only able to use leaf N as a proxy of photosynthetic potential. To further corroborate our findings regarding variation in shrub leaf N (productivity) between topographic positions, direct measures of photosynthetic capacity should be performed as additional factors such as leaf structure influence photosynthetic rates (Niinemets, 1999).

3.54 Stem water storage

In Chapter 2, we postulated that stem water storage may explain why sap flow was decoupled from leaf and whole-plant water use efficiency in our PCA. To test whether this is true, diurnal stem water storage measurements need to be made. One way to quantify the diurnal exchange of water between the transpiration stream and stem storage compartments is to simultaneously measure sap flow at the base of stems (a proxy for water withdrawn from the soil reservoir) and in upper branches (a proxy for water

leaving the plant via transpiration). The difference between basal sap flow and canopy transpiration can then be used to estimate the magnitude and direction of water flow between the transpiration stream and storage tissues (Wullschleger *et al.*, 1998). Using this technique, Goldstein *et al.* (1998) found that the amount of water withdrawn from storage tissues in five canopy tree species of a seasonal tropical forest in Panama represented 9-15% of the total daily water loss. Wood traits relating to stem hydraulic conductance, such as wood density and conduit diameter, could also be used in a more comprehensive, whole-plant economics spectrum to understand variability in water storage among shrubs (Chave *et al.*, 2009). These approaches should therefore be used in future tundra water use studies to understand how tall shrub water storage relates to water use efficiency, water stress with active layer development, and overall shrub function.

3.6 Chapter summary

Overall, this work provides valuable insight into the drivers of green alder function, and we provide suggestions for future work to further improve the current knowledge. Green alder is expanding rapidly across the low arctic tundra of the Northwest Territories and understanding the drivers of its productivity is critical for predicting future tundra conditions.

3.6 References

Benjamini Y, Hochberg Y (1995) Controlling the false discovery rate: A practical and powerful approach to multiple testing. *Journal of the Royal Statistical Society*, **57**, 289-300.

Bowman WD (1992) Inputs and storage of nitrogen in winter snowpack in an alpine ecosystem. *Arctic and Alpine Research*, **24**, 211–215.

Chave J, Coomes D, Jansen S, Lewis SL, Swenson NG, Zanne AE (2009) Towards a worldwide wood economics spectrum. *Ecology Letters*, **12**, 351–366.

Goldstein G, Andrade JL, Meinzer FC, Holbrook NM, Cavelier J, Jackson P, Celis A (1998) Stem water storage and diurnal patterns of water use in tropical forest canopy trees. *Environment*, **21**, 397–406.

Hardy RWF, Holsten RD, Jackson EK, Burns RC (1968) The acetylene-ethylene assay for N_2 fixation: Laboratory and field evaluation. *Plant Physiology*, **43**, 1185–1207.

Hurd T, Raynal D, Schwintzer C (2001) Symbiotic N_2 fixation of *Alnus incana* ssp. *rugosa* in shrub wetlands of the Adirondack Mountains, New York, USA. *Oecologia*, **126**, 94–103.

Jones DL, Willett VB (2006) Experimental evaluation of methods to quantify dissolved organic nitrogen (DON) and dissolved organic carbon (DOC) in soil. *Soil Biology and Biochemistry*, **38**, 991–999.

Mobley ML, Cleary MJ, Burke IC (2014) Inorganic nitrogen supply and dissolved organic nitrogen abundance across the US Great Plains. *PLoS ONE*, **9**, 1-5. DOI: 10.1371/journal.pone.0107775.

Myrold DD, Huss-Danell K (2003) Alder and lupine enhance nitrogen cycling in a degraded forest soil in northern Sweden. *Plant and Soil*, **254**, 47–56.

Niinemets Ü (1999) Components of leaf dry mass per area - thickness and density - alter leaf photosynthetic capacity in reverse directions in woody plants. *New Phytologist*, **144**, 35–47.

Rabley JM (2017) *The influence of topographic gradients and environmental drivers on the nodulation rate of* Alnus viridis *at a low arctic site* (unpublished undergraduate thesis). Wilfrid Laurier University, Waterloo, Canada.

Reich PB (2014) The world-wide "fast-slow" plant economics spectrum: A traits manifesto. *Journal of Ecology*, **102**, 275–301.

Ros GH, Hoffland E, van Kessel C, Temminghoff EJM (2009) Extractable and dissolved soil organic nitrogen - A quantitative assessment. *Soil Biology and Biochemistry*, **41**, 1029–1039.

Warren RK (2015) *Examining the spatial distribution of soil moisture and its relationship to vegetation and permafrost dynamics in a subarctic permafrost peatland*

(unpublished Master's thesis). University of Guelph, Guelph, Canada.

Wolters DJ, Akkermans ADL, Van Duk C (1997) Ineffective *Frankia* strains in wet stands of *Alnus glutinosa* L. Gaertn. in the Netherlands. *Soil*, **29**, 1707–1712.

Wright IJ, Reich PB, Westoby M et al. (2004) The worldwide leaf economics spectrum. *Nature*, **428**, 821–827.

Wullschleger SD, Meinzer FC, Vertessy RA (1998) A review of whole-plant water use studies in trees. *Tree Physiology*, **18**, 499–512.

3.7 Tables and figures

Table 3.1: Outputs of simple linear regressions used to test for relationships between metrics of *Frankia* nodulation and ordinated green alder functional traits representing leaf investment, productivity, and water use for 16 green alders in the Trail Valley Creek research basin. Estimates of average and total nodule biomass per shrub and nodule count per shrub were obtained from Rabley (2017). Predictor variables were visually inspected for normality and square root-transformed when necessary. We applied false discovery rates to all p-values from linear regressions that used the same response variables (three adjustments total to account for re-using each of the three principal components (PCs) as responses to each of the three nodulation metrics) using the Benjamini-Hochberg method (built-in R function 'p.adjust'; Benjamini & Hochberg, 1995).

Comparison	Formula	R^2	Adjusted p-value
Average nodule biomass per shrub vs. PC 1	y = 0.037x – 0.58	0.11	0.324
Average nodule biomass per shrub vs. PC 2	y = -0.03x + 0.44	0.11	0.324
Average nodule biomass per shrub vs. PC 3	y = 0.0095x – 0.15	0.017	0.634
Square root(total nodule biomass per shrub) vs. PC 1	y = 0.11 – 1.06	0.19	0.265
Square root(total nodule biomass per shrub) vs. PC 2	y = -0.036 + 0.33	0.035	0.694
Square root(total nodule biomass per shrub) vs. PC 3	y = 0.018 – 0.17	0.011	0.694
Square root(nodule count per shrub) vs. PC 1	y = -0.1209 + 0.59	0.046	0.469
Square root(nodule count per shrub) vs. PC 2	y = 0.083 – 0.41	0.038	0.469
Square root(nodule count per shrub) vs. PC 3	y = -0.078 + 0.38	0.045	0.469

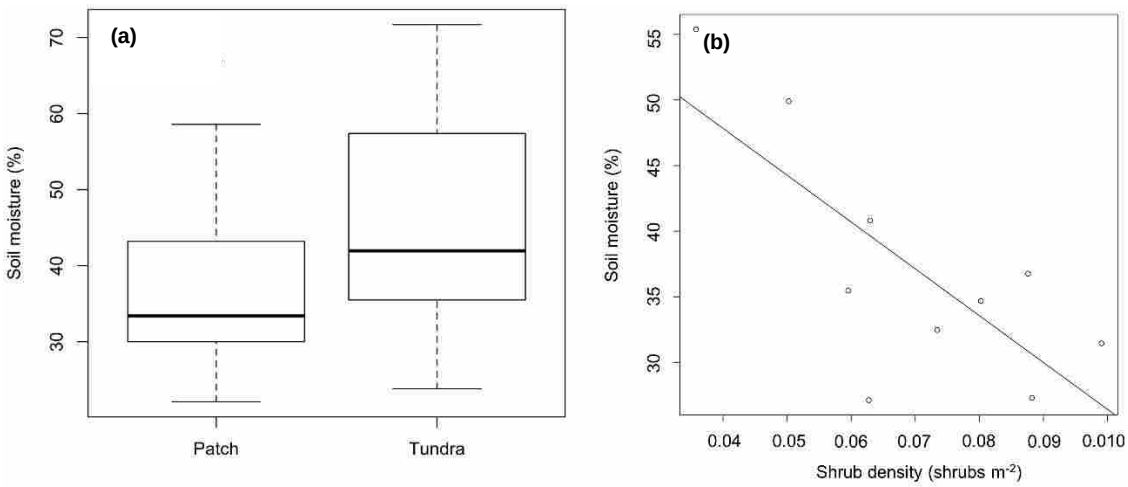

Fig. 3.1: (a) Boxplot displaying soil moisture (%) measured at a 5 cm depth at eight locations along 10 green alder patch transects and 10 paired open tundra transects from June 30th-July 2nd, 2015 in the Trail Valley Creek research basin on the low arctic tundra of the Northwest Territories (the eight locations along each transect were pooled for analysis). Each box encompasses the middle 50% of the distributions. The horizontal line within each box denotes the median. The whiskers represent the minimum and maximum values. Outliers (represented by open circles) are values that are 1.5 times greater than the interquartile range. Soil moisture was significantly higher in open tundra sites than in green alder patches (linear mixed effects model; $p = 3.70 \times 10^{-3}$). (b) Scatterplot showing the relationship between green alder density and soil moisture measured at a 5 cm depth (soil moisture measured in patches as explained above). Soil moisture data were pooled such that an average soil moisture per patch could be calculated (each point represents shrub density in a patch). Soil moisture significantly decreased with shrub density (simple linear regression; $p = 0.013$, $R^2 = 0.56$). Data in (a) and (b) were collected and analyzed by C. Wallace.

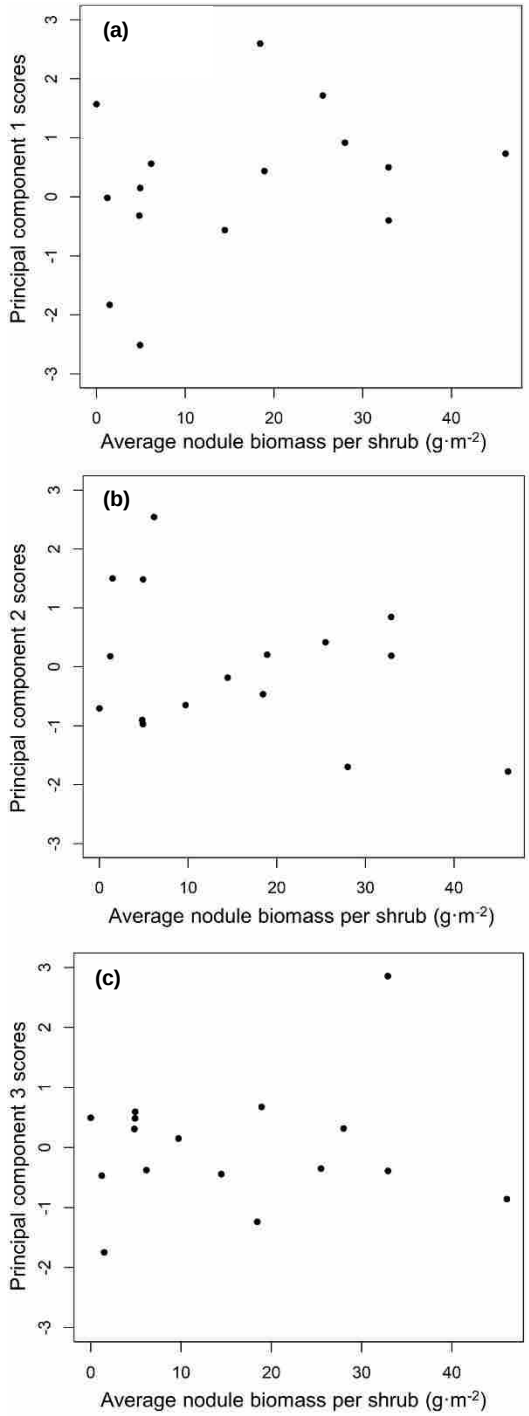

Figure 3.2: Scatterplots of average nodule biomass per shrub vs. ordinated green alder functional traits representing leaf investment, productivity, and water use for 16 green alders in the Trail Valley Creek research basin. Ordinated functional traits are represented by the scores of three principal component axes. Estimates of average nodule biomass per shrub were obtained from Rabley (2017). Average nodule biomass was not a significant predictor of principal component 1 (a), 2 (b), or 3 (b) (Table 3.1).

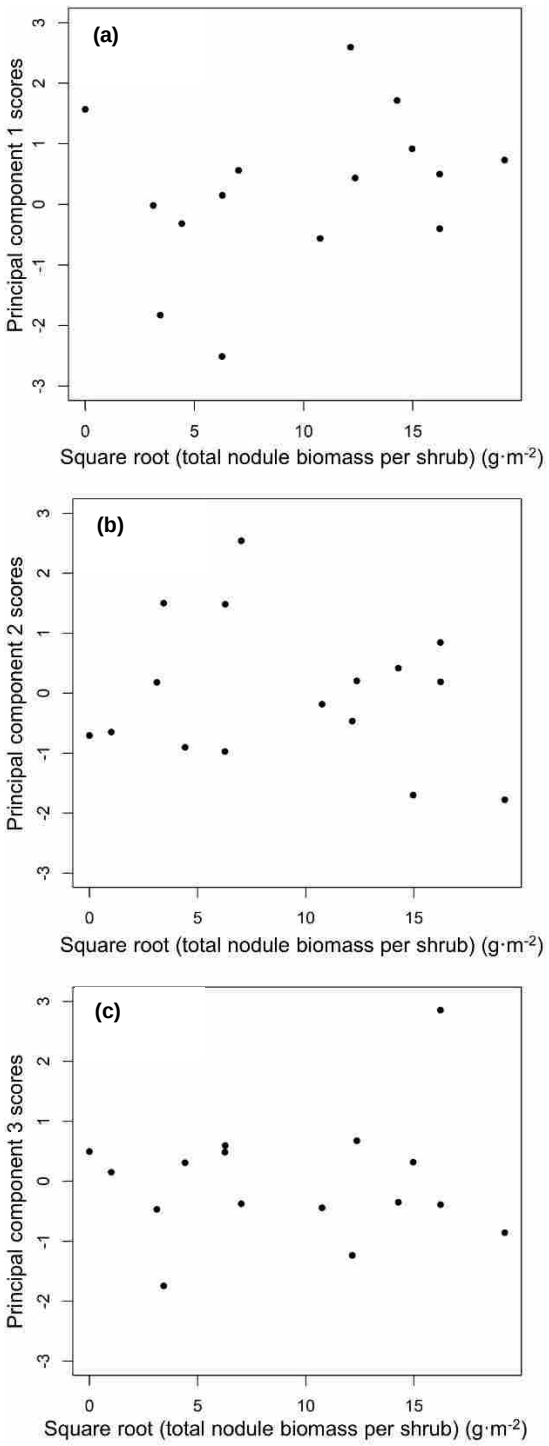

Figure 3.3: Scatterplots of square root-transformed total nodule biomass per shrub vs. ordinated green alder functional traits representing leaf investment, productivity, and water use for 16 green alders in the Trail Valley Creek research basin. Ordinated functional traits are represented by the scores of three principal component axes. Estimates of total nodule biomass per shrub were obtained from Rabley (2017). Square root (total nodule biomass) was not a significant predictor of principal component 1 (a), 2 (b), or 3 (b) (Table 3.1).

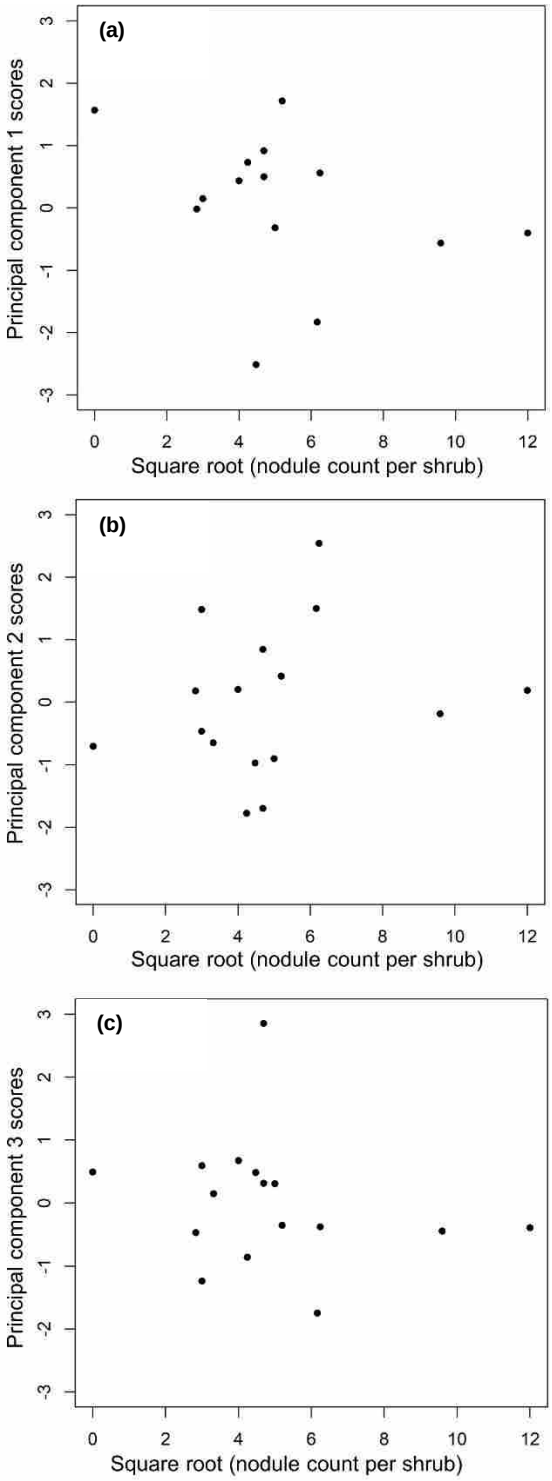

Figure 3.4: Scatterplots of square root-transformed nodule count per shrub vs. ordinated green alder functional traits representing leaf investment, productivity, and water use for 16 green alders in the Trail Valley Creek research basin. Ordinated functional traits are represented by the scores of three principal component axes. Estimates of nodule count per shrub were obtained from Rabley (2017). Square root (nodule count per shrub) was not a significant predictor of principal component 1 (a), 2 (b), or 3 (b) (Table 3.1).